PSYCHOPHYSICAL INVESTIGATIONS OF SPEED PROCESSING IN THE HUMAN VISUAL SYSTEM

Omar Hassan

A thesis submitted for the degree of

Doctor of Philosophy

Royal Holloway, University of London

2016

Declaration of Authorship

I Omar Hassan hereby declare that this thesis and the work presented in it is entirely my own. Where I have consulted the work of others, this is always clearly stated.

Signed:

Omar Hassan

Date: 16th March 2016

Abstract

A range of models of motion processing has been proposed (e.g. motion energy, gradient, Bayesian, ratio) but there is currently no consensus as to how the human visual system computes the speed of a moving image and there is insufficient data to adequately characterise the effects of even a few image parameters such as contrast, luminance and eccentricity upon perceived speed. A series of experiments was conducted in order to inform models of speed encoding and provide insight into the mechanisms underlying spatio-temporal processing in the visual system.

Measurements of the ramp after-effect suggest that the after-effect is determined by ramp amplitude rather than gradient and thus offer little support for the existence of gradient motion detectors. However, the findings of luminance-dependent ramp after-effects do provide support for the idea that the after-effect is mediated by ON- and OFF- pathways in the visual system.

Measurements of biases in speed perception indicated that speed encoding in the periphery is essentially similar to central vision whilst the results of a further study of speed biases indicated that at lower luminance there is significantly less reduction in perceived speed and greater increase in perceived speed (at low and high speeds respectively) and a concomitant reduction in the speed at which the bias is reversed. This luminance-dependent pattern of results is consistent with ratio-type models of speed encoding but inconsistent with all extant Bayesian models.

Overall the results of these experiments offer little support for gradient or Bayesian models. Whilst the results do not rule out other speed-encoding models, only ratio-class models can currently account for the entire pattern of results reported in this series of experiments.

Table of Contents

List of Figures

List of Tables

Acknowledgements

I am deeply indebted to my supervisor Dr Stephen Hammett for his invaluable guidance, encouragement, selfless time and care. I am grateful to my advisor Dr Jonas Larsson for the constructive discussions and friendly suggestions. To my friends and colleagues, I am thankful for the many stimulating discussions inside and outside the laboratory. I should also like to thank all the subjects who participated in the experiments. I am deeply grateful to my family, particularly my mother, Sahar, for her support over the years. I should also like to remember Dr George Harwood. Finally, to my constant, Christine, for always being there.

Publications

The data described in Chapter 6 were previously published in Hassan, O., and Hammett, S. T. (2015). Perceptual biases are inconsistent with Bayesian encoding of speed in the human visual system. *Journal of Vision*, *15*(2), 1-9.

Chapter 1

1 Introduction

Most of the experiments reported herein employ periodic stimuli to investigate the human visual system. This is predicated upon several assumptions, one of them being that the visual system may be considered linear over at least a part of its operating range. This assumption confers a number of advantages for systematic study of the system's properties.

1.1 Linear systems theory

For a system to be called *linear* it is required to have two properties: homogeneity and additivity. A system is said to be homogenous if an amplitude change, a, in the input signal, x, results in a proportional amplitude change in the output signal in the domain of the function, F, formally $F(ax) = aF(x)$ (Figure 1.1). A system complies with the principle of additivity if two signals can be added together and passed through the system without interacting. If the system's response to some stimulus, x_1, is x_1', and the response to some other stimulus, x_2, is x_2', then the response to the input signal, $x_1 + x_2$, is $x_1' + x_2'$, formally $F(x_1 + x_2 + \ldots) = F(x_1) + F(x_2) + \ldots$ (Figure 1.2). Taken together, homogeneity and additivity are often referred to as the principle of superposition.

Shift invariance, while not strictly a requirement for linearity, is a third property that is often found in linear systems. A system is said to be shift invariant when a shift in the input signal results in an identical shift in the output signal (Figure 1.3). This set of simple properties allows us to make predictions about how a system will respond given prior knowledge of its response to a restricted range of input waveforms. Moreover, if a system is linear and we know its response to

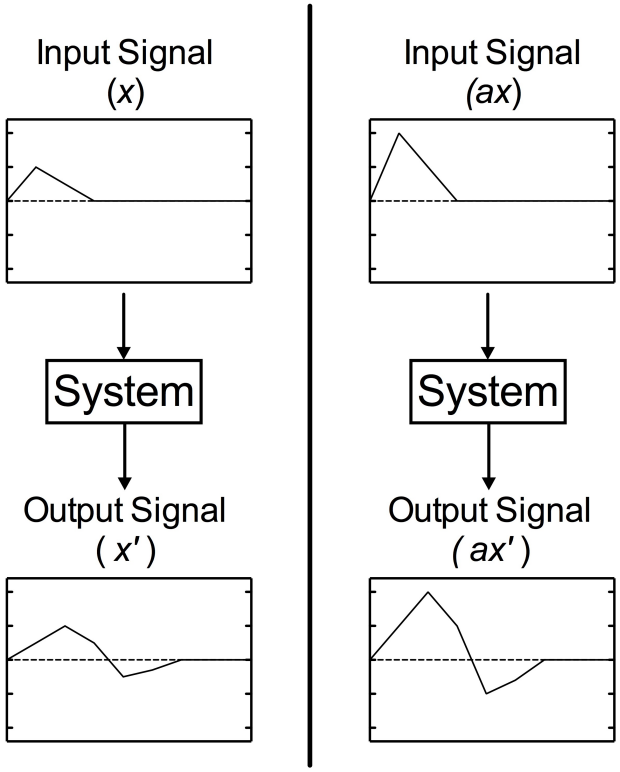

Figure 1.1: Illustration of homogeneity in a system. The amplitude of the input signal in the right column is twice (a = 2) that of the input signal in the left column, in a system with homogeneity, the output signal of the right hand column will result in an output signal with twice the amplitude of the output signal in the left column.

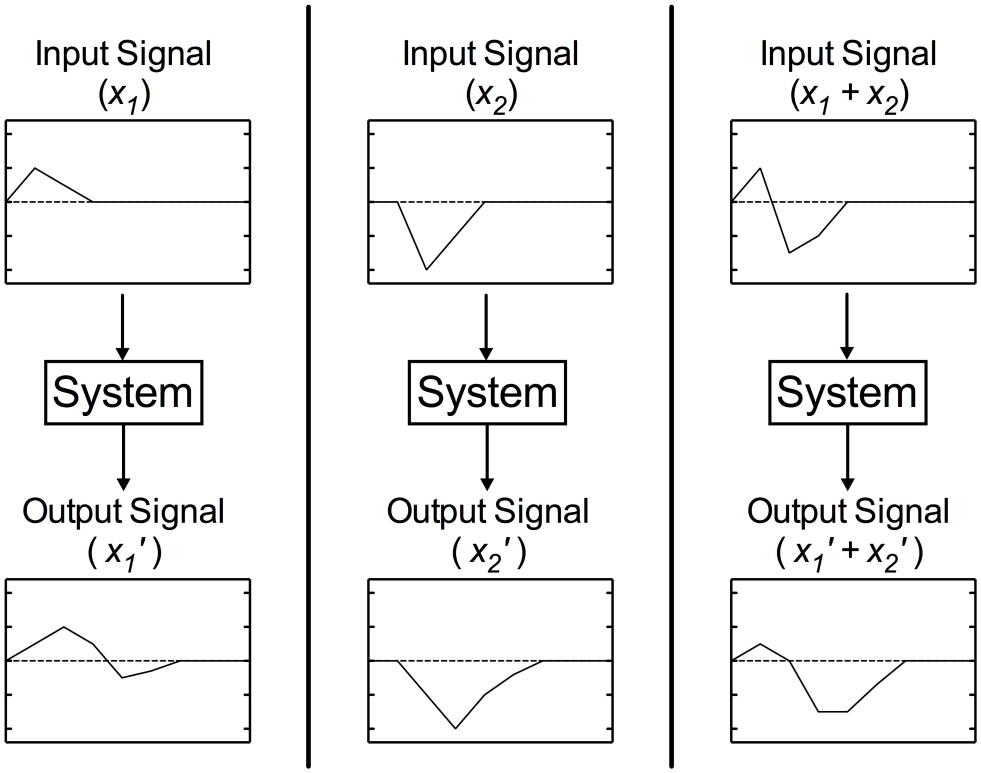

Figure 1.2: Illustration of additivity in a system. If the input, x_1, into a system results in the output, x_1', and the result of another input, x_2, is x_2', in a system with the property of additivity, the sum of the two inputs, $x_1 + x_2$, will yield the output, $x_1' + x_2'$.

some basis function, the response of the system to any input can be predicted by decomposing it into its component bases. Typically, such decomposition of complex signals is achieved by Fourier analysis. Fourier analysis is used preferentially over analogous mathematical transforms (e.g. the Hadamard transform decomposes complex signals into square waves) because basis functions other than sine waves are not passed linearly through the optics of the eye (e.g. De Valois & De Valois, 1988).

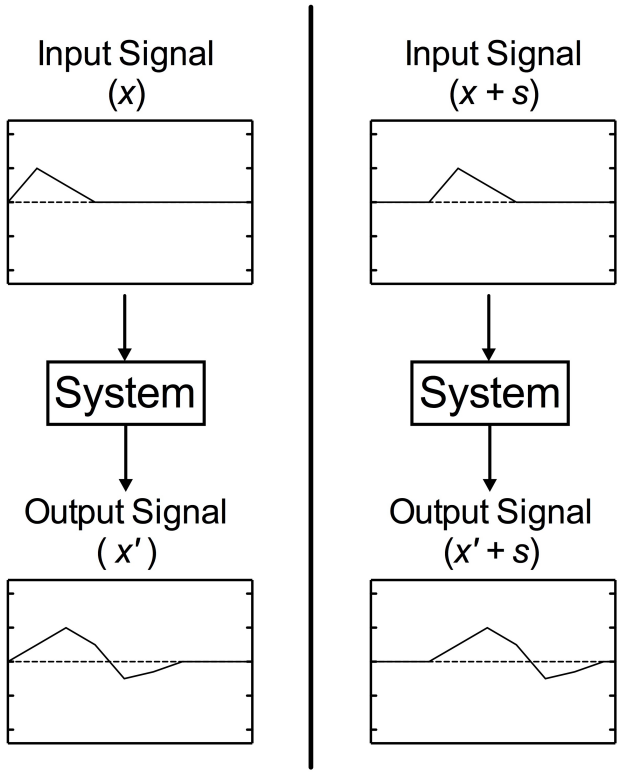

Figure 1.3: Illustration of shift invariance. In a system that is considered to be shift invariant, a shift (*s*) in the input (*x*) results in an identical shift in the output (*x'* + *s*).

1.2 Fourier Analysis

Fourier (1822) demonstrated that any function may be decomposed into a series of sinusoidal waveforms of different frequencies, amplitudes and phases.

1.2.1 Frequency

Frequency in the time domain is defined as cycles/second in Hertz (Hz). In the spatial domain, spatial frequency, or the rate at which luminance varies in cycles across a visual angle (degree), is defined as cycles/degree (c/deg), where the visual angle, V, of a stimulus of size, S, at a distance, D, from the eye is given by:

$$V = 2arctan\left(\frac{S}{2D}\right) \quad \text{..... (1.1)}$$

Figure 1.4 illustrates the calculation of visual angle. Given 2 cycles in S = 2 cm and an observer at 57 cm (D) from the image, the stimulus would subtend 2^o of visual angle (V). Thus, the spatial frequency of the sine wave would be 1 c/deg. Since:

$$V = 2arctan\left(\frac{S}{2D}\right) = 2arctan\left(\frac{2}{2(57)}\right) = 2^o \quad \text{..... (1.2)}$$

$$Spatial\ Frequency = \left(\frac{cycles}{degrees}\right) = \left(\frac{2}{2}\right) = 1\ c/deg \quad \text{..... (1.3)}$$

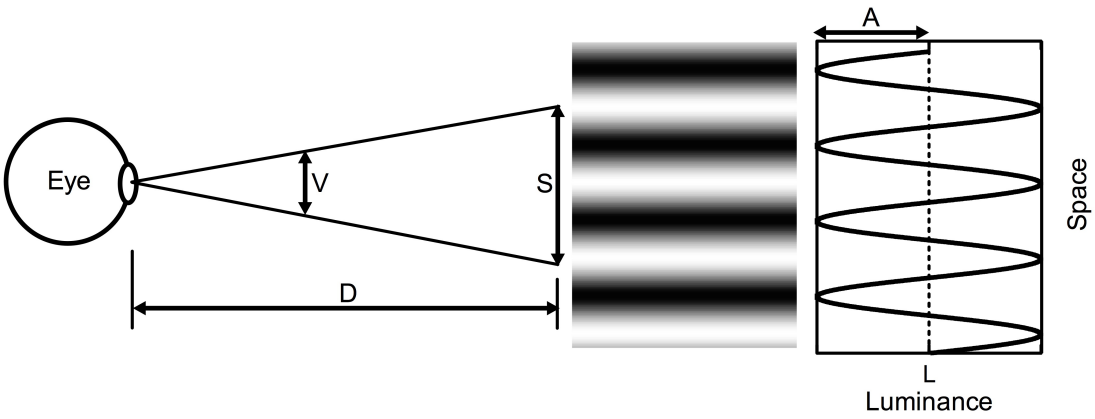

Figure 1.4: Illustration of a sine wave (right panel). In this example the sine wave oscillates about a mean luminance (L) with amplitude (A). The sine wave is depicted as an observer may see it on screen (central panel). The visual angle (V) in degrees is the angle the object of size (S) at a distance (D) subtends at the eye (left panel).

1.2.2 Amplitude

Amplitude refers to the maximum variation from mean that the waveform makes on some dimensional vector; in vision research this vector is usually luminance measured in candelas/m^2 (cd m^{-2}) (Figure 1.4, right panel). Luminance (or luminous intensity) is a photometric quantity, which represents the luminous intensity of a light source as perceived by the human eye. Formally, the candela is the luminous intensity, in a given direction, of a source that emits monochromatic radiation of frequency 540 x 10^{12} Hz and that has a radiant intensity in that direction of 1/683 watt per steradian (16th Conférence Générale des Poids et Mesures (CGPM), 1979).

Thus the amplitude (Figure 1.5) of an image is its contrast. For the purpose of this work the contrast of periodic spatial patterns shall be defined as Michelson contrast (*m*):

$$m = \frac{L_{max} - L_{min}}{L_{max} + L_{min}} \quad \text{..... (1.4)}$$

where L_{max} and L_{min} are maximum and minimum luminance respectively.

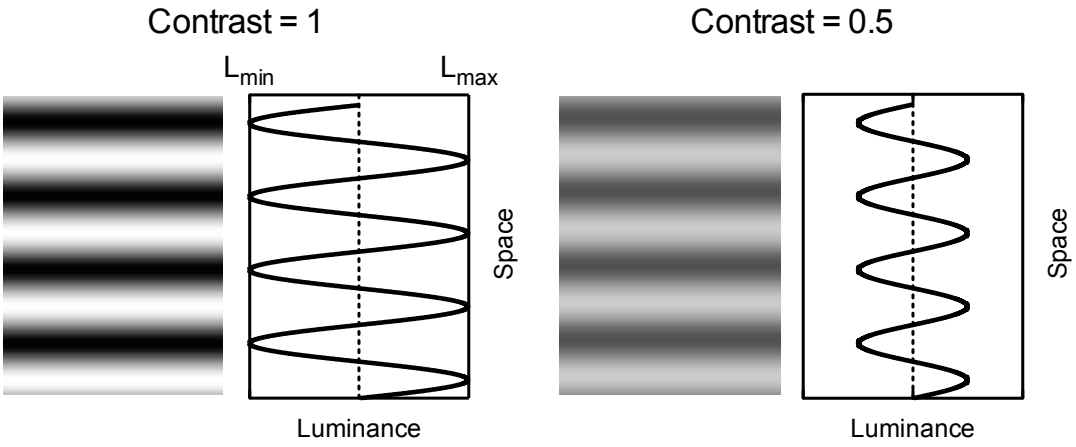

Figure 1.5: Illustration of two sinusoidal gratings with different contrasts (nominally 1 and 0.5) and corresponding luminance profiles.

1.2.3 Spatial and temporal phase

Phase denotes the point in a cycle of a waveform, measured in degrees (Figure 1.6). It is of particular importance when comparing several waveforms with each other. The phase angle of a waveform can be represented in space (spatial phase) and time (temporal phase).

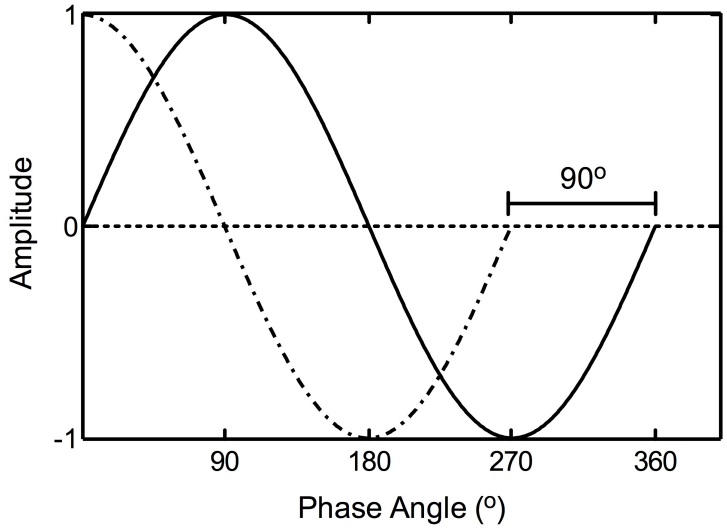

Figure 1.6: Illustration of two sine waves (solid line and dash-dot line) 90^{o} out of phase with each other (i.e. in phase quadrature).

1.2.4 The Fourier transform

A Fourier transform is a method of expressing a complex waveform as a series of sinusoidal components. Formally, the Fourier transform of a waveform is given by:

$$F(k) = \int_{-\infty}^{\infty} f(x) e^{-i2\pi kx}\, dx \quad \text{..... (1.5)}$$

where:

k is the spatial or temporal frequency,

x is the location in space or time,

i is $\sqrt{-1}$.

The inverse Fourier transform:

$$f(x) = \int_{-\infty}^{\infty} F(k) e^{i2\pi kx}\, dk \quad \text{..... (1.6)}$$

allows for Fourier synthesis, whereby spatial or temporal frequency may be transformed to space or time domains respectively. The Fourier inversion theorem states that a function in the space or time domain *f(x)* can be reconstructed from its Fourier transform *F(k)* (Bracewell, 1999).

For example, for an image that sharply transitions from an area of high luminance to an area of low luminance and back to an area of high luminance

e.g. a dark bar (Figure 1.7), the luminance profile would approximate a square wave.

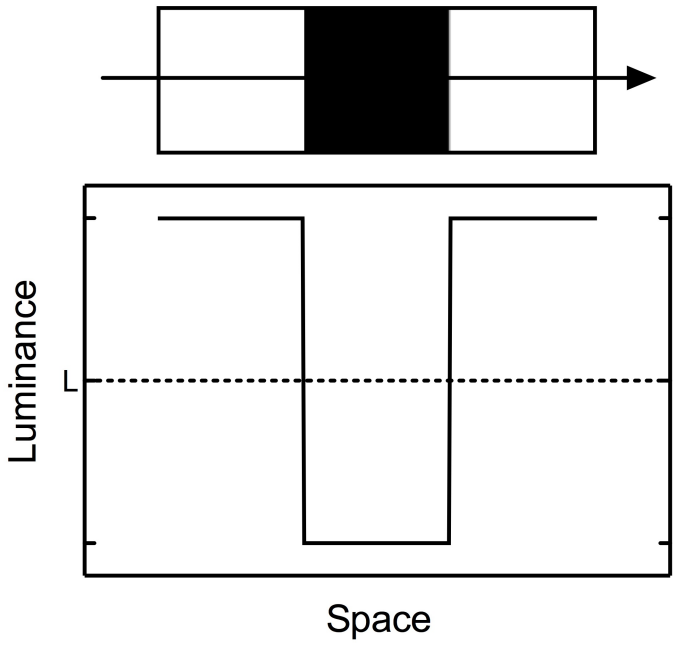

Figure 1.7: Illustration of a square wave (lower panel) with mean luminance (L) as a one-dimensional trace across an image of a dark bar surrounded by high luminance (upper panel).

A square wave is a periodic waveform that can be decomposed using Fourier analysis into odd harmonics of a fundamental sinusoidal component (the lowest frequency sinusoid in the sum) with varying amplitudes and phases.

The Fourier transform of a square wave of frequency *f* and amplitude 1 is given by:

$$\frac{4}{\pi}\left[sin(f) + \frac{sin\,(3f)}{3} + \frac{sin\,(5f)}{5} + \cdots + \frac{sin\,(nf)}{n}\right] \quad \text{..... (1.7)}$$

Thus, the amplitude of the fundamental sinusoidal component is $4/\pi$ or 1.273 times larger than the amplitude of the square wave. The amplitude of the third harmonic is 1/3 that of the fundamental, and so on. Figure 1.8 (left panels)

illustrates the first approximation to a square wave obtained by adding the fundamental (*f*) and third harmonic (3*f*), in these proportions and with equal phase. A progressively better approximation to a square wave may be obtained by continuing to add higher odd harmonics.

Similarly, a sawtooth wave of frequency *f* and amplitude 1 decomposes into both odd and even harmonics (Figure 1.8, right panels), and is given by:

$$\frac{2}{\pi}\left[sin(f) + \frac{sin(2f)}{2} + \frac{sin(3f)}{3} + \cdots + \frac{sin(nf)}{n}\right] \quad \text{..... (1.8)}$$

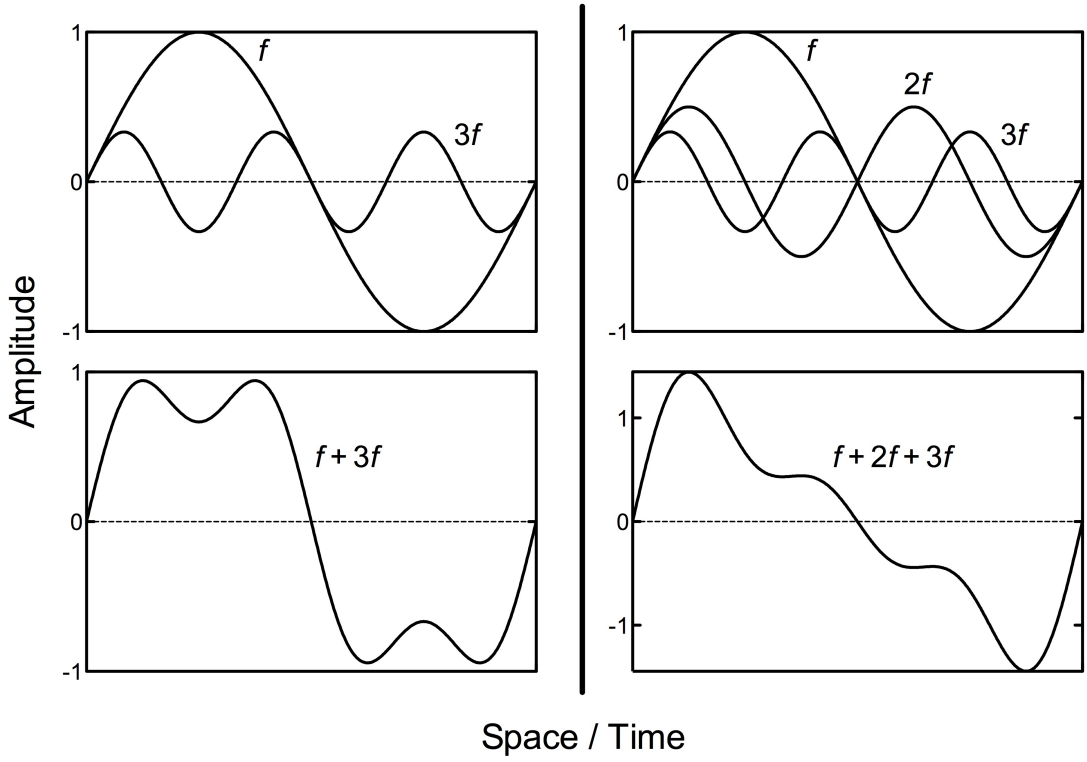

Figure 1.8: Synthesis of square (left panels) and sawtooth (right panels) waves. Left panels: The upper panel represents two component sine waves of frequencies *f* and 3*f*. The lower panel represents the first approximation to a square wave resulting from the sum of these components. Right panels: The upper panel represents three component sine waves of frequencies *f*, 2*f* and 3*f*. The lower panel represents an approximation to a sawtooth wave resulting from the sum of these components.

1.2.5 Linear systems analysis and the visual system

Fourier analysis may be applied to any stimuli, including aperiodic stimuli. As such, any image can be completely described by sinusoidal components of varying frequency, amplitude and phase. If we know how a system responds to a small set of sinusoidal components then we can predict its response to any complex signal, assuming the system is linear. Thus the assumption of linearity in the visual system is important in characterising the system's structure and to developing model systems.

However, neural information processing is predominantly nonlinear since the synaptic transmissions that propagate neural information primarily produce nonlinear input-output functions (e.g. Markram, 2003). Yet, surprisingly the visual system appears to exhibit a high degree of linearity. A review of linear and nonlinear systems analysis of the visual system by Shapley (2009) attributes the linearity of the retina to specialised ribbon synapses, while cortical linearity is described as a result of the interactions between excitatory and inhibitory synapses. Thus there is a presumptive case for employing the assumption of linearity in predicting the response of the visual system to complex images from knowledge of its response to basis functions.

1.3 Processing in the spatial domain

In principle the combination of linear systems theory and Fourier analysis should allow for the prediction of responses by the visual system, assuming it is linear. A great number of workers have sought evidence, that the visual system may be characterised as at least quasi-linear in the spatial domain.

1.3.1 The visual system as a Fourier analyser

Campbell and Robson (1968) addressed the question of whether the visual system could be considered a linear system that performs something akin to Fourier filtering by measuring threshold contrast (i.e., the contrast at which a stimulus becomes barely visible from a uniform grey background) for a range of periodic stimuli (e.g. sine-, square-, sawtooth- and rectangular-wave gratings), using a wide range of spatial frequencies (between 0.2 and 45 c/deg). Given that a square-wave comprises the sum of the odd harmonics of a fundamental sinusoid and that the amplitude of the fundamental component is 1.273 times greater than the amplitude of the square-wave (Figure 1.8), they postulated that contrast sensitivity (threshold contrast^{-1}) for a square-wave grating should be 1.273 times greater than that of a sine-wave grating of the fundamental frequency. Their measurements confirmed that the contrast sensitivity of a square-wave grating was approximately 1.273 times greater than that of a sine-wave grating. They concluded that the threshold contrast of complex gratings was determined by the amplitude of the fundamental Fourier component and that this was consistent with the notion that the visual system comprised multiple, independent linear spatial filters.

Further evidence consistent with this proposal was their finding that subjects were unable to discriminate between a sine wave and a square wave pattern until the contrast of the third harmonic of the square wave reached its own threshold. The third harmonic (3*f*) of a square wave grating has one-third the amplitude of the fundamental and three times the spatial frequency of the fundamental (Figure 1.8). Thus subjects appear to discriminate the stimuli upon the basis of the harmonic components of the square wave, leading Campbell

and Robson (1968) to suggest that the visual system uses linearly operating mechanisms that specifically respond to limited ranges of spatial frequencies. This multi-channel model assumes that the visual system performs an approximate Fourier analysis on the input stimulus, with separate channels analogous to spatial frequency filters with fixed ranges in the spatial frequency domain. The Contrast Sensitivity Function (CSF) of the system may thus be considered as the envelope of sensitivities of these independent spatial frequency channels (Figure 1.9) (The CSF indicates the relative contrast sensitivity (threshold contrast^{-1}) to spatial frequency).

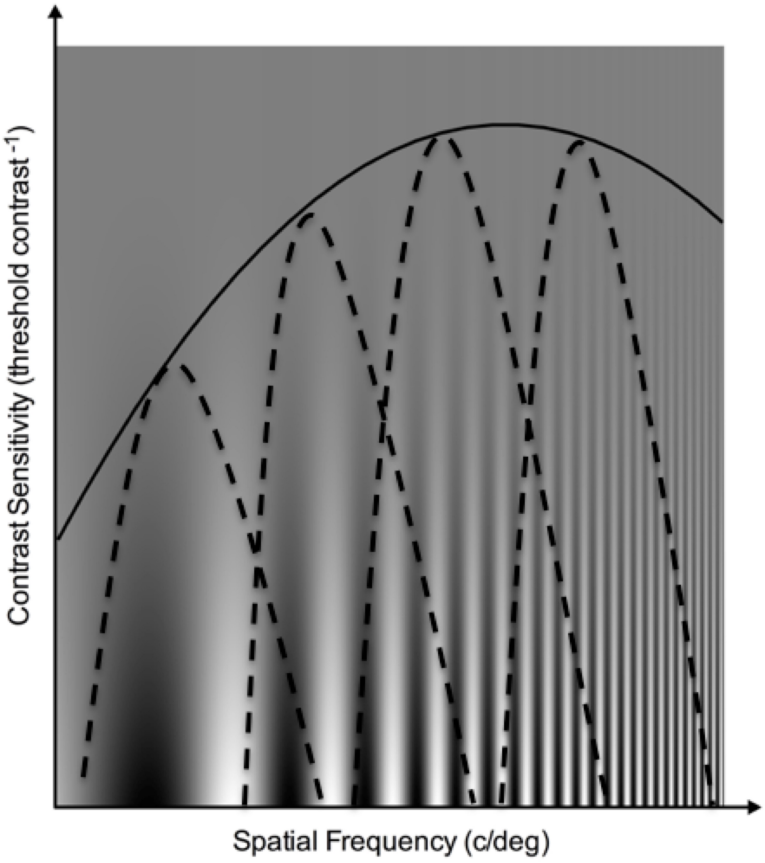

Figure 1.9: Illustration of the contrast sensitivity function (solid line) and some of the underlying channels (broken lines). Each channel responds to a limited range of spatial frequencies, the combination of these channels is what forms the CSF.

Further evidence for the existence of spatial frequency channels include spatial frequency-specific adaptation effects found by workers such as Pantle and Sekuler (1968) and Blakemore and Campbell (1969). They found that after viewing a high contrast grating at a particular spatial frequency, more contrast was required to detect similar frequency gratings (threshold elevation), whereas the contrast sensitivity for dissimilar spatial frequencies (approximately 2 octaves difference) was unaffected.

Blakemore and Campbell (1969) and Movshon and Blakemore (1973) found that threshold elevation did not occur exclusively at the adapting spatial frequency but across a limited range spanning around one to two octaves centred on the adapting frequency, suggesting that the channels are band-pass. Blakemore, Muncey, and Ridley (1973) measured the perceived loss of contrast after adaptation at several spatial frequencies and contrasts, and found that the width of the channels were also around two octaves centred on the adapting frequency. Measurements of the channels' widths seem to be consistent across studies that have employed different techniques (e.g. Blakemore & Campbell, 1969; Blakemore et al., 1973; Graham, 1972; Pantle & Sekuler, 1968; Stromeyer & Julesz, 1972) and are consistent with a model incorporating multiple independent band-pass spatial filters (or channels).

Some later work yielded evidence inconsistent with the assumption of *independent* channels (e.g. Barfield & Tolhurst, 1975; De Valois, 1977; Georgeson, 1975; Stecher, Sigel, & Lange, 1973; Tolhurst, 1972; Tolhurst & Barfield, 1978). For instance, Tolhurst and Barfield (1978) reported, that post-adaptation threshold was reduced for frequencies that differed from the

adapting pattern by one to two octaves (i.e., outside the range of a individual spatial channel), indicating that there may be inhibitory interconnections between channels. They hypothesise that in a resting state there is a steady level of inhibition across all channels. If a channel is then adapted, this channel will have less of an inhibitory effect on neighbouring channels causing an increase in their sensitivity.

While some inconsistency with Blakemore and Campbell's (1969) findings has been reported regarding the independence of channels (e.g. De Valois, 1977; Tolhurst, 1972; Tolhurst & Barfield, 1978) and channels selectively tuned to spatial frequency and not spatial phase (Jones & Tulunay-Keesey, 1975), evidence for their central finding of tuned spatial-frequency channels is abundant, and the multiple spatial-frequency channel model has subsequently become widely accepted (see reviews by: Braddick, Campbell, & Atkinson, 1978; De Valois & De Valois, 1980).

Figure 1.10 illustrates how these multiple spatial filters may approximate to a Fourier analyser of the visual scene.

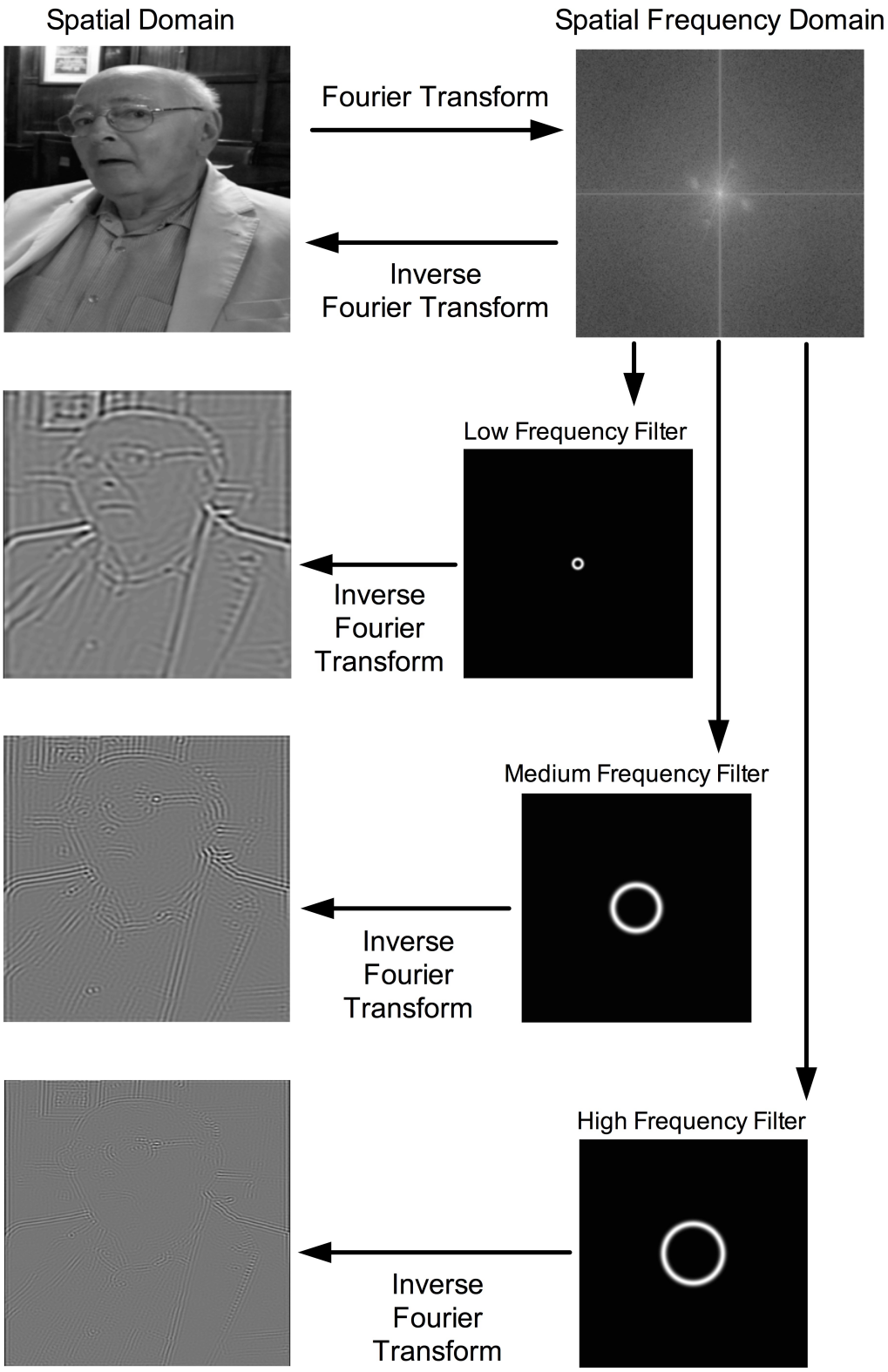

Figure 1.10: A 2-D Fourier transform of a natural image (top left) has been computed and its spectrum displayed (top right). The amplitude of each component is shown by the brightness of a pixel in the spectrum image. Low spatial frequencies are shown at the centre of the spectrum and high spatial frequencies are shown in the corners. Low, medium and high spatial frequency filters have been applied to the spectrum image and the spatial domain image has been recovered. Higher spatial frequencies contain information about feature details such as edges, while lower spatial frequencies contain information about the luminance variation over large scales.

1.3.2 Physiological implementation

In addition to the psychophysical evidence there is also substantial physiological evidence for the existence of tuned spatial-frequency channels in the visual system. Typically, retinal ganglion cells have circular antagonistic receptive fields with a variety of spatial extents. Enroth-Cugell and Robson (1966) proposed a plausible model of receptive field sensitivity comprising two Gaussian functions, the overall sensitivity given by the difference between the two functions (Figure 1.11).

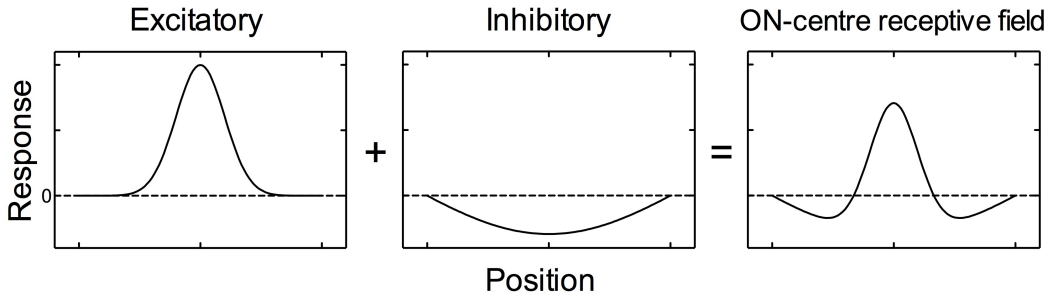

Figure 1.11: Illustration of how the combination of two Gaussian functions can produce an ON-centre receptive field (right panel). The trace in each panel illustrates the response to a point of light presented at various positions.

A cell with a receptive field based on this model would yield a strong response to gratings with a half cycle comparable to the width of the excitatory region. Little response would be shown to gratings with half cycles smaller than the excitatory region, and also little response to gratings with such a low frequency that both the excitatory and inhibitory regions fall within one half cycle. Thus, a cell that operates in such a way is sensitive to a narrow range of spatial frequencies, akin to the properties of a spatial frequency channel. However, quantitative estimates indicate the retinal cells' characteristics are not entirely consistent with behavioural evidence.

The spatial frequency bandwidths of retinal ganglion and Lateral Geniculate Nucleus (LGN) cells (Derrington & Lennie, 1984; Enroth-Cugell & Robson, 1966) appear to be broader relative to cortical cells and human psychophysical estimates (Campbell, Cooper, & Enroth-Cugell, 1969; De Valois, Albrecht, & Thorell, 1977; Maffei & Fiorentini, 1973). Furthermore, the spatial frequency response functions of cortical cells appear to be band-pass in nature, compared to the effectively low-pass response functions of retinal and LGN cells. Movshon, Thompson, and Tolhurst (1978) found that in the cat cortex the most common spatial bandwidth was around 1.3 octaves. De Valois, Albrecht, and Thorell (1982) found similar spatial bandwidths in the macaque cortex, most of the cells had bandwidths between 1 and 1.5 octaves, with the median bandwidth around 1.4 octaves. Thus cortical cells appear to be more consistent with behavioural estimates (e.g. Blakemore & Campbell, 1969; Movshon & Blakemore, 1973) of bandwidth than either retinal ganglion or LGN cells (Figure 1.12).

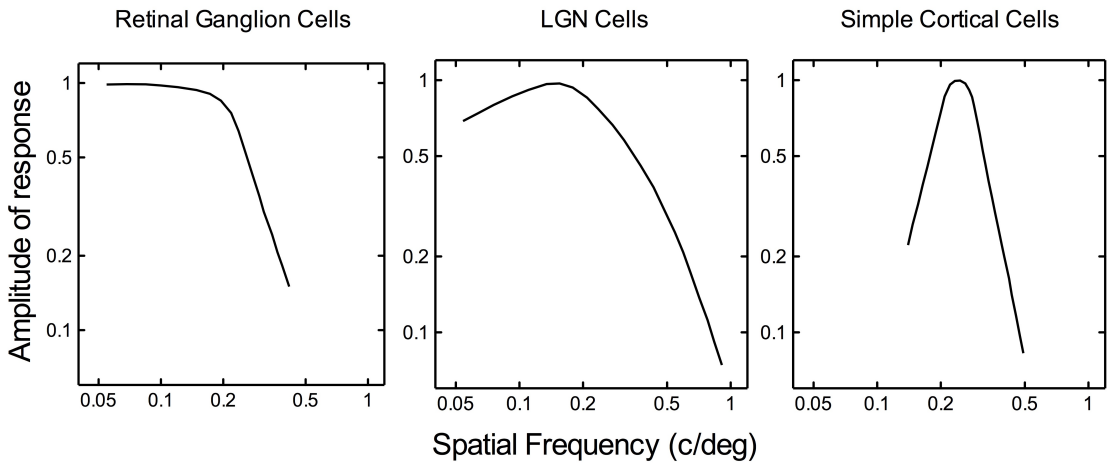

Figure 1.12: Examples of responses of single cells is the retina, LGN and cortex of the cat to a sinusoidal grating as a function of spatial frequency (after Maffei and Fiorentini (1973)). Sub-cortical cells appear to show low pass characteristics compared to the narrowly tuned band pass characteristics of cortical cells.

From this early work, a picture emerges whereby the visual system may be characterised, to a first approximation, as a quasi-linear system that processes spatial luminance signals in relatively independent, band-pass channels. The question therefore naturally arises as to whether its temporal processing is similarly structured.

1.4 Processing in the temporal domain

There is a relatively broad range of findings consistent with the notion that the human visual system analyses spatial patterns through multiple spatial filters (e.g. Braddick et al., 1978). The number of spatial channels has been estimated using a variety of techniques, e.g. spatial-frequency-specific adaptation (Blakemore & Campbell, 1969; Pantle & Sekuler, 1968), masking (Carter & Henning, 1971; Stromeyer & Julesz, 1972), subthreshold summation (Sachs, Nachmias, & Robson, 1971), and similarities between the spatial sensitivity profiles of these filters and single cells in the primary visual cortex have been noted (De Valois, De Valois, & Yund, 1979; Maffei, Morrone, Pirchio, & Sandini, 1979). However, early visual processing also involves temporal filtering. The nature of these temporal filters is not as well understood.

Early adaptation studies (Nilsson, Richmond, & Nelson, 1975; Pantle, 1971; Tolhurst, Sharpe, & Hart, 1973) suggested that whereas there are many narrowly tuned spatial frequency channels, there are few broadly tuned temporal frequency channels. Pantle (1971) used a staircase procedure to obtain flicker thresholds. Despite using a wide range of adapting frequencies Pantle's (1971) results showed little specificity of adaptation with similar profiles for the different flicker-sensitivity functions. However, subjects were adapted to

square wave flicker, whose harmonics may have resulted in the adaptation of temporal channels not sensitive to the fundamental frequency. Nilsson et al. (1975) used sinusoidally modulated adapting frequencies but reported that the maximum adaptation effect was not always the same as the adapting frequency. The findings of these early studies showed little specificity of adaptation and appear difficult to interpret.

More recent findings (e.g. Moulden, Renshaw, & Mather, 1984; Watson & Robson, 1981) provide clearer evidence consistent with the proposal of a few broadly tuned temporal channels. Moulden et al. (1984) used an adaptation protocol similar to earlier studies (Nilsson et al., 1975; Pantle, 1971; Tolhurst et al., 1973). They employed six adapting frequencies within the range 3 Hz to 20 Hz to investigate the threshold of five frequencies within the same range. Their results showed that, regardless of the adapting frequency, threshold elevation consistently peaked at one of two frequencies, 6 Hz and 14 Hz. They concluded that this suggests that there are only two temporal channels, one low-pass channel with an estimated peak sensitivity of 6 Hz, and one band-pass channel with an estimated peak sensitivity of 9 Hz.

Moulden et al. (1984) based their conclusion that only two temporal channels exist on adapting frequencies within the range 3 Hz to 20 Hz. Their data does not exclude the possibility of additional higher frequency channels with sensitivity profiles such that adapting frequencies of 3 Hz to 20 Hz yield little or no threshold elevation. Furthermore, their stimuli comprised light-emitting diodes (LEDs) (0.34 deg diameter) and were therefore spatially broadband.

Thus it is possible that their results reflect the responses of a number of independent, spatially tuned filters.

Watson and Robson (1981) addressed this issue by measuring temporal frequency discrimination performance using counterphase sinusoidal gratings near threshold at two spatial frequencies. The rationale for this methodology is that presenting frequencies near threshold will only lead to the activation of the channel most sensitive to that frequency. Whilst the sensitivity profiles of different channels may overlap, as reported in the spatial domain (Campbell & Robson, 1968), at threshold only the channel most sensitive will activate. Watson and Robson (1981) considered the possibility that detectors may be labelled, i.e., the output of a channel is associated with the frequency range over which the channel is sensitive, therefore an observer can distinguish between the response of any two channels. If the detection of frequencies presented near threshold is based upon the output of separate channels then those frequencies can be perfectly discriminated. Watson and Robson (1981) found that at both high (16 c/deg) and low (0.25 c/deg) spatial frequency, only relatively high and low temporal frequencies are discriminated perfectly. For example, at 0.25 c/deg, 8 Hz is perfectly discriminated from 0 Hz, but 2 Hz and 4 Hz are not; 2 Hz is perfectly discriminated from 16 Hz, but 4 Hz is not. At 16 c/deg, only 0 Hz and 8 Hz, and 0 Hz and 16 Hz are discriminated perfectly. Following the logic of perfect discrimination, Watson and Robson's (1981) results suggest that temporal frequency is encoded by two channels, at least at threshold.

Similar conclusions to Watson and Robson (1981) have been arrived at using different stimuli (Thompson, 1983) and different techniques (Anderson & Burr, 1985). Thompson (1983) employed drifting gratings and reported that only gratings with relatively large differences in drift speed could be discriminated. For instance, at 1 c/deg, 1 deg/sec and 7 deg/sec, 2 deg/sec and 12 deg/sec, and 3 deg/sec and 17 deg/sec, could be discriminated, suggesting that at threshold only two temporal filters are required for discrimination. Anderson and Burr (1985) reported evidence for two temporal channels using a masking paradigm. Employing drifting sinusoidal gratings of 0.1, 1 and 10 c/deg, at a constant temporal frequency, they measured the reduction in sensitivity to a test grating overlaid by a mask grating of variable temporal frequency. They found that regardless of temporal frequency the masking functions tended to show a single peak within the range 7 Hz to 13 Hz, for all test frequencies above 1 Hz. The exact location of the peak within the range 7 Hz to 13 Hz was dependent upon the spatial frequency of the test grating. Unlike in the spatial domain, masking functions did not peak at the same temporal frequency as the test gratings, as would be expected in a multi-channel configuration. Anderson and Burr (1985) conclude that their results suggest the existence of two temporal frequency detectors, one band-pass with a peak around 10 Hz, and a low-pass filter. In the case of low temporal frequencies, they found that masking functions did not have a specific peak.

Whilst there is strong evidence to support the notion of two temporal channels (e.g. Anderson & Burr, 1985; Foster, Gaska, Nagler, & Pollen, 1985; Moulden et al., 1984; Thompson, 1983; Watson & Robson, 1981) some psychophysical studies have suggested that there may be an additional third channel sensitive

only to high temporal frequencies. Hess and Plant (1985) replicated Watson and Robson's (1981) experiment and reported an improvement in discrimination performance at higher temporal frequencies. They found that at threshold and at very low spatial frequencies (0.2 c/deg) subjects were able to discriminate 0 Hz from 4 Hz and 4 Hz from 32 Hz. Similar results were obtained using suprathreshold stimuli, at low spatial frequencies (0.2 c/deg), there was an improvement in higher temporal frequency discrimination performance, suggesting a third channel. However, when a higher spatial frequency (2 c/deg) was employed, for both threshold and suprathreshold stimuli, their results were similar to those of Watson and Robson (1981), indicating the presence of only two temporal frequency mechanisms. It is difficult to account for the discrepancies between the results of Hess and Plant (1985) and Watson and Robson (1981). One possibility is that small differences between the stimuli used in each experiment may account for the differences. Hess and Plant (1985) used a lower spatial frequency (0.2 c/deg) compared to Watson and Robson (1981) (0.25 c/deg) and a slightly larger Gaussian spread of 2 periods compared to 1.5 periods.

Mandler and Makous (1984) motivated their experiment with the same labelled channels logic as Watson and Robson (1981), yet their results do not help to clarify this discrepancy between a two-channel or three-channel model of temporal processing. The data of one subject corresponded with a three-channel model, where 1 Hz, 4 Hz and 45 Hz were discriminated from one another, whereas, the data of another subject were more inline with the existence of two channels, one channel that could detect frequencies below 6 Hz and another channel that could detect frequencies above 6 Hz. Despite this

difference in subject performance, Mandler and Makous (1984) propose that a three-channel model adequately describes their results (Mandler, 1984). Finally, Hess and Snowden (1992) used a masking paradigm to investigate temporal processing in the visual system, and also suggested the existence of three temporal channels.

One of the main pieces of evidence for the existence of a third temporal channel is the improvement in discrimination performance at higher temporal frequencies, yet this may be due to an artifact. It is well known that viewing a flickering region over a prolonged period of time reduces sensitivity to that flicker (Pantle, 1971). Furthermore, prolonged viewing of peripheral flickering regions result in the perceptual fading and eventual disappearance of those flickering regions (Schieting & Spillmann, 1987). Hammett and Smith (1992) proposed that subjects in earlier experiments supporting the existence of three temporal channels were able to improve their discrimination performance at higher temporal frequencies due to fading cues which are enhanced by the relatively long presentation times (1-3 sec) as used by Mandler and Makous (1984) and Hess and Plant (1985). Perceptual fading will affect both stimuli in a discrimination task, but not necessarily with equal measure. Schieting and Spillmann (1987) reported that perceptual fading time was reduced as the temporal frequency of stimuli increased. Therefore, in a discrimination task with two stimuli of different temporal frequencies, perceptual fading times would be different. This difference in perceptual fading time is made more salient with long presentation times (1-3 sec) and as the temporal frequencies of the stimuli in the discrimination tasks are increased.

In order to investigate whether perceptual fading improved discrimination performance at higher temporal frequencies Hammett and Smith (1992) used three different presentation durations 3000, 1500 and 300 msec. They report that at 1500 msec duration at 0.5 c/deg, discrimination performance was best bellow 20 Hz and then improves again above 30 Hz. At the same presentation duration but higher spatial frequency (4 c/deg) there was no improvement in performance above 30 Hz, similar to previous findings. In order to reduce the effect of perceptual fading, presentation duration was reduced to 300 msec at 0.5 c/deg, the improvement in discrimination above 30 Hz disappeared. To demonstrate how much of an effect presentation duration had on discrimination performance, Hammett and Smith (1992) increased presentation duration to 3000 msec, in order to make the fading cues more salient. They found that discrimination performance at higher temporal frequencies (35 Hz) could be improved even at high spatial frequencies (4 c/deg).

Studies prior to Hammett and Smith (1992) that used an increase in discrimination performance at higher temporal frequencies to infer a third temporal channel used relatively long presentation durations. Furthermore, Hess and Plant (1985) suggested that an improvement in discrimination performance was confined to lower spatial frequencies yet, Hammett and Smith (1992) showed that this improvement was present at higher spatial frequencies but that longer presentation durations were required. Subsequently, Fredericksen and Hess (1998) developed a model to best fit their set of psychophysical data and found that only two-temporal filters were necessary to describe the performance of three subjects. While some researchers (e.g. Hess & Plant, 1985; Hess & Snowden, 1992; Mandler & Makous, 1984) have

suggested the existence of three temporal channels it is now generally believed that there are just two temporal channels: one tonic (low-pass) and one phasic (band-pass) (Anderson & Burr, 1985; Fredericksen & Hess, 1998; Hammett & Smith, 1992).

1.4.1 Magnocellular and Parvocellular pathways

Single-cell studies on the macaque have revealed cortical cells with low-pass and band-pass temporal tuning characteristics (Foster et al., 1985; Hawken, Shapley, & Grosof, 1996), similar to the temporal filters suggested by Anderson and Burr (1985). Foster et al. (1985) reported most neurons in V1 and V2 were broadly tuned for temporal frequency and exhibited either band-pass or low-pass characteristics within the range of 0.5 Hz to 16 Hz. Hawken et al. (1996) suggested that the temporal frequency tuning in V1 appears to be a filtered version of the signals from the Lateral Geniculate Nucleus (LGN). Furthermore, early physiological research established the existence of two functionally distinct groups of retinal ganglion cells, parasol and midget cells, that correspond to the Magnocellular (M) and Parvocellular (P) layers in the LGN, respectively (e.g. Kaplan & Shapley, 1986; Lennie, Trevarthen, Van Essen, & Wässle, 1990; Merigan & Maunsell, 1993). One striking difference between cells in the M and P pathways is the temporal characteristics of their responses to visual stimuli (Gouras, 1968). When presented with a step change in luminance, P cells show a more tonic (or sustained) response, whereas, M cells show a more phasic (or transient) response (Purpura, Tranchina, Kaplan, & Shapley, 1990). Furthermore, P cells are most sensitive to low temporal frequencies and reduce their sensitivity as temporal frequency increases, whereas, M cells are less sensitive to low temporal frequencies and more

sensitive to high temporal frequencies (Merigan & Maunsell, 1993). While both M and P cells have centre-surround receptive fields that can be described by Gaussian functions (Derrington & Lennie, 1984), M cells' receptive fields are typically 2-3 times larger than P cells' (Lennie et al., 1990).

Another physiological difference between M and P cells is their sensitivity to stimulus colour. P cells have a colour opponent structure (ether red/green or blue/yellow), making them sensitive to "chromatic" stimuli regardless of the relative luminance of the colours (Derrington & Lennie, 1984). M cells, on the other hand, are less sensitive to colour and more sensitive to achromatic "luminance" modulation (Callaway, 2005; Derrington, Krauskopf, & Lennie, 1984; Michael, 1988; Wiesel & Hubel, 1966). The superior sensitivity to luminance modulation of M cells is particularly noticeable at higher temporal frequencies. Derrington and Lennie (1984) reported that macaque M cells are more sensitive to higher temporal and lower spatial frequencies than P cells. P cells were optimally sensitive to stimuli modulated at temporal frequencies around 10 Hz, M cells to stimuli modulated at around 20 Hz.

Behavioural evidence from localised lesions to the M and P pathways also highlight the functional specialisation of the two pathways. Lesions to the M pathway cause a decrease in luminance contrast sensitivity to high temporal and low spatial frequency stimuli (Merigan, Byrne, & Maunsell, 1991). This reduction in sensitivity results in the reduced visibility of fast flickering or fast moving stimuli, consistent with physiological evidence. Lesions to the P pathway result in complementary effects, thus a decrease in luminance contrast sensitivity to low temporal and high spatial frequencies (Merigan, Byrne, et al.,

1991; Merigan & Eskin, 1986; Merigan, Katz, & Maunsell, 1991). There appears to be an approximately four-fold decrease in visual acuity caused by P pathway lesions, which suggests that the P pathway plays a large role in detecting high spatial frequencies (Merigan, Katz, et al., 1991). Furthermore, M pathway lesions cause no change to colour contrast sensitivity, while P pathway lesions cause an almost complete loss of colour vision (Merigan, Katz, et al., 1991; Schiller, Logothetis, & Charles, 1990).

There is considerable physiological and behavioural evidence showing functional specialisation between the M and P pathways. This has led many (e.g. Callaway, 2005; Lennie et al., 1990; Merigan & Maunsell, 1993) to associate the M and P pathways with motion and form perception, respectively. There is thus a speculative link that can be made between physiological and psychophysical findings. Psychophysical research suggests that there are probably only two temporal channels and the M and P pathways may possibly form their substrate. Regardless, of the substrate of these temporal filters they are tuned for flicker but not speed. But many cortical cells are tuned for speed (e.g. Maunsell & Van Essen, 1983; Rodman & Albright, 1987; Simoncelli & Heeger, 2001). A range of models has therefore been proposed to account for how early spatial and temporal information is transformed into a cortical representation of speed.

1.5 Motion models

1.5.1 Reichardt detectors

Exner (1894) was one of the earliest to consider how a motion signal could be generated from neural connections, suggesting that to detect the direction of motion it is necessary that an image be sampled at more than one point in space and that these samples be summed. Direction and speed of a moving object can be obtained in this type of system, by comparing the differences in time delay of signals reaching the point of summation from different locations in the retina. Reichardt (1961) proposed the first formal model of motion detection, known as the Reichardt detector or Hassenstein-Reichardt model (Hassenstein & Reichardt, 1956), based on the optomotor response of insects. A Reichardt detector has two input channels that sample the visual field at two spatially adjacent points. The luminance pattern from one of the input channels is delayed (by a low-pass temporal filter) and correlated with the luminance pattern from the non-delayed input channel at a multiplication unit. The multiplication unit is included in the model because if either a light increment (ON) or a light decrement (OFF) were presented to the two inputs, the resulting response would follow the sign rule of multiplication in all sequence combinations. Thus, a Reichardt detector would only respond when the luminance patterns at both inputs are the same (Figure 1.13). In this way the Reichardt detector operates as a spatio-temporal correlator allowing for motion detection.

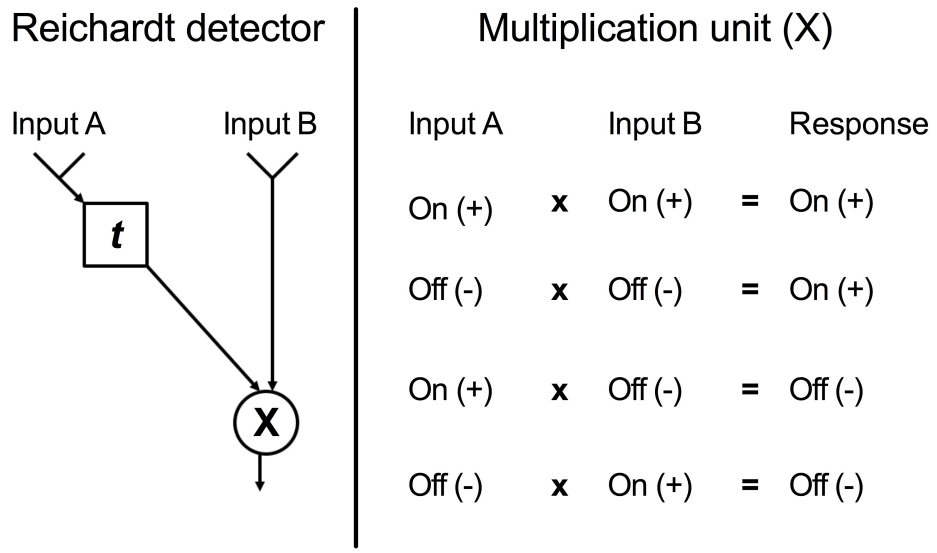

Figure 1.13: Left panel: Schematic of a Richard detector. Input A is delayed by a temporal filter (*t*) before both input (A and B) signals are compared at the multiplication unit (X). Right panel: The response of a multiplication unit based on luminance patterns at inputs.

An Elaborated Reichardt Detector (ERD) consists of two mirror-symmetrical Reichardt detectors (subunits) that are tuned to motion in opposite directions (e.g. left and right). The component subunits share two input channels that sample the visual field at two spatially adjacent points. The response of each subunit reflects how well the luminance pattern from each input correlates. Subtracting the response of the left subunit from the response of the right subunit yields the detector's response.

The Reichardt detector was developed based on the compound eyes of insects, composed of many ommatidia, for which point shaped receptive fields may have seemed appropriate, however mammalian eyes are structured differently. Physiological studies involving the visual pathways of higher mammals (e.g. cats and monkeys) have shown that cells in the retina and LGN are not directionally sensitive (e.g. Hubel & Wiesel, 1961; Shapley & Lennie, 1985). Although, neurons in V1 are found to be directionally sensitive, the receptive fields of these neurons are not sensitive to single points, but rather to large

areas of the visual field. Furthermore, for the Reichardt detector to signal motion accurately, the outputs of several detectors need to be combined; how this combination is achieved is undefined in the original model. Another limitation of the Reichardt detector is that it is susceptible to spatial aliasing. If the distance between the input channels (spatial sampling rate) were between one half and one spatial period of the input stimulus, the detector would signal the incorrect direction, as predicted by the Nyquist-Shannon sampling theorem (Nyquist, 1928; Shannon, 1949).

Van Santen and Sperling (1985) developed a version of the Elaborated Reichardt Detector in order to overcome some of the limitations of previous versions that attempt to model low-level motion detection in humans. To prevent spatial aliasing, the receptors of the ERD are linear spatial input filters out of phase by 90^{o}, as opposed to point shaped receptive fields in the original detector. To prevent temporal aliasing, the temporal filters are modified in order to delay temporal frequencies compared at the multiplication unit by 90^{o}. Consequently, the receptive fields of the input spatial filters and succeeding temporal filters are in quadrature phase (differ in phase by 90^{o}). Combining these spatio-temporally separate spatio-temporal impulse responses, yield spatio-temporally inseparable responses tuned to motion in opposite directions. Moreover, Van Santen and Sperling (1985) specify an algorithm (voting rule) for how the responses from independent ERDs, sensitive to different spatial frequencies, are combined in order to produce the final response to motion by the visual system. A voting rule is necessary when applying the Reichardt detector model to human vision because the many detectors may present conflicting information at the decision stage.

1.5.2 Motion energy models

Motion energy models (Adelson & Bergen, 1985) are formally equivalent to Van Santen and Sperling's (1985) version of an ERD. Motion energy models filter the input image through spatial and temporal filters out of phase by 90^{o} in order to produce four spatio-temporally separable responses. These separable responses can be added or subtracted to produce spatio-temporally inseparable filters, which signal a preferred direction of motion. There are two rightward tuned linear filters and two leftward tuned filters, with each directional pair in quadrature phase. Adelson and Bergen (1985) note that while spatio-temporally inseparable filters are useful in analysing motion, they possess a few drawbacks. Firstly they are phase sensitive, for example, a moving sine wave pattern would elicit a response that also oscillated sinusoidally over time. At any point in time, the output of a spatio-temporally inseparable filter may be negative, zero or positive, so that at any given moment the output does not directly indicate motion. Adelson and Bergen (1985) suggest that an output with a constant value for constant motion would be more inline with the behaviour of many direction-selective complex cells. Secondly, the sign of a response from a spatio-temporally inseparable filter is dependent upon the sign of the stimulus contrast. For example, a white bar on a black background and a black bar on a white background moving in the same direction would give inverse responses.

To overcome these drawbacks Adelson and Bergen (1985) introduce phase-independence to their model by squaring and summing the responses of each directional pair of spatio-temporally inseparable filters and extracting a measure of local motion energy. The resulting motion energy responses for each direction are always positive and phase independent. The motion energy

responses would also be the same regardless of the sign, but not magnitude, of the stimulus contrast. The opponent motion energy (e.g. difference between the motion energy signals for rightward and leftward motion) gives a clear directional signal, but still confounds velocity and contrast.

In order to extract a velocity estimate invariant from contrast Adelson and Bergen (1986) suggested that the opponent motion energy be scaled by some 'static energy' signal. This in essence renders the modified motion energy models into a ratio model of speed encoding, comparing the outputs of 'fast' (opponent motion energy) and 'slow' (static energy) mechanisms. However, how the output of an array of spatiotemporally oriented motion detectors, each tuned to different velocities is combined to encode speed is not considered. Furthermore, the notion that speed is encoded in a 'labelled lines' manner as the output of an ensemble of narrowly tuned channels is not consistent with our current understanding of speed perception. Firstly, as previously mentioned (see section 1.4) there exist two (or may be three) broadly-tuned temporal frequency channels, one low-pass (or 'slow') and one (or two) band-pass (or 'fast') channel. Secondly, adaptation to a moving stimulus changes the perceived speed of a subsequently viewed moving test stimulus (e.g. Carlson, 1962; Smith & Edgar, 1994; Thompson, 1981). The effect of adaptation was not confined to test speeds within a narrow range about the adapting speed as would be expected from a 'labelled lines' approach. In fact, the perceived speed of all stimuli moving at speeds slower than the adapting speed appeared slower for stimuli moving in the same direction, when the adapting speed was slower than the test speed the perceived speed of the test stimuli appeared faster (e.g.

Hammett, Champion, Morland, & Thompson, 2005; Smith & Edgar, 1994; Thompson, 1981).

Physiological studies (De Valois, Cottaris, Mahon, Elfar, & Wilson, 2000) have shown that the properties at each stage in the motion energy model are comparable to behaviour of cells across successive areas in the brain. In the cat visual cortex some simple cells have linear spatio-temporally separable responses, while other simple cells have spatio-temporally inseparable responses (McLean & Palmer, 1989; McLean, Raab, & Palmer, 1994; Pollen & Ronner, 1981). Direction selective complex cells haven been show to behave much like the non-linear transformation stage, producing phase-independent signals corresponding to motion energy (Emerson, Bergen, & Adelson, 1992). In the primate visual cortex Perrone and Thiele (2002) describe how V1 neurones are tuned to certain spatial and temporal frequencies while neurones in the middle temporal (MT) area have spatio-temporally inseparable receptive fields oriented in the spatio-temporal frequency domain. They suggested that velocity tuning in MT occurs via a ratio of the low-pass and band-pass channels in V1. Furthermore, Perrone (2005) showed how a motion sensor with variable speed tuning could be produced from just two V1 neurons.

1.5.3 Recovering direction of motion

Neither Bayesian nor ratio approaches to speed encoding explicitly address the encoding of direction but a range of studies have addressed this key parameter. Both Reichardt and motion energy approaches have an explicit spatial component that encodes local velocity (speed and direction) but the recovery of motion direction in complex two-dimensional patterns requires further

computation. Adelson and Movshon (1982) suggested a two stage intersection of constraints (IOC) model to extract motion direction in multiple (e.g. sinusoidal plaid) component two-dimensional stimuli. Stage one of the model comprises the extraction of the (ambiguous) component velocities which are defined by a line of constraint parallel to the components' orientations. The second stage determines overall pattern (plaid in the case of two sinusoidal components) motion by identifying the intersection of the constraint lines (Figure 1.14).

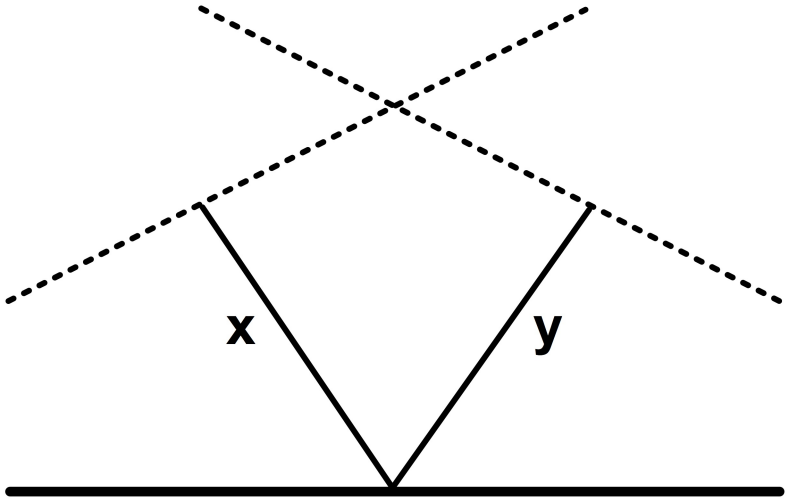

Figure 1.14: The IOC model: x and y represent the velocity vectors of the two components. Constraint lines are represented by the broken lines. The intersection of these lines determines velocity.

The IOC model has proven successful in predicting perceived velocity for a range of two-dimensional patterns. However, the model fails to predict perceived direction when the two components differ in either contrast (Stone, Watson, & Mulligan, 1990) or spatial frequency (Smith & Edgar, 1991). Stone et al. (1990) reported that perceived direction is biased toward the direction of the higher contrast pattern component and Smith and Edgar (1991) found that perceived direction was biased toward the lower spatial frequency pattern component. Both groups suggested that the bias in perceived direction was due to an underlying bias in the perceived speed of the pattern's components. Thus

the IOC model can predict direction but only if the input to its second stage is that of the *perceived* rather than physical component speeds. Derrington and Suero (1991) provided further support for this modified form of the IOC model by showing that perceived direction was also biased after motion adaptation in a manner consistent with the IOC being computed by inputs of perceived speed. However, Champion, Hammett and Thompson (2007) demonstrated that biases in perceived speed induced by changing pattern component contrast does not lead to the perceived direction biases predicted by the modified IOC model. Moreover, Ferrera and Wilson (1990) demonstrated that the IOC model fails to predict direction for 'Type II' plaids. These plaids are two-dimensional patterns comprising components of very similar orientation but different speeds – the resultant pattern has an IOC that is not coincident with its vector sum. Wilson, Ferrera and Yo (1992) constructed a model that could predict the perceived direction of these Type II patterns by computing the vector sum of first-order and second-order components of the image. However, Champion et al. (2007) point out that Wilson et al.'s model cannot predict the perceived direction biases induced by unequal component contrast since the model incorporates an early gain control mechanism that makes it almost immune to contrast manipulations. Furthermore, Victor and Conte (1994) reported further evidence that the IOC approach may not reflect how the brain encodes motion direction. They found that a patient with posterior cortical atrophy had superior direction discrimination for moving plaids than for their component gratings – the opposite of that which would be predicted by the IOC model but, as Victor and Conte note, consistent with the model of Heeger (1987).

1.5.4 Heeger's model of the extraction of image flow

In constructing his model of velocity extraction, Heeger takes as his starting point the observation that band-pass spatio-temporal filters such as those implemented in motion energy models are not velocity selective mechanisms. Instead, they are tuned to a range of spatio-temporal frequencies and, as such, cannot disambiguate variations in spatial and temporal frequency within that range nor changes in contrast. Heeger's (1987) model sets out to demonstrate how an unambiguous velocity code may nevertheless be computed by combining the outputs of a large array of such mechanisms whose tuning characteristics vary.

Heeger's (1987) model employs quadrature pairs of band-pass, three-dimensional spatio-temporal filters. The quadrature relationship of these filters indicates that the maximum response in one filter is coincident with the minimum responses in the other – in order to achieve this property Heeger uses sine and cosine functions multiplied by a Gaussian (Gabors). The result of this quadrature phase is that the summed (and first squared) outputs of these filters gives a motion energy signal that is phase invariant. While these filters respond to motion, Heeger points out that they do not provide an unambiguous code for velocity. However, by varying the width of the Gaussian independently for space and time the filters can be tuned for a variety of different orientations and frequencies. Heeger's (1987) model uses a 'family' of such filters, each of which produces an energy measure within a different Gaussian region of the Fourier frequency domain. Moreover, the model normalises its response by dividing each filter output by the average of all filters of a particular orientation, thus reducing the ambiguity of the output with respect to contrast. In order to extract

velocity the model estimates the least squares fit of the filters' responses to calculate the orientation of the plane through frequency space that accounts for the greatest measure of motion energy. Finally, Heeger shows that this final stage can be modelled by combining the outputs of the motion energy filters in a non-linear (squaring) manner to produce velocity-tuned units that have properties similar to the velocity tuned cells found in macaque MT.

Heeger's (1987) model deals well with a variety of natural stimuli and psychophysical estimates such as plaid direction with unequal contrast components and plaid coherence as a function of component angular separation. It is also consistent with Victor and Conte's (1994) report of a patient with cortical atrophy whose direction discrimination was better for plaids than their components – the model would predict precisely this since the combination of the outputs of the family of spatio-temporal filters allows for the disambiguation of the filter outputs. In the case of single gratings this ability to disambiguate is diminished. The model also has a good deal of physiological plausibility which was further enhanced in the model described by Simoncelli and Heeger (1998). Their model was conceptually similar to that of Heeger's (1987) original scheme although differing in implementation.

Simoncelli and Heeger's (1998) model comprises two stages that map onto cortical areas V1 and MT. The model V1 cells are characterised by linear receptive fields. A disadvantage of using such linear filters is that their responses can be negative whilst neural responses (spike rates) are positive. Simoncelli and Heeger deal with this by half wave rectifying and then squaring the weighted sum (over space and time) of the input contrast, thus ensuring that

the model's response is always positive. This response is then normalised by dividing the output by a value proportional to the summed activity of all neurones (regardless of orientation and spatio-temporal tuning) within the 'cortical neighbourhood'. This divisive stage serves to normalise the model neurone's response with respect to contrast and thus limits the dynamic range. These V1 model neurones do not unambiguously signal velocity but respond only to the velocity component of a pattern that is orthogonal to the preferred spatial orientation. In the second stage of the model, Simoncelli and Heeger (1998) describe how an unambiguous velocity code can be derived in model MT cells by combining the outputs of V1 model neurones whose differing space-time orientations are consistent with a specific velocity. The stages of computation in the model MT cells are essentially similar to those of the V1 neurones but, due to the combination of inputs across a range of spatio-temporal orientations, the resultant units provide a true velocity-tuned estimate that closely matches the characteristics of real MT cells. Thus this class of model can be demonstrated to possess widespread biological plausibility and a computationally efficient method for encoding image velocity. However, its reliance on the detection of Fourier energy does pose a serious challenge for it in relation to the processing of 'non-Fourier' or second-order motion, a class of stimuli that will be described below.

1.5.5 Motion energy, second order stimuli and feature tracking

Models that rely on the extraction of Fourier energy to encode velocity have shown impressive success in simulating a range of motion-related phenomena in a biologically plausible way. However, there is a range of stimuli that do not provide an unambiguous cue to such models but are yet clearly discernible to

the human observer. The possibility thus arises that there may be more than one mechanism that encodes velocity.

Braddick (1974) was among the first to propose two sub-systems of motion perception, naming them ‘short-range’ and ‘long-range’ processes. He proposed that the detection of short-range motion was sub-served by motion detectors that are sensitive to local spatio-temporal changes in luminance whereas long-range motion occurs after the shape of the relevant feature has been extracted. The short-range and long-range processes are defined by the characteristics of their spatio-temporal ranges (Anstis, 1980; Braddick, 1980). The short-range process operates over small spatial (≤ 15 arcmin) and temporal intervals (inter-stimulus intervals ≤ 100 msec) while the long-range process operates over many degrees and longer durations (inter-stimulus intervals up to 500 msec) (Braddick, 1974; Cavanagh & Mather, 1989). Many early studies provided evidence distinguishing between the two sub-systems. The short-range process produces motion after-effects (Anstis & Cavanagh, 1981; Banks & Kane, 1972), does not respond to equiluminant stimuli defined by colour (Ramachandran & Gregory, 1978) and is not driven dichoptically (Braddick, 1974). The long-range process appears to have the inverse properties of the short-range process, no or weak motion after-effects are produced (Anstis, 1980; Anstis & Moulden, 1970; Banks & Kane, 1972; Papert, 1964), apparent motion can be perceived with equiluminant stimuli defined by colour (Ramachandran & Gregory, 1978) and it can operate dichoptically (Shipley, Kenney, & King, 1945). The most important distinction between the two processes is the way in which they extract motion information from a retinal image. The short-range process is thought to correspond to low-level motion detectors which work in parallel across the

visual field while the long-range process is thought to correspond to higher-level visual processing which can identify forms and infer motion from the changes in spatial position of object features over time.

However, subsequent studies have suggested that the distinction between the two-subsystems may not be as clear as previously thought. Short-range motion can be perceived over long distances (Cavanagh, Boeglin, & Favreau, 1985; Chang & Julesz, 1983), for equiluminant stimuli defined by colour (Cavanagh et al., 1985; Sato, 1988) and can be driven dichoptically (Shadlen & Carney, 1986). Furthermore, the long-range process can produce motion after-effects (Von Grünau, 1986).

One possible resolution of these discrepancies was offered by Cavanagh and Mather (1989) who suggested that the different properties identified with the short-range and long-range processes are due to the differences in the stimuli used rather than an indication of the existence of two motion sub-systems. Instead, they proposed that all motion is sub-served by the same early motion detectors but is subsequently processed in different ways depending upon the stimulus characteristics. Early studies investigating the characteristics of apparent motion (e.g. Anstis, 1980; Anstis & Moulden, 1970; Banks & Kane, 1972) used short-range motion stimuli, such as ‘random-dot kinematograms’ (RDKs) (Julesz, 1971) and long-range motion stimuli consisting of large isolated objects. Random-dot kinematograms consist of random dot images presented in quick succession. The dots in one (e.g. the central) region of these images are spatially shifted by the same distance in each image, while the dots in the surrounding areas remain stationary. Thus the dots in the central region of the

images are perceived as a coherent object moving smoothly. Braddick (1974) identified 15 arcmin as the maximum spatial shift (D_{max}) at which discrete motion could be identified and thus the upper-limit of the short-range process. However, a number of subsequent studies have been able to obtain D_{max} values greater that 15 arcmin (e.g. Baker & Braddick, 1985; Chang & Julesz, 1983; Nakayama & Silverman, 1984). Chang and Julesz (1983) and Nakayama and Silverman (1984) manipulated the spatial frequency of the random-dot kinematograms and found that the largest D_{max} was obtained for random-dot kinematograms containing predominantly low spatial frequencies. Cavanagh et al. (1985) found that once the elements in a random-dot kinematogram were greater than 15 arcmin, D_{max} scaled linearly with element size. Thus long-range motion stimuli consisting of predominantly low spatial frequencies would allow motion to be seen for larger spatial displacements.

Physiological evidence suggests that directionally selective neurons with large receptive fields are stimulated by large stimuli or large spatial shifts of apparent motion stimuli than neurons with smaller receptive fields (e.g. Baker & Cynader, 1988). Thus, the spatial frequency content of apparent motion stimuli may account for the differences in maximum spatial shift. Cavanagh and Mather (1989) suggest that a more useful dichotomy than the short-range and long-range processes would be one based on stimulus attributes, distinguishing between first- and second-order stimuli.

Cavanagh and Mather (1989) describe first-order motion as the movement of luminance or colour defined patterns, whereas second-order motion is described as the movement of image characteristics not defined by luminance

or colour such as contrast modulation and texture. Fourier motion models, such as the motion energy model (Adelson & Bergen, 1985) (see Section 1.5.2) and those of Heeger (1987) and Simoncelli and Heeger (1998) reviewed above have been successful at modelling first-order motion detection. However, Chubb and Sperling (1988) showed mathematically that low-level motion detectors which operate by detecting motion energy are insensitive to second-order motion.

Three possible explanations of how second-order motion is detected have been proposed. First, Chubb and Sperling (1988) suggested that first- and second-order motion are initially processed in parallel by separate low-level mechanisms before conventional (Fourier) motion computation. In order for a second-order motion pathway to detect second-order motion the retinal image is first filtered linearly and then rectified or squared. Rectification is a mathematical process by which all negative signal values are made positive. There are two types of rectification possible, full wave rectification converts all negative values into positive values and retains them, and half wave rectification discards all negative values. This non-linear rectification stage renders the output signal visible to conventional motion-energy detectors. A second possibility is that first- and second-order motion are detected by a single common mechanism with non-linear properties (e.g. Benton & Johnston, 2001; Benton, Johnston, McOwan, & Victor, 2001; Johnston, McOwan, & Buxton, 1992). A third possibility is that second-order motion detection is mediated by a post-attentive feature-tracking mechanism, such as that proposed by Cavanagh (1992). The occurrence of motion may be inferred by tracking the same target feature (e.g. regions of high and low contrast) over successive positions and Ullman (1979)

proposed a model that makes such motion correspondence matches. In Ullman's (1979) minimal mapping theory a cost is associated with the perceived movement of any image element from one image (or frame of view) to the next. This cost is proportional to the distance between the positions of the element in the two frames of view. The smaller the distance is, the lower the cost of motion. This is because when motion in a three-dimensional scene is projected onto a two-dimensional surface (e.g. the retina), shorter movements are more probable than longer movements. Ullman's model computes the most probable motion correspondence between image elements using this logic.

To date the majority of empirical evidence suggests that first- and second-order motion are initially encoded by independent low level mechanisms (e.g. Baker, 1999; Lu & Sperling, 1995; Smith, 1994). For example, Ledgeway and Smith (1994) employed multi-frame motion sequences in which the frames altered between sinusoidal variations in luminance (first-order) and similar variations in contrast (second-order) to investigate whether unambiguous motion could be detected. The motion sequences were designed in such a way that unambiguous motion would be produced only if observers were integrating both types of frame (first- and second-order). If observers were analysing each type of frame independently then they would perceive ambiguous motion. Ledgeway and Smith (1994) found that observers were unable to integrate the frames of the multi-frame motion sequences, suggesting that first- and second-order motion are initially detected by distinct mechanisms, each of which is only sensitive to one type of motion. Ledgeway and Smith (1997) provide further psychophysical evidence for second-order motion detectors. They employed luminance-modulated (first-order) and contrast-modulated (second-order)

adaptation stimuli to investigate whether adaptation to second-order motion could cause changes in perceived speed. They found a similar pattern of results for both types of motion. When adaptation speed was faster than the test speed, adaptation resulted a reduction in perceived speed. When adaptation speed was slower than the test speed, there was an increase in perceived speed. These results suggest that first- and second-order motion are encoded by similar computational procedures, but not necessarily the same mechanisms in the visual system. While Ledgeway and Smith (1997) found some crossover adaptation (influence of adaptation to one type of motion transferring to the other type of motion) other studies have found that crossover adaptation does not generally occur, supporting the idea of distinct first- and second-order motion processing mechanisms (Ledgeway & Smith, 1994; Nishida, Ledgeway, & Edwards, 1997; Pavan, Campana, Guerreschi, Manassi, & Casco, 2009).

Seiffert and Cavanagh (1998) presented observers with a luminance-modulated (first-order) and contrast-modulated (second-order) gratings oscillating sinusoidally to investigate whether observers were relying on a velocity-sensitive motion energy mechanism or a position-sensitive feature tracking mechanism to detect motion. If observers were relying on a feature tracking mechanism to detect motion, then only the amount of spatial change would determine near-threshold motion. Alternatively, if motion was detected by a motion energy mechanism both amplitude and frequency oscillation would determine thresholds. Seiffert and Cavanagh (1998) found that observers were relying on motion energy mechanisms to detect the motion of luminance-modulated gratings, but relied on a feature tracking mechanism to detect the motion of second-order gratings, further supporting the idea that first- and second-order motion may be processed by distinct mechanisms.

Additional evidence consistent with discrete mechanisms is found in neurophysiological studies. A number of studies has described patients with cortical lesions who have selective impairment of first- and second-order motion discrimination, suggesting that the two regions may be regionally separate at an early stage of cortical processing (Plant, Laxer, Barbaro, Schiffman, & Nakayama, 1993; Plant & Nakayama, 1993; Vaina, Cowey, & Kennedy, 1999; Vaina, Makris, Kennedy, & Cowey, 1996, 1998; Vaina & Soloviev, 2004). Moreover, O'Keefe and Movshon (1998) measured individual neurons in monkey area MT and found selectivity for the direction of first-order motion but not for the direction of second-order motion. However, fMRI has shown that some neurons in human area MT are activated by second-order motion (Smith, Greenlee, Singh, Kraemer, & Hennig, 1998). Thus, neurophysiological evidence suggests that functionally distinct first- and second-order mechanisms may exist but their precise anatomical characterisation is not entirely clear.

To date evidence suggests that early stage second-order motion detectors work with feature-tracking mechanisms. Smith (1994) employed an ambiguous motion stimulus and demonstrated that both a mechanism that involves non-linear rectification followed by motion energy detection and a feature-tracking mechanism can detect second-order motion under certain conditions. He found that observers normally reported the direction associated with a rectification followed by motion energy mechanism scheme. However, when an inter-stimulus interval was introduced between the updates in stimulus position observers reported the direction associated with feature motion. Further evidence for the stimulus-dependent nature of motion detection was reported by

Lu and Sperling (1995) who used a pedestal-plus-test display, in which a drifting and a stationary grating are superimposed in order to investigate whether motion detection is affected when features are masked by a stationary pattern. They found evidence for both first- and second- order motion mechanisms and a third feature-tracking mechanism. However, in essence their scheme can be reduced to two mechanisms since their second-order mechanism is simply applies motion energy processing upon a rectified signal. Both Smith, (1994) and Lu and Sperling (1995) found that feature-tracking mechanisms are slower (tuned for lower temporal frequencies) than motion-energy mechanisms. Other studies using the pedestal paradigm have shown that at low contrast second order motion is dependent upon feature-tracking mechanisms (Derrington & Ukkonen, 1999; Seiffert & Cavanagh, 1998). Seiffert and Cavanagh (1998, 1999) showed that at low contrast and low speeds second-order motion detection is based upon a feature-tracking mechanism, while at high contrast and high speeds second-order motion detection is based upon a motion-energy system.

Attention has also been shown to affect the detection of second-order motion. When observers were required to attend to one of two spatially-adjacent patterns containing either first-order (luminance-defined) or second-order (contrast-defined) motion they were better able to discriminate the direction of second-order motion in the attended pattern, as opposed to the unattended pattern. When the two patterns contained first-order motion there was no difference in the observers' performance with the attended and unattended patterns (Lu, Liu, & Dosher, 2000). However, Allen and Derrington (2001) employed a distractor task to distract attention and found that there is little

difference due to the effect of attention in detecting motion of fist- and second-order stimuli with or without a distractor. Allen and Ledgeway (2003) replicated the results of Lu et al. (2000) with attended and unattended patterns but found that the enhancement in direction discrimination of second-order motion patterns due to attention was dependant upon the speed and duration of the stimuli. These results suggest that while attention-driven feature-tracking mechanisms may contribute to the detection of second-order motion, the level of influence that these mechanisms have is, again, dependent upon stimulus parameters.

Thus a picture has emerged which is broadly consistent with the notion that two mechanisms sub-serve motion processing – one that extracts motion signals using low-level local changes in luminance (with or without a non-linear stage to aid detection of second-order) and a feature tracking mechanism that effectively infers motion after the relevant segment of the image has been extracted. A range of models have proposed various algorithms for how these two processes are implemented. Whilst these models vary in detail, it is now apparent that it is the precise stimulus configuration that is critical to which process is activated.

1.5.6 Gradient models

While there is physiological evidence consistent with motion energy models alternative models that use gradient detectors have also been proposed to model motion perception (e.g. Fennema & Thompson, 1979; Heeger & Simoncelli, 1993; Horn & Schunck, 1981; Johnston, McOwan, & Buxton, 1992; Marr & Ullman, 1981). Gradient models compute velocity by dividing the temporal derivative of local luminance by its spatial derivative.

Spatio-temporal gradient models, unlike Reichardt models, produce a signal that is proportional to the local velocity at each point in the image, independent of pattern properties. Notably, as long as the velocity is constant no modulations are expected in the local signals and the global velocity signal does not change with the spatial wavelength of the pattern. However, velocity estimation using the gradient model varies widely. Under conditions in which the spatial gradient of intensity is reduced the unreliability of velocity estimation is increased. Where the spatial gradient of intensity equals 0, for example, a uniform space of equal luminance, no motion information can be computed. As such, the gradient model provides the best estimates of velocity at edges, where there is a peak in spatial gradient (Marr & Ullman, 1981).

For the visual system to encode velocity in such a way as described by gradient models, at least two kinds of visual mechanisms are required that respond to local spatial and temporal differences in image intensity. There is some psychophysical support for the existence of such mechanisms. Anstis (1967) reported an effect in which the visual system adapts to the direction of change of illumination - the “ramp after-effect” (Arnold & Anstis, 1993). Anstis (1967) found that after adapting to a spatially uniform field of light that gradually brightened, a subsequently viewed uniform test field of constant luminance appeared to dim over time. Conversely, adaptation to a gradually dimming pattern yielded a percept of a gradual brightening in a constant test stimulus (Anstis, 1967; Anstis & Harris, 1987; Arnold & Anstis, 1993; Cavanagh & Anstis, 1986). This after-effect suggests that there are visual mechanisms tuned to the direction of temporal luminance gradients. Moreover, following adaptation to a

luminance ramp, a static test field that contained a spatial luminance gradient appeared to move (Anstis, 1967). This perceived motion is consistent with a gradient model of motion perception, in which motion is a ratio of temporal and spatial gradient signals. The apparent temporal gradient due to luminance ramp adaptation is combined with the physical spatial gradient in the test field to signal motion.

1.6 Speed perception

The models discussed thus far deal well with predicting direction of motion but fail to provide a clear account of speed encoding. Gradient models fare badly where the spatial gradient of intensity is reduced and motion energy models are confounded by contrast. To date, there is little agreement as to how the human visual system encodes speed (see e.g. Hammett et al., 2005; Hammett, Champion, Thompson, & Morland, 2007). Previous psychophysical studies have shown that the human perception of speed can be influenced by many factors (e.g. Brown, 1931) including contrast, luminance and temporal frequency (e.g. Hammett et al., 2007). Much of the work that addresses the problem of how we perceive speed has looked to biases in our perception to inform both formal and informal models of speed encoding.

1.6.1 Effect of contrast upon perceived speed

One such perceptual bias first reported by Thompson (1982) is the effect of contrast upon perceived speed. Subjects were tasked with matching gratings of varying contrast to a standard grating of fixed contrast for speed at a range of temporal frequencies (1 - 16 Hz). Thompson's (1982) results showed that at slow (< 8 Hz) speeds, low contrast decreased perceived speed but at faster

speeds (> 8 Hz) low contrast increased perceived speed. Stone and Thompson (1992) re-examined the effect of contrast on the perceived speed of moving gratings over a wider range of contrasts and spatial frequencies. Their results and others' (e.g. Thompson, Brooks, & Hammett, 2006; Thompson, Stone, & Swash, 1996; Thompson & Stone, 1997) confirmed Thompson's (1982) original findings. For convenience and following others (e.g. Brooks, 2001; Snowden, Stimpson, & Ruddle, 1998) I will refer to these biases in perceived speed as the Thompson Effect. Thompson (1982) suggested that speed is encoded as the ratio of two channels, one 'slow' and one 'fast'. The 'slow' speed channel of this ratio model is assumed to be more sensitive to slow (< 8 Hz) speeds than the 'fast' speed channel and at slow (< 8 Hz) speeds the 'slow' channel is also assumed to have higher sensitivity than the 'fast' channel (Thompson, 1982) (Figure 1.15). Thus, a reduction in the contrast of a slow moving stimulus would result in the 'slow' speed channel becoming relatively more sensitive to the stimulus than the fast speed channel producing a reduction in perceived speed. Similarly, a reduction in the contrast of a fast moving stimulus would result in the 'fast' speed channel becoming relatively more sensitive to the stimulus than the slow speed channel producing an increase in perceived speed.

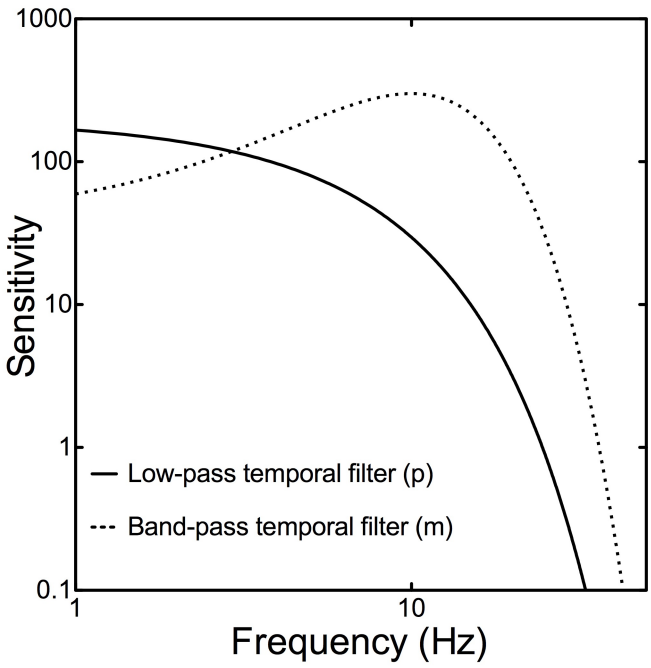

Figure 1.15: The temporal frequency sensitivity profiles of low-pass (or 'slow' channel) and band-pass (or 'fast' channel) temporal filters (after Smith and Edgar (1994)).

1.6.2 Effect of adaptation upon perceived speed

The findings of adaptation experiments reported by Thompson (1981) are also consistent with a ratio model of speed encoding. For example, following adaptation to a moving stimulus the perceived speed of a subsequently viewed test stimulus and all slower speeds moving in the same direction appeared reduced. However, when adaptation speed was slow and test speed was fast perceived speed increased. Adaptation of the 'fast' speed channel with fast adaptation speeds would result in the 'slow' speed channel becoming relatively more sensitive thus biasing the output of the ratio to lower values. Similarly, adaptation of the 'slow' speed channel with slow adaptation speeds would result in the 'fast' speed channel becoming relatively more sensitive and biasing the ratio to higher values. Later, Hammett et al. (2005) also found that adaptation can result in both increases and decreases in perceived speed under certain conditions and outlined a formal ratio model to explain this effect.

1.6.3 Ratio models and physiology

The ratio model proposed by Thompson (1981, 1982, 1983) and others (e.g. Adelson & Bergen, 1986; Fredericksen & Hess, 1998; Hammett, Thompson, & Bedingham, 2000; Harris, 1980; Perrone & Thiele, 2002; Smith & Edgar, 1994) computes speed as the ratio of a low-pass (or 'slow' channel) and a band-pass (or 'fast' channel) temporal filter. Hammett et al. (2005) proposed a formal model that employed Perrone's (2005) temporal filters. The bases of these temporal filters are two types of V1 complex neurons: transient and sustained, which have band-pass and low-pass temporal frequency tuning respectively. As previously mentioned (see Section 1.4.1) physiological studies have shown that the M and P cells in the primate LGN have transient and sustained responses respectively (e.g. Livingstone & Hubel, 1987, 1988; Maunsell, 1987; Maunsell & Schiller, 1984; Schiller & Malpeli, 1978) and behavioural evidence shows that the contrast sensitivity of M and P cells appear complementary, P cells are more sensitive to low temporal frequencies while M cells are more sensitive to high temporal frequencies (Merigan, Byrne, et al., 1991; Merigan & Eskin, 1986; Merigan, Katz, et al., 1991). While the physiological substrates of the low-pass and band-pass filters described in the ratio model are unknown previous workers have highlighted the similarity between these filters and the M and P pathways (e.g. Hammett et al., 2005; Thompson et al., 2006).

1.6.4 Effect of luminance upon perceived speed

The ratio model has also been invoked to explain the perceptual bias of luminance upon speed perception (Hammett et al., 2007). A reduction in the luminance of fast moving (> 4 Hz) stimuli increased the perceived speed of those stimuli (Hammett et al., 2007; Vaziri-Pashkam & Cavanagh, 2008).

Similar to the explanation of how contrast may bias speed perception, Hammett et al. (2007) assume that at low luminance the sensitivity of the 'slow' speed filter is reduced relative to the sensitively of the 'high' speed filter, thus perceived speed is increased. This assumption has some physiological support, as Purpura, Kaplan, and Shapley (1988) reported that at low luminance levels the response of P cells is reduced proportionately more than that of M cells.

1.6.5 Bayesian models

Recently, Bayesian operators have been used to model perceptual biases such as the Thompson Effect (e.g. Ascher & Grzywacz, 2000; Hürlimann, Kiper, & Carandini, 2002; Stocker & Simoncelli, 2006; Weiss & Adelson, 1998; Weiss, Simoncelli, & Adelson, 2002). In general, Bayesian models assume that speed is encoded as the output of the combination of a likelihood estimate and a 'slow' prior function. The likelihood function represents the noisy sensory signal. The prior function represents the probability of encountering a particular speed. Proponents of the Bayesian model make the assumption that most speeds we encounter are slow, thus a 'slow' speed prior is used, although this is not readily supported by data – as Weiss et al. (2002) point out "*we have no direct evidence (either from first principles or from empirical measurements) that this assumption is correct.*" (p. 599).

The Bayesian model relies on the logic that as the sensory signal becomes less precise (i.e. as the Signal-to-Noise Ratio decreases) the greater the influence of the 'slow' speed prior becomes. For example, as the contrast of a target stimulus is reduced its' speed signal becomes increasingly difficult to estimate

and the influence of the ‘slow’ speed prior increases resulting in a reduction of perceived target stimulus speed.

However, while the Bayesian model is able to account for the reduction of perceived speed at low contrast it is unable to predict the increase in perceived speed as contrast is reduced at temporal frequencies above 8 Hz, since a reduction in contrast always increases the influence of the ‘slow’ speed prior (Weiss et al., 2002).

However, it is not only Bayesian models that struggle to account for empirical findings. Krekelberg, van Wezel, and Albright (2006) have shown that no current models of perceived speed can adequately account for the response properties of speed-tuned cells in the monkey cortex. The Bayesian model is successful in explaining reductions in perceived speed (e.g. for low contrast slow moving stimuli and for peripherally moving stimuli) but is not as successful at dealing with increases in perceived speed. There is currently no full model of speed encoding in humans and insufficient data to adequately characterise the effects of contrast, luminance or eccentricity upon perceived speed. There is therefore a clear need for further studies of how image attributes modulate perceived speed.

1.7 Chapter summaries

A series of experiments was conducted in order to inform models of speed encoding and provide insight into the mechanisms underlying spatio-temporal processing in the visual system.

Chapter 2 documents some preliminary methodological issues. In Chapter 3 the work of Anstis (1967) and Arnold and Anstis (1993) was extended to investigate which parameter/s of the visual scene determine/d the ramp after-effect – often considered key evidence for gradient models of motion detection. Chapter 4 described an experiment that measured the biases in speed perception attributable to contrast. Chapter 5 documents an investigation of whether perceived slowing of stimuli in the periphery may be accounted for in terms of a perceived reduction in contrast. In Chapter 6 the effects of contrast and luminance on speed perception are reported. Chapter 7 comprises a discussion of these results and consideration of potential future research.

Chapter 2

2 Some Methodological Considerations

2.1 Acquiring data

Psychophysical studies have commonly used binary decision tasks in order to investigate the point at which a difference between a perceived property of two stimuli is matched. For example, in contrast matching, the subject is presented with both stimuli and indicates which stimulus pattern has greater contrast. On each trial (or set of trials) the independent variable, for example, contrast of one of the stimuli (test stimulus) is changed, while the contrast of the other (standard stimulus) is kept constant. After several trials the point of subjective equality (PSE) is reached, the point at which the subject perceives the stimulus level as equal across stimuli.

There are two common ways in which the contrast of the test stimulus may be determined. Classical research used fixed procedures where all the values of the test stimulus levels are predetermined for a sequence of trials. Adaptive procedures sequentially change the test stimulus level from trial to trial based on previous trial responses. Adaptive procedures are theoretically more efficient than fixed procedures because measurements converge toward the PSE. Since the emergence of adaptive procedures in the 1940s (Anderson, McCarthy, & Tukey, 1946; Dixon & Mood, 1948; von Békésy, 1947) they have become widely used in psychophysics (Cornsweet, 1962; Levitt, 1971; Taylor & Creelman, 1967).

2.2 Adaptive procedures

Adaptive procedures differ in the systems they use to efficiently place stimulus levels in a sequence of trials (or adaptive track) and to provide the final estimate

of threshold. Simple staircase procedures use the previous one or more trial responses to select the next stimulus level. A one up – one down staircase decreases the stimulus level when the subject's response is 'correct' on the previous trial and increases the stimulus level when the subject's response is 'incorrect'. A change in the direction of the stimulus level along the adaptive track is called a reversal point. In general, the threshold estimate is derived by averaging the values at the reversal points along an adaptive track. A one up – one down staircase tends towards the 50% performance level on a psychometric function, the adaptive track targets the stimulus level for which the probability of a 'correct' or 'incorrect' response is 50%.

A psychometric function describes the relationship between a stimulus level and a subject's response, generally represented as the probability of 'success' over a number of trials at that stimulus level. 'Success' in this case is dependent upon the subject's task and predefined rules (e.g. in Experiment 3a the subject's task was to indicate which pattern (standard or test) appeared to have greater contrast).

The Parameter Estimation by Sequential Testing (PEST) algorithm developed by Taylor and Creelman (1967) provided more efficiency in estimating threshold by changing step size (the change in independent variable level when a directional change is made) as the adaptive track progressed. The PEST routine requires some initial parameters such as a starting stimulus level, step size, target performance level (e.g. 50% correct detections) and stopping criterion (final step size). Several trials are presented at a stimulus level and statistical analysis is used to specify whether the subject's performance at that

level is better or worse than the targeted performance level. Based on the outcome of the statistical analysis a new stimulus level and step size may be defined and a series of trials presented again followed by statistical analysis. The PEST routine terminates at the criterion step size and typically the stimulus level on the final trial is taken as the final threshold estimate.

Taylor and Creelman (1967) coined the term ‘sweat factor’ in order to evaluate the efficiency of psychophysical measurements. The sweat factor is the product of the number of trials and the variance of independent variable measures across all trials in a sequence. To generate the ideal sweat factor Taylor and Creelman (1967) simulated an experimenter with complete understating of the probabilities at each stimulus level, who always selects the stimulus level that will produce a performance level equal to the target performance level. They also simulated the PEST routine under various conditions to determine its sweat factor and conclude that the PEST procedure is 40%-50% efficient.

In order to make the PEST routine more efficient in estimating threshold others have proposed a hybrid PEST routine that used PEST rules and a ‘maximum-likelihood’ method to vary the stimulus level (e.g. Hall, 1981, 1983; Pentland, 1980). After each trial the responses from all preceding trials are used to make a maximum-likelihood estimate of the parameters of a psychometric function, from which the next stimulus level and final threshold value are obtained.

Similar to the hybrid PEST routine, the QUEST routine (Watson & Pelli, 1983) also uses all of the response information from previous trials to set the next stimulus level, with the addition of prior knowledge (e.g. previous research and

literature). Crucially, Watson and Pelli (1983) make a distinction between the use of prior knowledge to set stimulus levels during a sequence of trials and deriving the final threshold estimate, which only uses the response information from a sequence of trials. While the original PEST routine was 40%-50% efficient, Watson and Pelli (1983) reported that a QUEST routine was 84% efficient.

The use of prior assumptions in the QUEST routine may appear to introduce inherent biases in an experiment. However, Leek (2001) reviewed several adaptive procedures and concluded that most biases could be compensated by a careful consideration of experimental parameters and techniques. As such, where adaptive procedures have been used herein, a QUEST routine was employed to set stimulus levels on each trial. However, the termination for the QUEST routine at a criterion step size would result in unequal numbers of trials (*n*) across trial sequences. The changing of *n* may change the variance of the psychometric function underlying subject performance, the time taken to complete a sequence of trials, and confound the final threshold estimate with adaptation and fatigue effects. Thus estimates of PSE were not derived from parameters of the last *n* steps, or only the last trial. Rather, to ensure every estimate was derived from the same *n* observations QUEST was terminated after 50 trials. The data were subsequently fit to a cumulative Gaussian function and the 50% point of the function was taken as PSE.

2.3 Fitting the Psychometric Function

In order to estimate PSE a psychometric function must be fit to the data. This is generally done by assuming that the underlying function can be described by a

particular psychometric model (e.g. a cumulative Gaussian, Weibull, reverse Weibull or Logistic ogive). However, psychometric functions are monotonic (i.e. the function's first derivative does not change sign). It follows that as the signal strength of a stimulus increases a subject's task performance also increases. However, psychophysical data (including some herein) are frequently non-monotonic (Figure 2.1). Most of the data reported herein were analysed by fitting a cumulative Gaussian to the data and determining the 50% point which was taken as an estimate of PSE. In order to ensure that these estimates of PSE were not biased by breaches of the assumption of monotonicity I compared these estimates with those derived by a recently described assumption-free fit (Żychaluk & Foster, 2009) (Figure 2.1 and Figure 2.2). The assumption-free model makes no assumptions about the underlying psychometric function of a data set. Rather, the assumption-free model uses local linear fitting to estimate the function locally point-by-point.

A comparison was made between the PSE estimates derived from fitting a cumulative Gaussian function with the PSE estimates derived from an assumption-free fit to the data of Experiment 3a. Experiment 3a investigated the perceptual bias of contrast perception attributed to speed. Two patterns were presented simultaneously for 500 msec on each trial. Standard patterns constantly drifted at 1 deg/sec throughout, test patterns drifted at one of four speeds (1, 2, 4, or 8 deg/sec). The Michelson contrast of the standard pattern was constant throughout at 0.1. Five blocks were run at each speed. The subject's task was to indicate which pattern appeared to have the greater contrast (see Chapter 4 for full details of Experiment 3a). The Michelson contrast of the test pattern was altered by a QUEST routine (Watson & Pelli,

1983) depending on the subject's responses. For each block the QUEST procedure was terminated after 50 trials, for the purpose of this chapter the data were fit to both a cumulative Gaussian function using the method of least squares fit and to an assumption-free function, and the 50% point of each function was taken as the PSE.

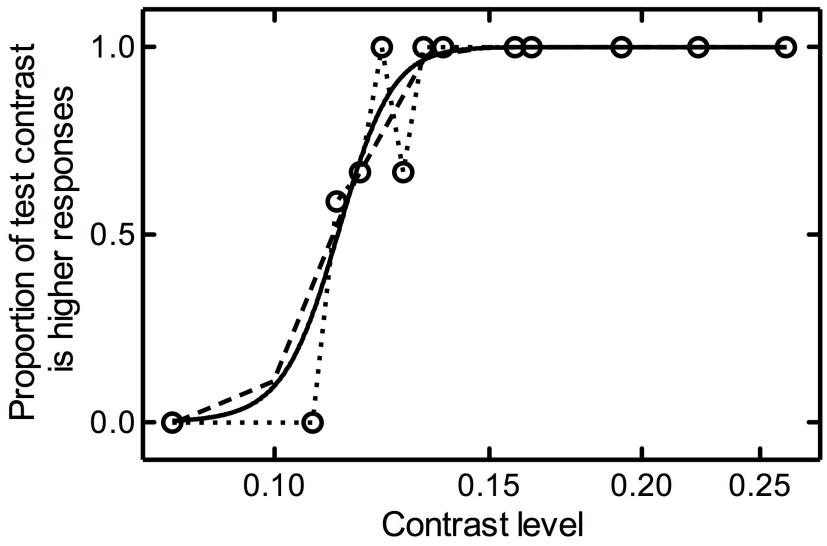

Figure 2.1: The data yielded by one QUEST procedure for one subject from Experiment 3a (open circles / dotted line) fit to a cumulative Gaussian function (broken line) and assumption-free (solid line).

Figure 2.1 plots typical non-monotonic data from Experiment 3a fit to both a cumulative Gaussian function and an assumption-free function. A subject's responses for each QUEST procedure (or sequence of 50 trials) were binned by contrast level and fit to a cumulative Gaussian function using the method of least squares fit. The assumption-free model provides a very similar estimate of PSE. All subject data sets from Experiment 3a were fit to both cumulative Gaussian functions and assumption-free models in order to investigate whether breaches of the assumption of monotonicity for a cumulative Gaussian function biased the estimate of PSE (Figure 2.2).

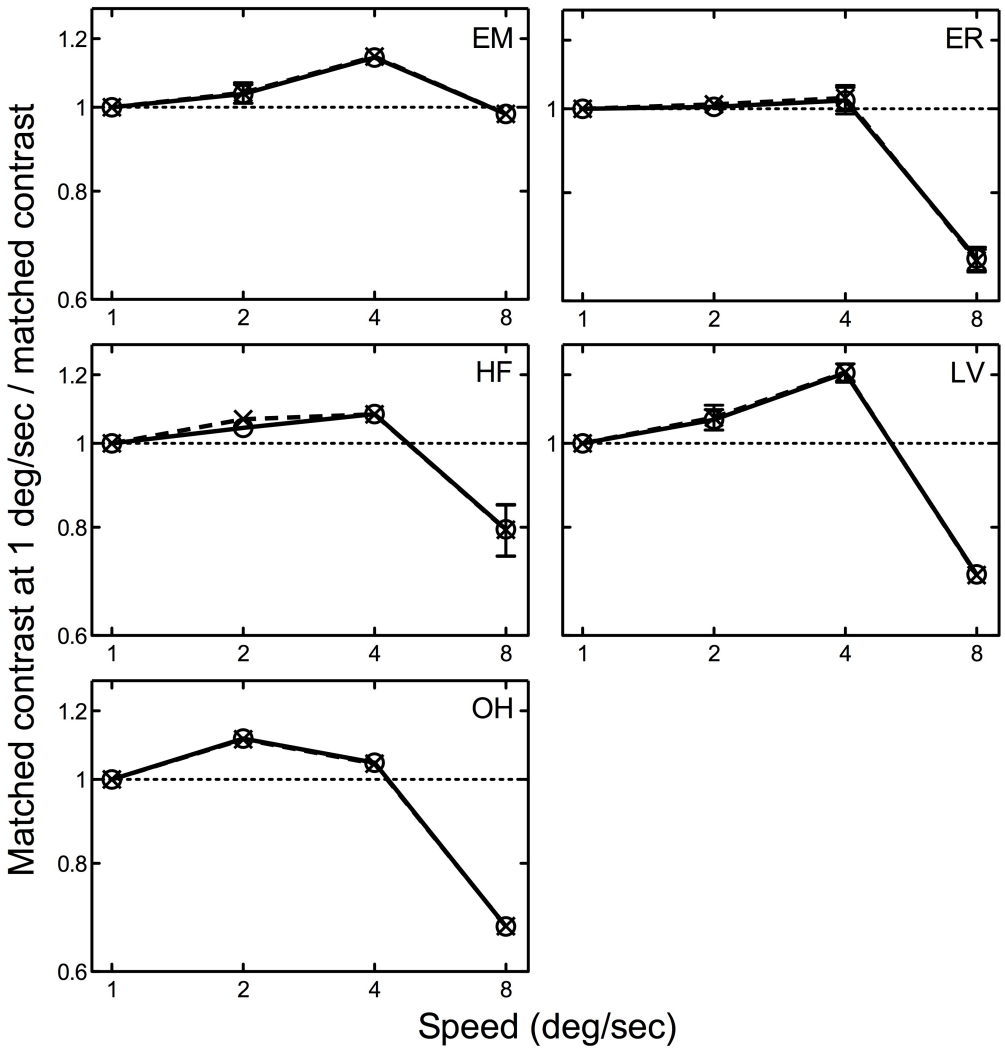

Figure 2.2: The ratio of matched contrast at 1 deg/sec to matched contrasts at higher speeds is plotted as a function of grating speed (deg/sec) for all subjects from Experiment 3a. The mean of five PSE estimates derived from a cumulative Gaussian function (circles) and mean of five PSE estimates derived from an assumption-free fit (crosses) are plotted. Error bars represent ±1 SEM.

For all subjects in Experiment 3a, two-way ANOVAs revealed no significant main effect of fitting method, a significant main effect of speed, and no significant interaction between fitting method and speed (Table 2.1).

Table 2.1: Two-way analysis of variance (ANOVA) for fitting method and speed on matched contrast for each subject in Experiment 3a. * The effect is significant at the .001 level.

Subject					
EM	Source	*df*	Mean square	*F*	*p*
	Fitting method	1	0.000	0.00	0.945
	Speed	3	2.724	16.03	0.000*
	Interaction Fitting method X Speed	3	0.000	0.00	0.999
	Error	32	0.169		
ER	Source	*df*	Mean square	*F*	*p*
	Fitting method	1	0.000	0.00	0.960
	Speed	3	37.822	144.25	0.000*
	Interaction Fitting method X Speed	3	0.008	0.03	0.992
	Error	32	0.262		
HF	Source	*df*	Mean square	*F*	*p*
	Fitting method	1	0.036	0.05	0.826
	Speed	3	20.454	27.38	0.000*
	Interaction Fitting method X Speed	3	0.024	0.03	0.991
	Error	32	0.747		
LV	Source	*df*	Mean square	*F*	*p*
	Fitting method	1	0.007	0.03	0.873
	Speed	3	76.925	270.45	0.000*
	Interaction Fitting method X Speed	3	0.002	0.01	0.999
	Error	32	0.284		
OH	Source	*df*	Mean square	*F*	*p*
	Fitting method	1	0.000	0.00	0.953
	Speed	3	64.656	391.81	0.000*
	Interaction Fitting method X Speed	3	0.000	0.00	0.999
	Error	32	0.165		

In order to estimate PSE the experiments reported herein have therefore employed a standard least-squares fit of a cumulative Gaussian to the data. This choice was motivated by (a) the good agreement with the assumption-free method and (b) computational efficiency.

Whilst traditionally psychophysical studies assume that low level processing is essentially the same across human subjects it has recently become popular to include analysis of variance in results. Whilst I adhere to the assumption that low-level processing is similar across subjects, ANOVAs are reported here to evaluate differences between conditions rather than subjects.

Chapter 3

3 Ramp after-effects: the effect of luminance and ramp profile

3.1 Introduction

It is well known that the visual system adjusts its sensitivity to the prevailing level of illumination. Adaptation does not occur instantly, moving from a dark environment to a light one or vice versa requires a short period of time before the visual system adjusts to seeing at the new level of illumination. These processes are known as light and dark adaptation respectively. However, Anstis (1967) reported a new effect in which the visual system adapts not to the intensity of illumination, but to the direction of change of illumination.

Anstis (1967) measured the effect of adapting to stimuli whose luminance increased or decreased over time as a sawtooth function (Figure 3.1). He found that after adapting to a spatially uniform field of light that gradually brightened, a subsequently viewed uniform test field of constant luminance appeared to dim over time. Conversely, adaptation to a gradually dimming pattern yielded a percept of a gradual brightening in a constant test stimulus. This phenomenon is termed the ramp after-effect. Anstis (1967) reported that the temporal frequency and amplitude of luminance modulation were not critical to the effect but that a temporal frequency of 1 Hz and amplitude of 40 dB was near optimum for eliciting the longest duration of the perceived motion. This was the only combination of frequency and amplitude reported by Anstis (1967).

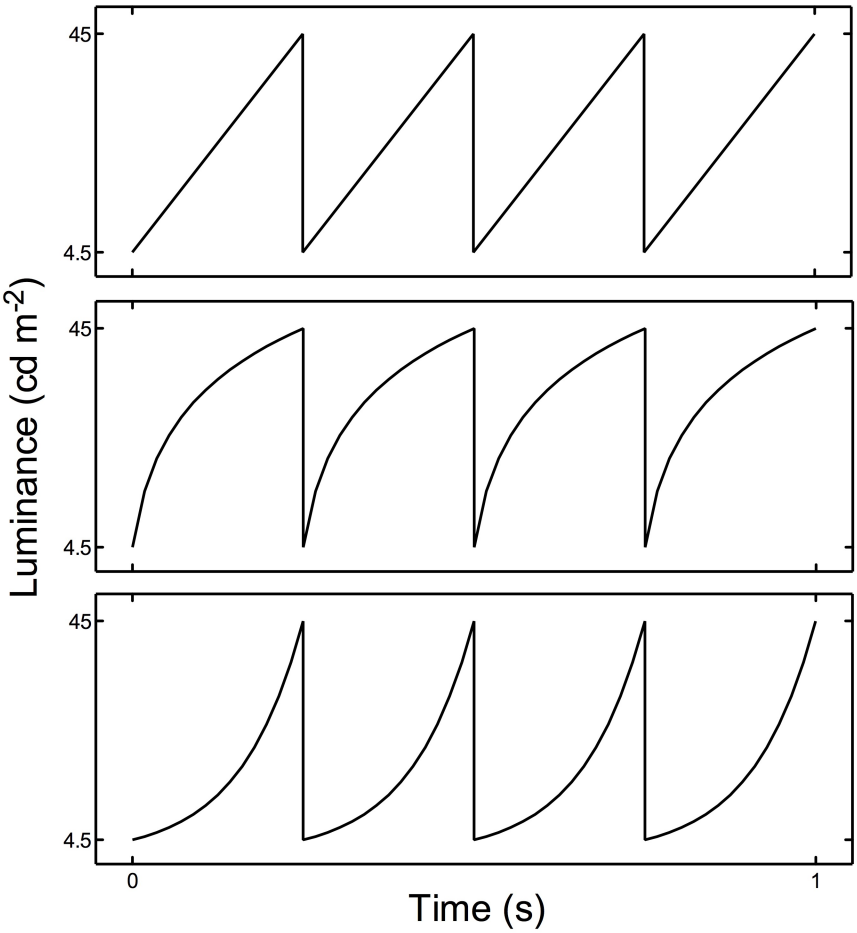

Figure 3.1: Linear (upper panel), logarithmic (middle panel) and exponential (lower panel) luminance ramps. The linear and logarithmic luminance ramps as used in Anstis (1967) and Arnold and Anstis (1993), respectively.

Anstis (1967) also reported that, following adaptation to a luminance ramp, a static test field that contained a spatial luminance gradient appeared to move. Viewing a spatially uniform adapting field, whose luminance was modulated by an ascending sawtooth ramp, followed by a test field consisting of a spatial luminance gradient darkest on the left, rightward motion is perceived along with apparent dimming. Subsequently viewing a test field consisting of a spatial luminance gradient darkest on the right, there is apparent dimming and leftward motion. However, without a spatial luminance gradient present in the test field, no motion is perceived, only dimming. Anstis (1967) concluded that this motion after-effect was an artefact due to the presence of a post-adaptation spatial

luminance gradient. The ascending luminance ramp is adapting the visual system to a continually brightening scene. As such, the parts of the visual system that code for increasing luminance may be reducing their baseline activity, tilting the balance in favour of descending luminance signals. Thus, a post-adaptation spatially uniform test field appears to be dimming. With a spatial luminance gradient present post-adaptation, the dimming after-effect causes the perceived luminance across the spatial luminance gradient to decrease. This decrease in perceived luminance creates the illusion of the darker shades of the spatial luminance gradient encroaching upon the lighter shades.

The ramp after-effect does not transfer interocularly (Anstis & Harris, 1987; Anstis, 1967) which implies a sub-cortical locus of the underlying mechanism as it is commonly believed that there are few cells that receive monocular input in any visual cortical areas other than V1 (Hubel & Wiesel, 1972; Hubel, Wiesel, & Stryker, 1977; Lund & Boothe, 1975).

Arnold and Anstis (1993) further investigated the ramp after-effect using a nulling method rather than using Anstis's (1967) measure of the duration of the perceived motion. Adapting stimuli comprised a spatially uniform field whose luminance was modulated by a sawtooth waveform presented for 5 sec, followed by a spatially uniform test field of 1 sec. Subjects indicated whether the test field appeared to be brightening or dimming. After adaptation, luminance ramps of the same polarity to the adapting pattern were presented for 1 sec. The amplitude of these nulling ramps was varied until test fields appeared to be neither dimming nor brightening. The slope of this nulling ramp was used to indicate the strength of the ramp after-effect. Using this method they found that

the after-effect was proportional to the amplitude of the adapting waveform and not its gradient. Since the gradient of a logarithmic luminance ramp (Figure 3.1) as used by Arnold and Anstis (1993) is constantly changing it is possible that a number of gradient detectors are being adapted. Thus no one gradient detector is being adapted for a prolonged period of time. A consequence of this may be that amplitude would appear to drive the after-effect rather than gradient. Moreover, Anstis (1967) employed a linear adapting luminance ramp for which gradient was constant. However, only one adapting gradient was reported. In order to fully evaluate the role of gradient in determining the ramp after-effect I therefore measured its duration for a range of amplitudes and gradients (Experiment 1) and for linear, logarithmic and exponential ramps (Experiment 2).

3.2 Experiment 1: The effect of adaptation frequency, amplitude and luminance upon the ramp after-effect

An understanding of which parameters of the adapting stimulus determine the ramp after-effect may provide important clues to the underlying physiological substrate of the phenomenon which, in turn, may yield insight into a fundamental aspect of the visual system's ability to adapt to prevailing dynamic conditions. For instance, Anstis (1967) speculates that the effect may be mediated by 'ON' and 'OFF' retinal cells. Arnold and Anstis (1993) suggest that ascending luminance ramps selectively adapt the ON-channels, whereas, descending ramps selectively adapt the OFF-channels. This proposition is simply tested by comparing the duration of the perceived motion to ascending and descending luminance ramps at high and low luminance since OFF cell responses are known to be reduced at low luminance (Dolan & Schiller, 1989,

1994; Ramoa, Freeman, & Macy, 1985). I therefore measured the duration of the after-effect at both high and low luminance.

3.3 Methods

3.3.1 Subjects

Five (two male and three female) subjects aged between 20 and 27 participated in this experiment. One of the subjects (OH) was an author; the other four were naïve to the purpose of the experiment. All subjects had normal or corrected-to-normal acuity.

3.3.2 Apparatus and stimuli

Stimuli were generated using the Psychophysics Toolbox extensions (Brainard, 1997; Kleiner, Brainard, & Pelli, 2007; Pelli, 1997) for MATLAB 7.11 (MathWorks, Cambridge, UK) and displayed on an EIZO 6600-M (Hakusan, Ishikawa, Japan) monochrome monitor at a frame rate of 60 Hz. The monitor was gamma corrected using the CRS Optical photometric system (Cambridge Research Systems, Rochester, UK). The display subtended $47^{o} \times 34^{o}$ at a viewing distance of 40 cm. Mean luminance was 24.75 cd m^{-2} for the high luminance conditions and 2.475 cd m^{-2} in the low luminance conditions. In the low luminance conditions 1 log unit neutral density filters (NDF) (Thorlabs Inc., Newton, New Jersey, USA) were inserted into drop-cell trial frames (Skeoch, Sussex, UK) that were worn by subjects in all conditions.

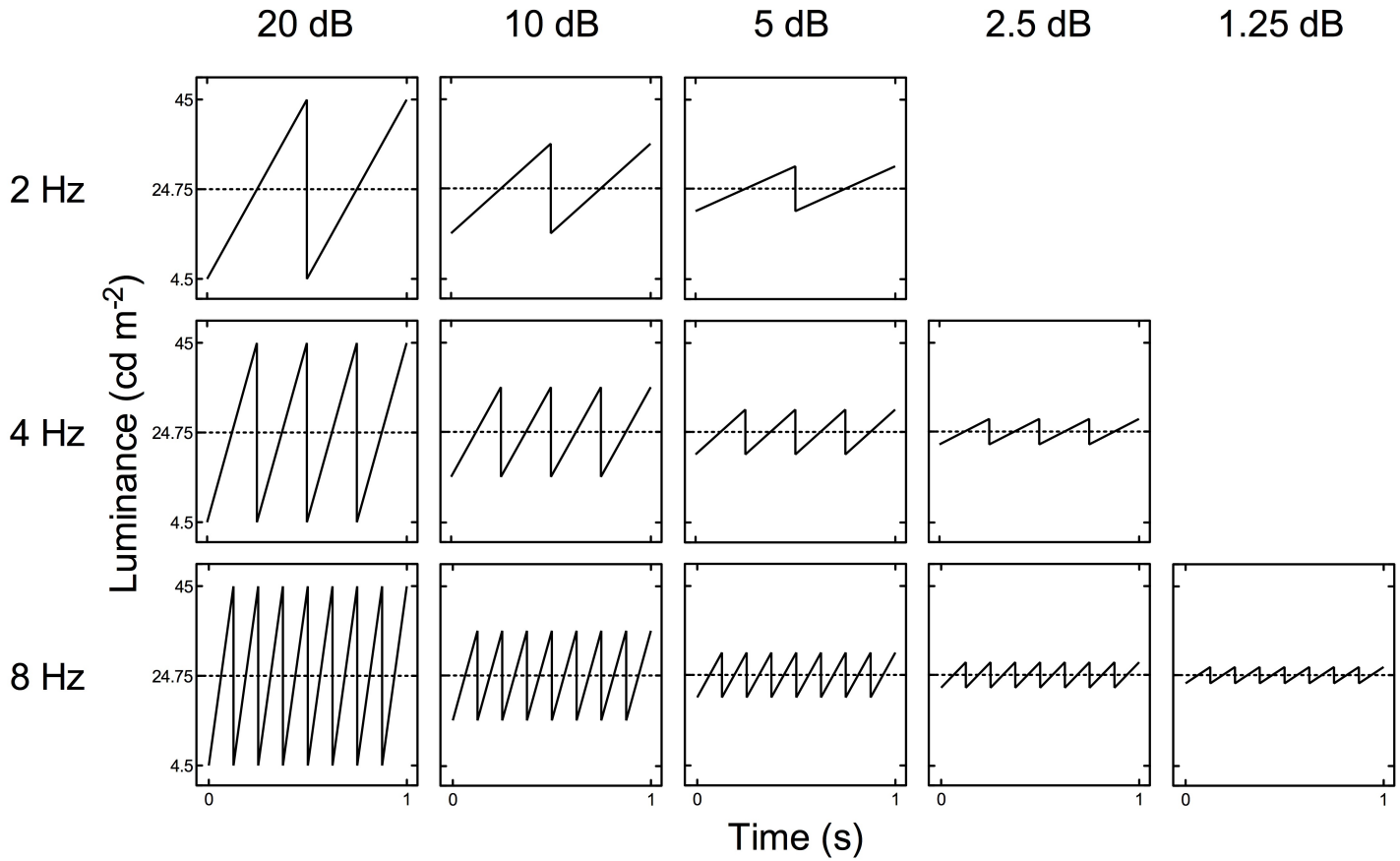

Figure 3.2: Ascending sawtooth luminance waveforms as a function of time. Nominal amplitude is indicated above each column and temporal frequency to the left of each row. The broken line represents mean luminance.

Adapting stimuli (Figure 3.2) comprised spatially uniform fields subtending 47° × 34° (horizontal × vertical). Luminance was modulated using ascending and descending sawtooth waveforms at 2, 4 or 8 Hz. The amplitude of luminance modulation ranged across 1.25, 2.5, 5, 10, and 20 decibels (dB) where:

$$dB = 20log_{10}\left(\frac{L_{max}}{L_{min}}\right) \quad \text{..... (3.1)}$$

where L_{max} and L_{min} are maximum and minimum luminance respectively. All test stimuli consisted of a 0.023 cycle/deg horizontally orientated half-cosine edge, subtending 25° × 22° (horizontal x vertical) with a nominal Michelson contrast (m) of 1 (actual 0.99), where:

$$m = \frac{L_{max} - L_{min}}{L_{max} + L_{min}} \quad \text{..... (3.2)}$$

The same test stimulus was used throughout for the purpose of comparison with Anstis (1967).

3.3.3 Procedure

Before beginning the experiment subjects were dark adapted for at least 5 min. A trial consisted of an adaptation interval of 16 sec followed by a test interval. All stimuli were presented at high and low luminance for ascending and descending linear luminance ramps. Each trial block consisted of a single temporal frequency and luminance. Within each block the amplitude of luminance modulation was randomised from trial to trial. The frequency and luminance tested was randomised from block to block. Subjects were required

to fixate on the centre of the screen during the adaptation interval and to indicate when the perception of motion had ceased during the test interval by pressing a mouse button. The test edge was alternated between 0^{o} and 180^{o} (darkest at the top or darkest at the bottom) on each trial. A blank screen of mean luminance was presented for at least 30 sec between each trial. The mean of 5 estimates was taken as the duration of the after-effect for each condition. Ten practice trials were presented at the beginning of each trial block. The experiments were conducted binocularly in a semi-darkened room using a chin and headrest.

3.4 Results

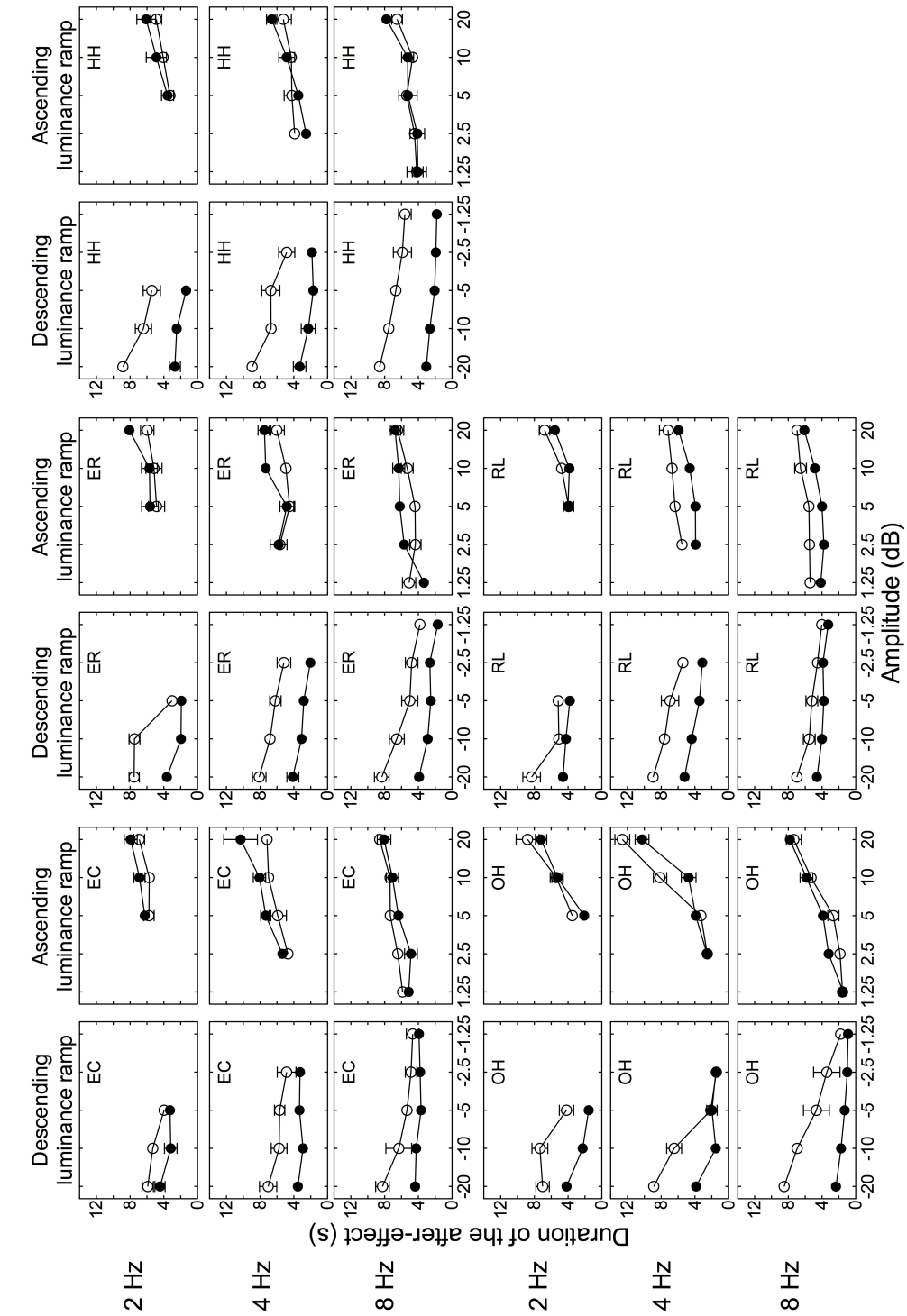

Figure 3.3: The duration of the after-effect is plotted as a function of adaptation luminance amplitude for high (open circles) and low luminance (closed circles) conditions for 2, 4 and 8 Hz for all subjects. Subjects' initials are indicated in the top right of each panel. Luminance amplitudes greater than zero represent ascending ramps, negative values represent descending ramps. Error bars represent ±1 SEM.

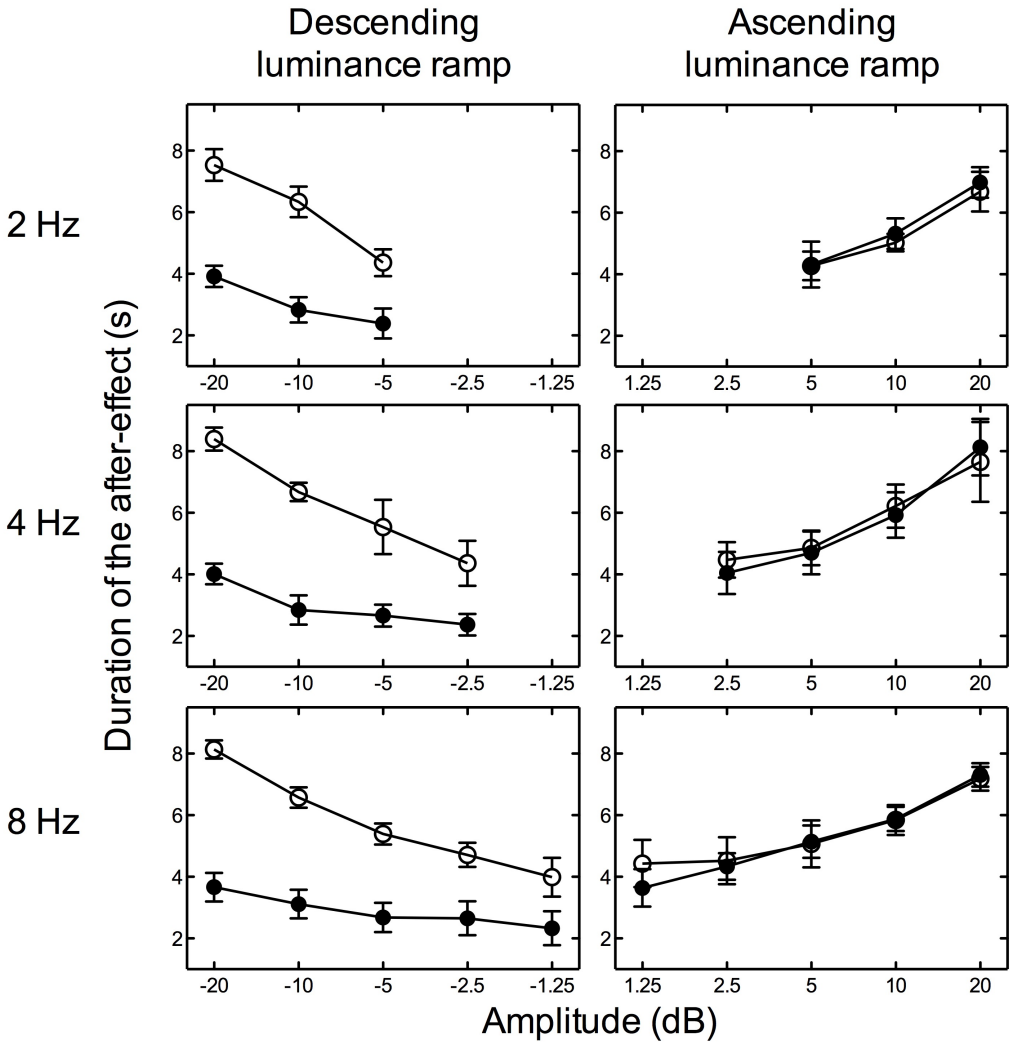

Figure 3.4: The average duration of the after-effect is plotted as a function of adaptation luminance amplitude for high (open circles) and low luminance (closed circles) conditions for 2, 4 and 8 Hz. Luminance amplitudes greater than zero represent ascending ramps, negative values represent descending ramps. Error bars represent ±1 SEM.

For ascending luminance ramps, the results indicate that as the amplitude of the adapting ramp increases the duration of the after-effect also increases for all temporal frequencies tested (Figure 3.3 and Figure 3.4). A two-way repeated measures ANOVA revealed no significant main effect of luminance, $F(1, 4) = 0.01$, $p = 0.931$; no significant main effect of frequency, $F(2, 8) = 0.66$, $p = 0.542$; and no significant interaction between luminance and frequency, $F(2, 8) = 0.26$, $p = 0.776$, on the duration of the after-effect. At high luminance, the duration of the after-effect also increases monotonically with amplitude in the

descending luminance ramp condition. However, at low luminance, the duration of the after-effect is consistently shorter than at high luminance. A two-way repeated measures ANOVA revealed a significant main effect of luminance, $F(1, 4) = 41.74$, $p < 0.005$; but no significant main effect of frequency, $F(2, 8) = 0.72$, $p = 0.516$; and no significant interaction between luminance and frequency, $F(2, 8) = 0.58$, $p = 0.583$, on the duration of the after-effect.

For all temporal frequencies at high luminance, two-way repeated measures ANOVAs revealed no significant main effect of adapting luminance ramp direction (ascending or descending), a significant main effect of ramp amplitude, and no significant interaction between ramp direction and ramp amplitude, on the duration of the after-effect (Table 3.1).

Table 3.1: Two-way repeated measures ANOVA for adapting luminance ramp direction and ramp amplitude on the duration of the after-effect at each temporal frequency at high luminance. * The effect is significant at the 0.01 level. ** The effect is significant at the 0.001 level.

Temporal Frequency					
2 Hz	Source	*df*	Mean square	*F*	*p*
	Luminance ramp direction	1	4.209	1.41	0.300
	Luminance ramp amplitude	2	19.460	22.89	0.000**
	Interaction Luminance ramp direction X Luminance ramp amplitude	2	0.953	0.89	0.444
	Error	8	0.850		
4 Hz	Source	*df*	Mean square	*F*	*p*
	Luminance ramp direction	1	1.951	0.36	0.580
	Luminance ramp amplitude	3	24.815	5.82	0.010*
	Interaction Luminance ramp direction X Luminance ramp amplitude	3	0.373	0.67	0.585
	Error	12	0.556		
8 Hz	Source	*df*	Mean square	*F*	*p*
	Luminance ramp direction	1	0.962	0.25	0.642
	Luminance ramp amplitude	4	21.055	21.60	0.000**
	Interaction Luminance ramp direction X Luminance ramp amplitude	4	0.521	2.56	0.078
	Error	16	0.202		

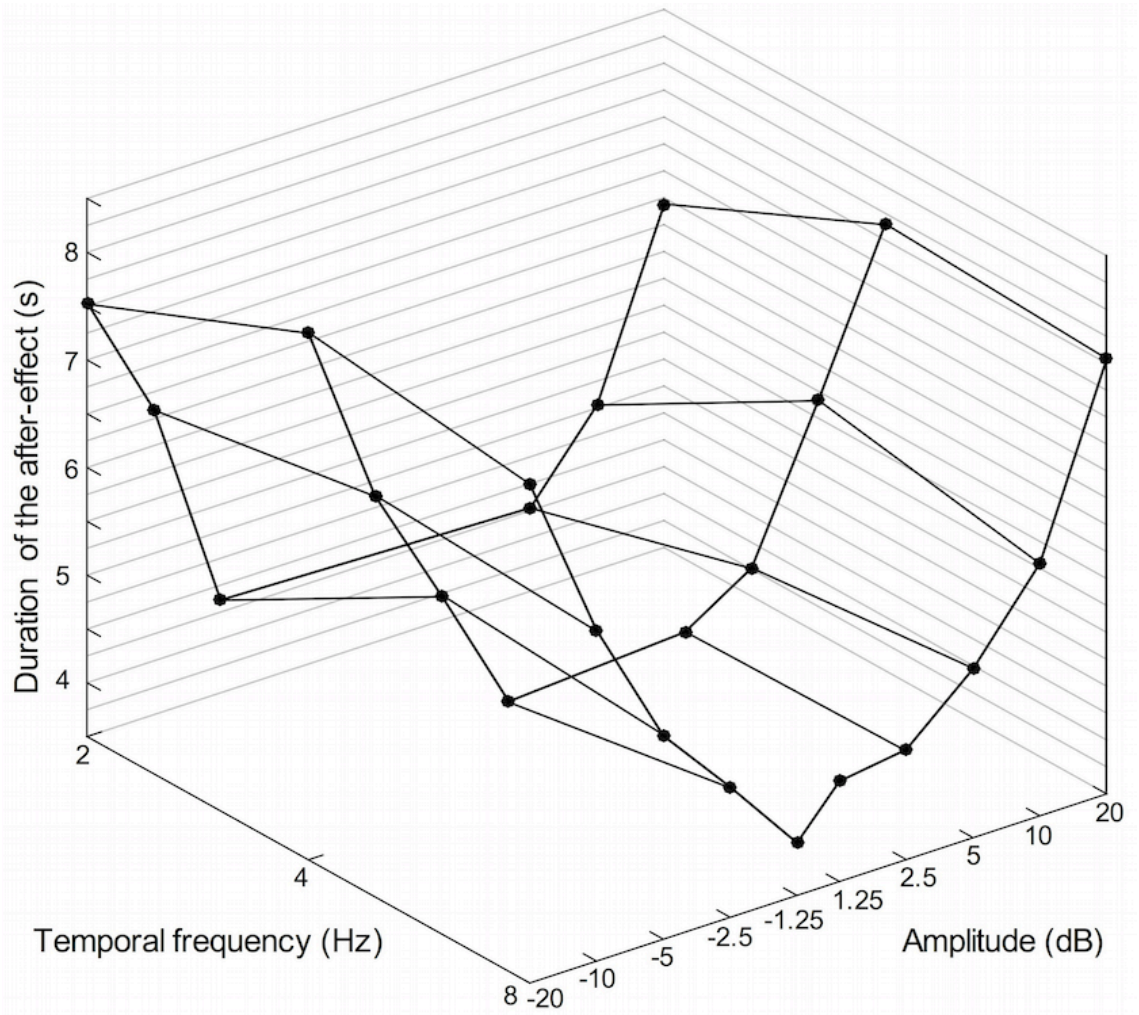

Figure 3.5: Three-dimensional plot of the results from the high luminance condition in Experiment 1. The duration of the after-effect is plotted as a function of adaptation luminance amplitude and temporal frequency. Luminance amplitudes greater than zero represent ascending ramps, negative values represent descending ramps. Symbols represent the mean of five subjects.

For each adapting amplitude across all frequencies the duration of the after-effect is comparatively constant (Figure 3.5). The ramp after-effect appears to be closely related to adapting amplitude and relatively independent of adapting temporal frequency. The maximum duration of the after-effect was consistently found at peak amplitude, irrespective of frequency, suggesting that the after-effect is determined by ramp amplitude rather than gradient.

In order to evaluate the relative contribution of gradient and amplitude quantitatively, two regression analyses were run to examine the relationships

between duration of the after-effect and (a) ramp amplitude, and (b) ramp gradient. For the amplitude model R^2 = 0.481, $F(1, 118) = 109.22$, $p < 0.001$. For the gradient model R^2 = 0.332, $F(1, 118) = 58.53$, $p < 0.001$. Thus both models could explain a significant proportion of the variance in duration of the after-effect. The correlation between the two models was significant (r = 0.732, $p < 0.001$). The predictive utility of the two models was therefore compared using Hotelling's t-test for non-independent correlations. The results indicate that the amplitude model accounted for significantly more variance than the gradient model, $t(117) = 2.40$, $p < 0.050$.

3.5 Experiment 2: The effect of linear, logarithmic and exponential luminance ramps upon the ramp after-effect

While Arnold and Anstis (1993) suggest that the after-effect was strongly driven by amplitude, they employed logarithmic adapting ramps for which gradient constantly changed whereas Anstis (1967) used linear ramps (Figure 3.1). As the gradient of the temporal ramp changes, so does the preferred temporal frequency of temporally tuned mechanisms that detect it optimally. Thus it is possible that differing ramp profiles recruit different populations of temporally tuned units. Furthermore a relatively limited range of parameters has been previously measured. For instance, Arnold and Anstis (1993) measured the effect between 0.5 and 4 Hz for amplitudes ranging from 5 to 20 dB using logarithmic ramps whereas Anstis (1967) used a linear ramp of 1 Hz and 40 dB (Figure 3.1). In order to evaluate the effect of ramp characteristics on the duration of the after-effect I have measured the effect of luminance ramp adaptation for a wider range of frequencies (2 – 8 Hz) and luminance amplitudes (1.25 – 20 dB) for both ascending and descending, linear, logarithmic and exponential luminance ramp profiles.

3.6 Methods

The experimental details were identical to those described for Experiment 1 except that only the high luminance condition was included and the profile of adaptation luminance was modulated using ascending and descending logarithmic and exponential waveforms as opposed to linear waveforms (Figure 3.6). Each trial block consisted of a single luminance ramp profile.

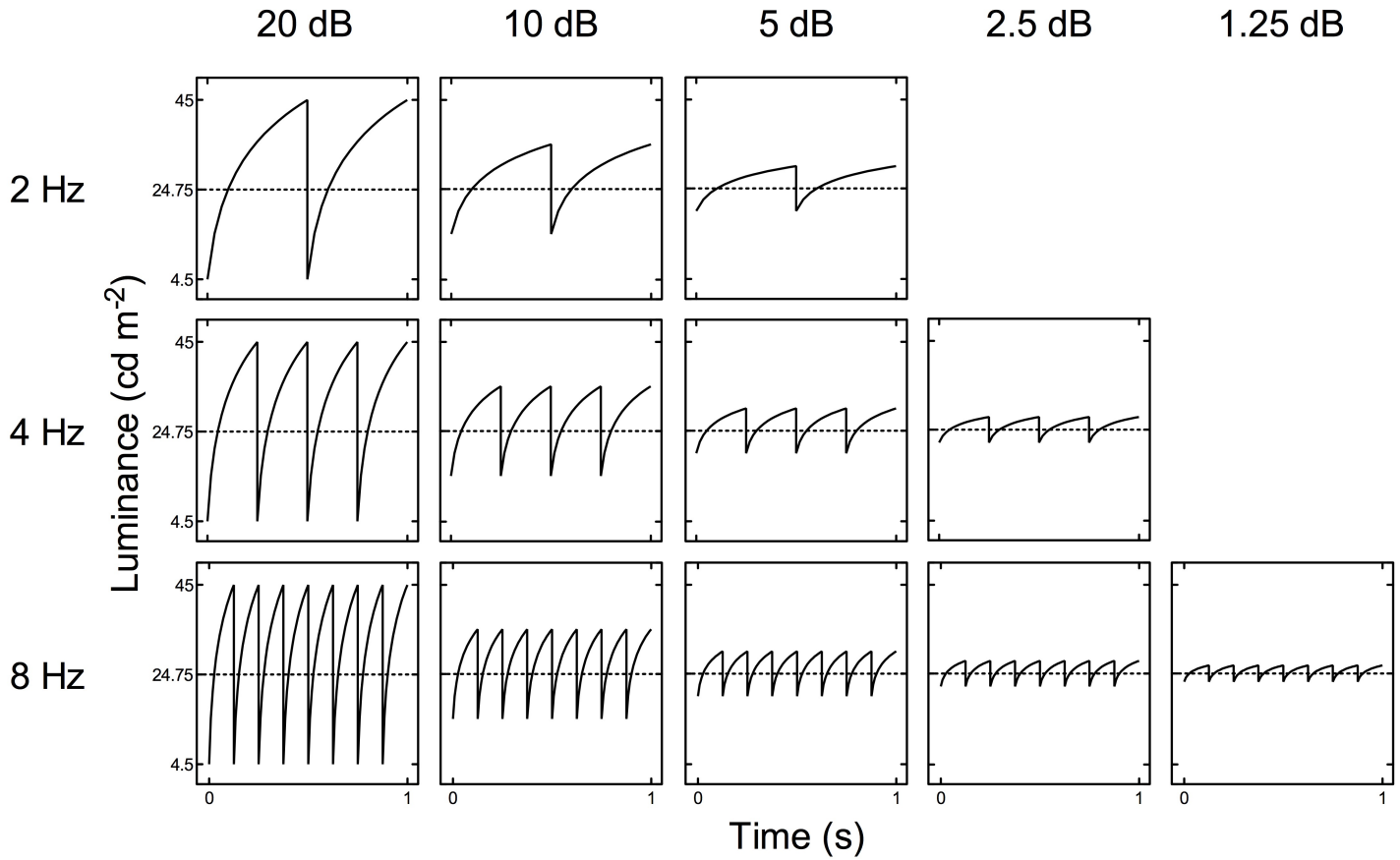

Figure 3.6: Ascending logarithmic luminance waveforms, as a function of time. Nominal amplitude is indicated above each column and temporal frequency to the left of each row. The broken line represents mean luminance.

3.7 Results

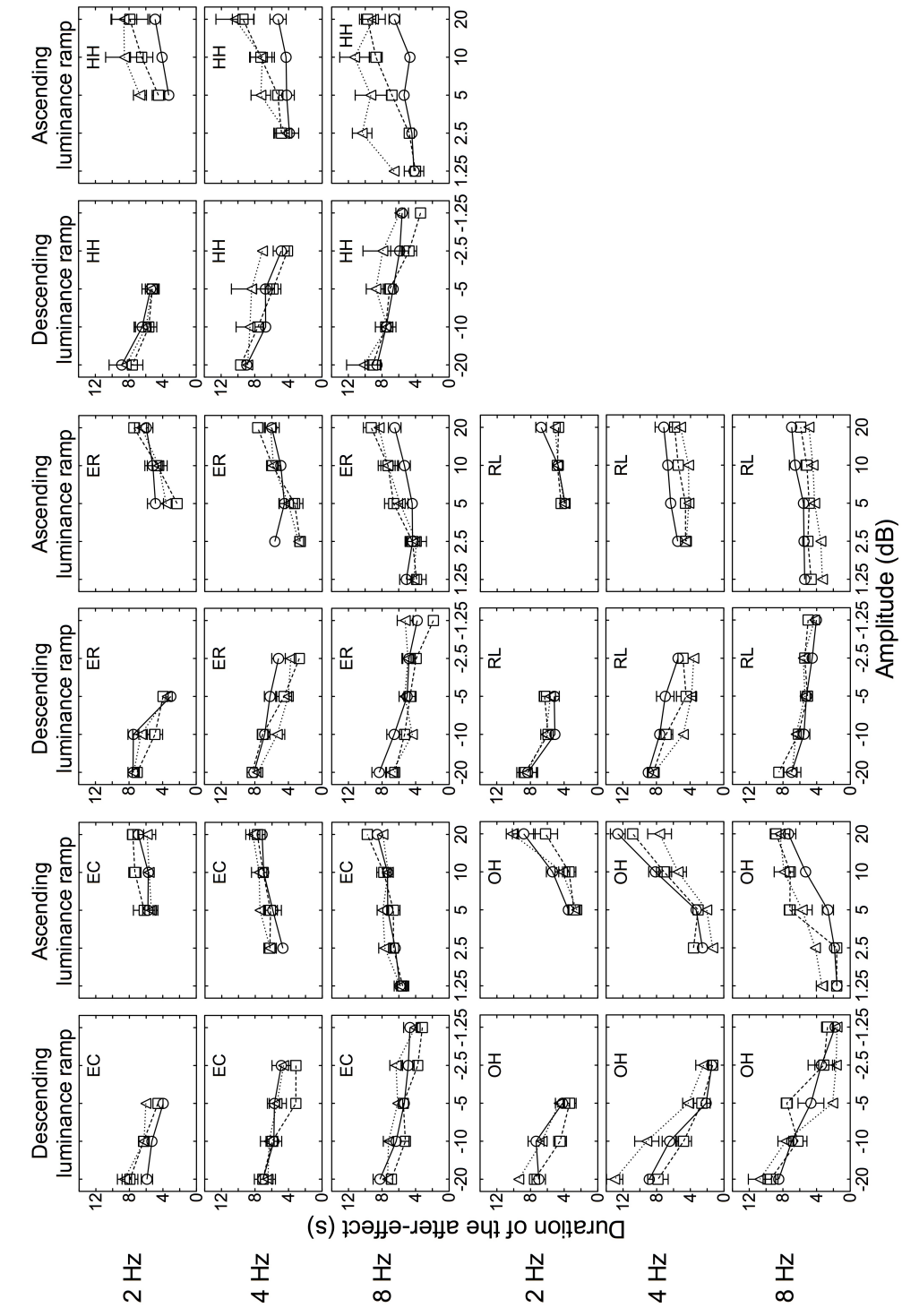

Figure 3.7: The duration of the after-effect is plotted as a function of adaptation luminance amplitude for linear (circles/solid line) (from Experiment 1), logarithmic (squares/broken line) and exponential (triangles/dotted line) luminance ramps for 2, 4 and 8 Hz for all subjects. Subjects' initials are indicated in the top right of each panel. Luminance amplitudes greater than zero represent ascending ramps, negative values represent descending ramps. Error bars represent ±1 SEM.

For both ascending and descending linear, logarithmic and exponential luminance ramp adaptation, the results indicate that as amplitude increases the duration of perceived motion increases for all temporal frequencies tested (Figure 3.7 and Figure 3.8).

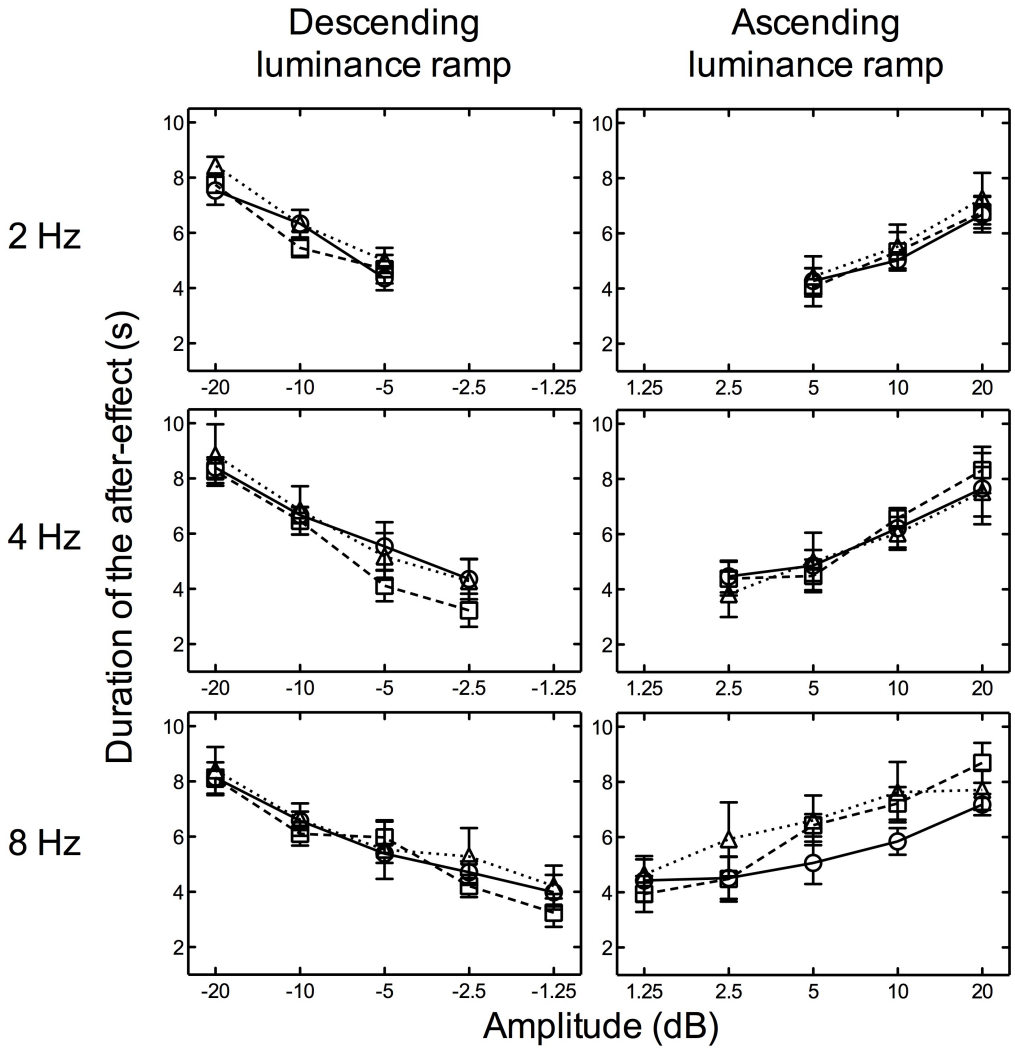

Figure 3.8: The duration of the after-effect is plotted as a function of adaptation luminance amplitude for linear (circles/solid line) (from Experiment 1), logarithmic (squares/broken line) and exponential (triangles/dotted line) luminance ramps for 2, 4 and 8 Hz. Luminance amplitudes greater than zero represent ascending ramps, negative values represent descending ramps. Symbols represent the mean of five subjects, error bars represent ±1 SEM.

There was no significant difference between the durations of the after-effect after adaption to linear, logarithmic or exponential ramps (Figure 3.8). Two-way repeated measures ANOVAs revealed no significant main effects of luminance ramp profile for ascending, $F(2, 8) = 0.25$, $p = 0.786$, and descending, $F(2, 8) =$

2.42, p = 0.150 stimuli. No significant main effects of frequency (ascending: F(2, 8) = 2.21, p = 0.172) (descending: F(2, 8) = 1.92, p = 0.208), and no significant interactions between luminance ramp profile and frequency (ascending: F(4, 16) = 0.99, p = 0.443), (descending: F(4, 16) = 0.22, p = 0.925), were found.

3.8 Discussion

The results from Experiment 1 indicate that, at high luminance, the duration of the after-effect is well characterised by the amplitude of the adapting linear ramp. Had the ramp after-effect been driven by gradient the subjective duration of perceived motion would peak at different adapting amplitudes for different adapting temporal frequencies. This was not the case in Experiment 1; rather, regardless of adaptation frequency the maximum duration of the after-effect was found at the maximum amplitude. These findings are consistent with Arnold and Anstis's (1993) observation that the ramp after-effect is driven by amplitude, particularly large sweeps in amplitude of at least 20 dB. Although, in Experiment 1 I used linear luminance ramps whereas Arnold and Anstis (1993) adapted subjects to logarithmic luminance ramps (Figure 3.1) the results are consistent. However, in order to better assess whether differences in ramp profile could influence the ramp after-effect, in Experiment 2 I adapted subjects to exponential, and logarithmic luminance ramps as used by Arnold and Anstis (1993) and replicated their finding that the effect is monotonically related to amplitude. The ramp profile had no effect on the duration of the after-effect. The same test stimulus was used throughout and perhaps other test stimuli would reveal other properties but for the purposes of comparison with Anstis (1967) it was necessary to use that stimulus. I cannot rule out that different test

amplitudes and different test stimulus profiles might have revealed other patterns.

Anstis (1997) concluded that since ramp after-effects can be interpreted as motion after-effects, "*motion detectors include a filter to detect gradual change of luminance, dI/dT*" (p. 65) and several other researchers (e.g. Ashida & Scott-Samuel, 2014; Scarfe & Johnston, 2010) have suggested that the ramp after-effect is consistent with a gradient model of motion encoding (e.g. Marr & Ullman, 1981). This proposal is predicated upon the assumption that the neural mechanism which ordinarily detects motion also mediates the ramp after-effect. However this may not be the case, instead the percept may be mediated simply upon the basis of changes in the response of spatial mechanisms. More critically, the results of Experiment 1 show that it is *amplitude* rather than gradient that determines the illusory perception of motion and the results of Experiment 2 reveal that the gradient profile does not influence the after-effect. Gradient motion detectors would however, by definition, be tuned for gradient rather than amplitude. Although amplitude was the best predictor of performance across both experiments, nonetheless gradient had a weaker, albeit significant, effect under some conditions (even if it did not predict the peak aftereffect).

The effect of luminance

A similar pattern of results to that of adaptation at high luminance is found at low luminance, for ascending luminance ramp adaptation. However, the duration of the after-effect was significantly attenuated at low luminance when the adapting pattern comprised descending luminance ramps. How could this

difference be explained? One possibility is that the after-effect is mediated by adapting the ON- and OFF- pathways in the visual system that are selectively tuned for increments and decrements in luminance. ON retinal ganglion cells are stimulated by local increments in illumination whereas OFF ganglion cells respond to local decrements in illumination (Schiller, 1982, 1984, 1992; Schiller, Sandell, & Maunsell, 1986). Thus, the ramp after-effect might be due to selective adaptation of the ON or OFF cells by ascending or descending luminance ramps. Moreover, the response properties of feline cortical ON and OFF cells are significantly altered by absolute luminance level. At low luminance, OFF cell responses are reduced or absent, while ON responses are unaffected (Dolan & Schiller, 1989, 1994; Ramoa et al., 1985). I find a significant reduction in the ramp after-effect under precisely these conditions – at low luminance and exclusively for descending (OFF) luminance ramps. Thus the significant reduction in the duration of the after-effect found is entirely consistent with adaptation of cortical ON and OFF pathways. I conclude that my results demonstrate that the visual system processes brightness within a metric that explicitly represents the amplitude of luminance over time and is optimally sensitive to large amplitudes. The local gradient of these changes does not appear critical to the system's response. The most likely neural substrate of this representation of brightness is amplitude-tuned ON and OFF pathways. The results offer no support for gradient models of motion processing.

Chapter 4

4 The effect of speed-induced perceived contrast changes upon speed matching

4.1 Introduction

Thompson (1982) first reported that perceived speed depends on stimulus contrast. When two parallel gratings moved at the same low speed (below 8 Hz) a reduction in the contrast of one of the gratings, resulted in the perceived speed of that grating being under-estimated (Brooks, 2001; Stone & Thompson, 1992; Thompson, 1982). However, at higher speeds (above 8 Hz) a reduction in contrast resulted in perceived speed being over-estimated (Blakemore & Snowden, 1999; Thompson, 1982; Thompson et al., 2006). The under-estimation of perceived speed due to reduced contrast, has been shown to occur over a wide range of contrasts (2.5 – 50%) (Stone & Thompson, 1992). It is possible that the over-estimation of perceived speed at low contrast (at speeds above 8 Hz) may reflect differences in the perceived contrast of patterns at different temporal frequencies rather than being an effect of speed processing *per se*.

Just as perceived speed is affected by changes in contrast, perceived contrast also changes as temporal frequency changes (Georgeson, 1987). Georgeson (1987) found that contrast appears lower at higher temporal frequencies than at lower temporal frequencies. Thompson (1982) proposed that the increase in perceived speed at lower contrast and higher speeds was due to the relatively larger attenuation of the slow mechanism's contribution to the computation of speed due to its relative insensitivity at higher speeds. However, if perceived speed depends upon perceived (rather than physical) contrast, it may be that these increases in perceived speed reported by Thompson and others (e.g.

Hammett et al., 2005) are due to the lower perceived contrast of fast speeds and that, at equal perceived contrast this increase in perceived speed may be reversed or attenuated. Thus the increase in perceived speed at high temporal frequencies could reflect these changes in perceived contrast rather than a change in the speed code *per se*. No previous studies have tested this possibility since they (Blakemore & Snowden, 1999; Brooks, 2001; Stone & Thompson, 1992; Thompson et al., 2006) used physically constant contrast values across the speed ranges measured. In order to examine the possibility that changes in the perceived contrast of the low contrast pattern in these speed-matching tasks might explain the over-estimation of speed at high frequencies I measured the perceived speed of low contrast patterns (relative to a standard pattern of 0.7 contrast) for a range of speeds at both constant physical and matched contrast.

4.2 Experiment 3a: The effect of speed upon perceived contrast

4.3 Methods

4.3.1 Subjects

Five (three male and two female) subjects aged between 23 and 32 participated in this experiment. One of the subjects (OH) was an author; the other four were naïve to the purpose of the experiment. All subjects had normal or corrected-to-normal acuity.

4.3.2 Apparatus and stimuli

All stimuli were horizontally orientated sinusoidal gratings of 2 c/deg generated using the Psychophysics Toolbox extensions (Brainard, 1997; Kleiner et al., 2007; Pelli, 1997) for MATLAB 7.11 (MathWorks, Cambridge, UK) and

displayed on an EIZO 6600-M (Hakusan, Ishikawa, Japan) monochrome monitor at a frame rate of 100 Hz. The monitor was gamma corrected using the CRS Optical photometric system (Cambridge Research Systems, Rochester, UK). The display subtended $68^{o} \times 47^{o}$ at a viewing distance of 28.5 cm. Mean luminance was 25 cd m^{-2}. Stimuli were presented through two 6 degrees diameter circular windows with hard edges. Each window was located equidistant from the horizontal centre of the screen and separated by 2^{o}. A small bright fixation spot was situated at the centre of the display.

4.3.3 Procedure

Before beginning the experiment subjects were dark adapted for at least 5 min. Two patterns were presented simultaneously for 500 msec on each trial. Standard patterns (always presented on the left) constantly drifted at 1 deg/sec throughout, test patters drifted at one of four speeds (1, 2, 4, or 8 deg/sec). The spatial phase of both the standard and test gratings was randomised on each trial. The standard and tests patterns always drifted in a downward direction. The Michelson contrast of the standard pattern was constant throughout at 0.1. The Michelson contrast of the test pattern was altered by a QUEST routine (Watson & Pelli, 1983) depending on the subject's responses. For each block the QUEST procedure was terminated after 50 trials, the data were fit to a cumulative Gaussian function using the method of least squares and the 50% point of the function was estimated. The mean of five such estimates was taken as the PSE. A blank screen of mean luminance was presented between each test pair and subjects pressed a mouse button in order for each test pair to be presented. The subject's task was to indicate which pattern appeared to have the greater contrast, by pressing a mouse button. The experiments were

conducted binocularly in a semi-darkened room using a chin and headrest.

4.4 Results

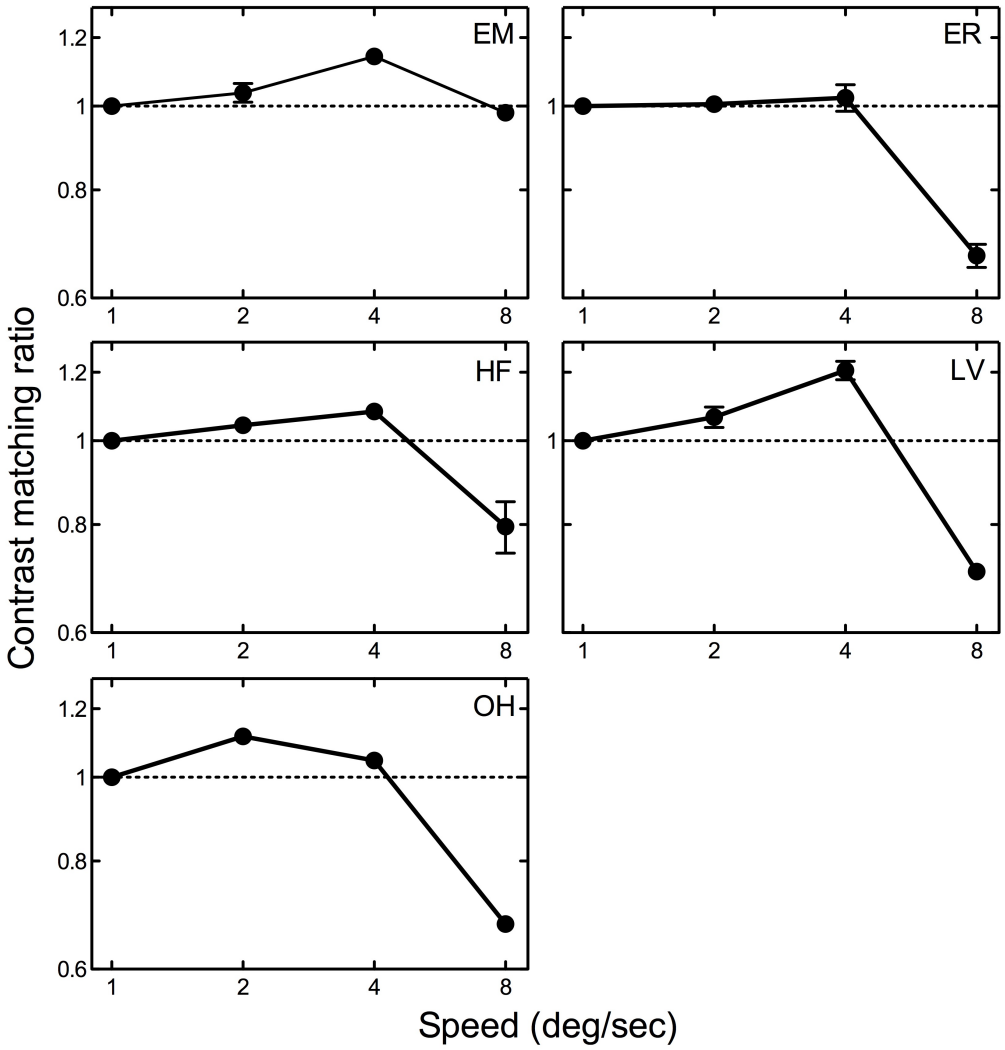

Figure 4.1: The ratio of perceived contrast at 1 deg/sec to perceived contrasts at higher speeds is plotted as a function of grating speed for all subjects. Subjects' initials are indicated in the top right of each panel. Values greater than 1 indicate an increase in perceived contrast, values less than 1 indicate a reduction in perceived contrast. Error bars represent ±1 SEM.

Figure 4.1 and Figure 4.2 plot the results. There were hemi-field differences in perceived contrast for some of the subjects, consistent with previous reports (Beaton & Blakemore, 1981; Edgar & Smith, 1990; Rao, Rourke, & Whitman, 1981; Rovamo & Virsu, 1979). Due to these hemi-field differences each contrast match was normalised with respect to each subject's perceived contrast at 1

deg/sec. All subjects over-estimated contrast at speeds below 4 deg/sec, conversely, subjects under-estimated contrast at the higher speed of 8 deg/sec i.e. perceived contrast at 2 and 4 deg/sec was greater than that at 1 deg/sec.

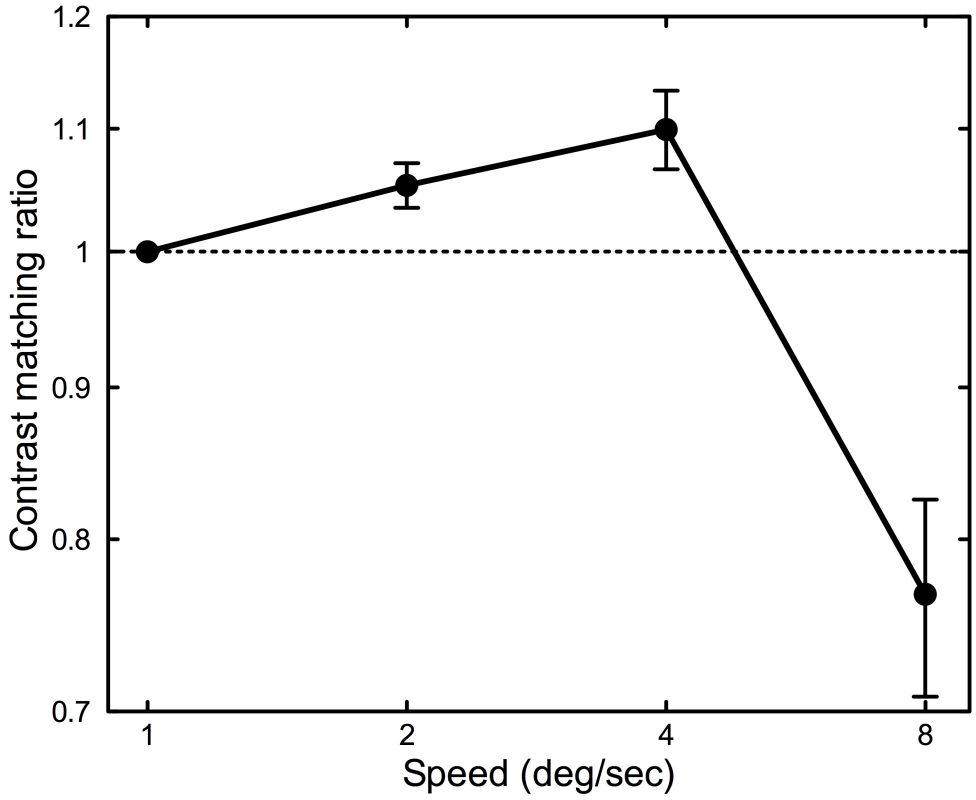

Figure 4.2: The average ratio of perceived contrast at 1 deg/sec to perceived contrasts for higher speeds is plotted as a function of grating speed. Values greater than 1 indicate an increase in perceived contrast, values less than 1 indicate a reduction in perceived contrast. Error bars represent ±1 SEM.

One sample t-tests revealed significant differences from a match ratio of 1 (veridical), at 2, 4 and 8 deg/sec ($t(4) = 2.88$, $p < 0.050$, $t(4) = 2.97$, $p < 0.050$, $t(4) = -3.99$, $p < 0.050$), respectively.

4.5 Experiment 3b: The effect of perceived contrast upon biases in perceived speed

4.6 Methods

The experimental details were identical to those described for Experiment 3a except that the subject's task was to indicate which pattern appeared faster, the speed of the test pattern was altered by a QUEST routine depending upon the subject's response. Perceived speed was measured for stimuli of unequal contrast. In the control condition, the contrast of the standard patterns was fixed at 0.7 and the test at 0.1. In the other condition, the standard pattern was fixed at 0.7 and the test contrast was set to that of the subject's contrast match value estimate in Experiment 3a. Five estimates were taken at each speed and contrast. The order of each condition was randomised.

4.7 Results

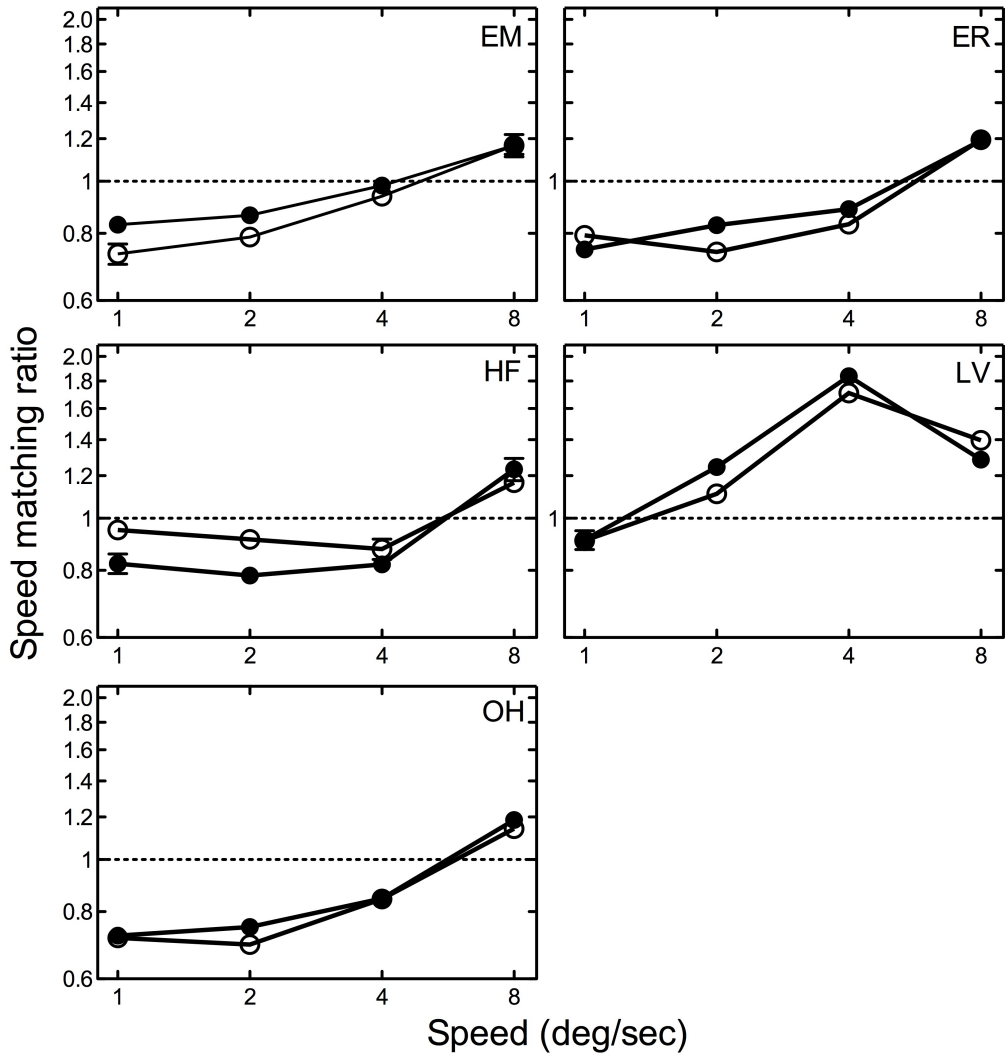

Figure 4.3: The ratio of physical test speed to matched speed for all subjects is plotted as a function of speed for constant physical contrasts (closed symbols) and matched contrast (open symbols). Subjects' initials are indicated in the top right of each panel. Values greater than 1 indicates an over-estimation of speed, values less than 1 indicate an under-estimation of speed. Error bars represent ±1 SEM.

Figure 4.3 and Figure 4.5 plot the results of the speed matching experiment for both constant physical and matched contrast. All subjects apart from LV, showed an under-estimation of speed below 4 deg/sec, and an over-estimation of speed at 8 deg/sec, for both physical and matched contrasts. It is not possible to entirely account for this discrepancy between subjects. However,

LV's data take the same shape as those of her contrast matching and thus it may be that the subject misunderstood the task (Figure 4.4).

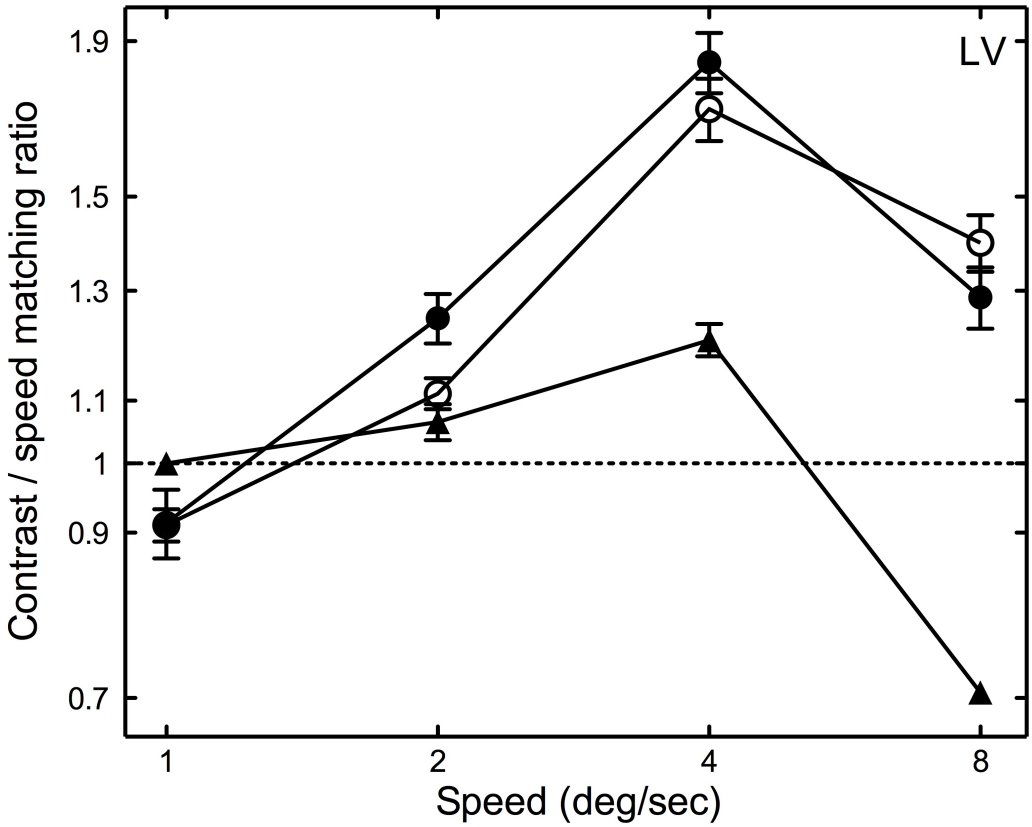

Figure 4.4: LV's results for contrast matching (triangles), speed matching with constant physical contrasts (closed circles) and matched contrast (open circles) are re-plotted for comparison. Error bars represent ±1 SEM.

Given the likelihood that LV misunderstood the task her data have been excluded from subsequent analysis. The results for all other subjects indicate that, across all speeds tested, there is no difference between speed matching with physical or matched contrasts.

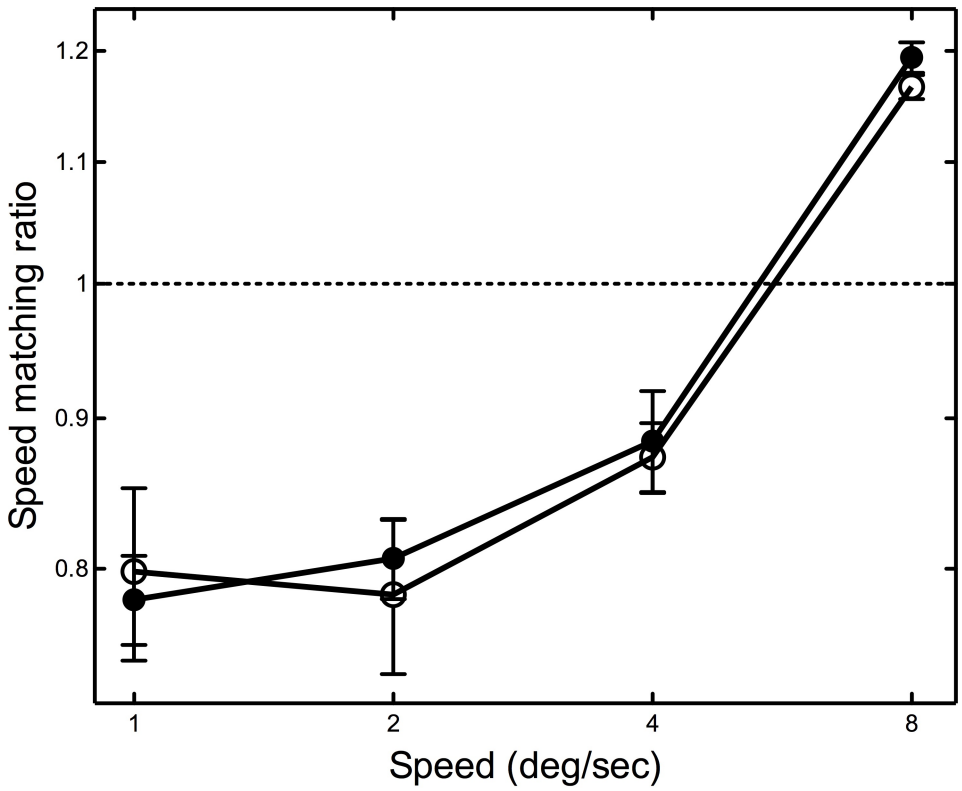

Figure 4.5: The average ratio between the physical test speed and matched speed as a function of grating speed for constant physical contrasts (closed symbols) and matched contrast (open symbols). Values greater than 1 indicates an over-estimation of speed, values less than 1 indicate an under-estimation speed. Error bars represent ±1 SEM.

At speeds below 4 deg/sec, with both constant physical and matched contrast, lower contrast yielded an under-estimation in perceived speed. At speeds above 4 deg/sec, with both constant physical and matched contrast, lower contrast yielded an over-estimation in perceived speed. A paired sample t-test revealed no significant difference ($t(3) = -1.09$, $p = 0.355$, two-tailed) between the ratio of perceived speed with constant physical contrasts and with matched contrast. With LV's data included another paired sample t-test also showed no significant difference ($t(3) = -1.17$, $p = 0.324$, two-tailed).

4.8 Discussion

Georgeson (1987) reported that as temporal frequency increased perceived contrast increases up to 4 Hz and reduces between 8 and 16 Hz. Consistent with this, the results showed that subjects required lower contrasts at 4 (2 deg/sec) and 8 Hz (4 deg/sec) in order to match 10% contrast at 2 Hz (1 deg/sec), whereas, at 16 Hz (8 deg/sec) a higher contrast was required to make the same match. However, for all temporal frequencies tested there was no significant difference between speed matching with constant physical contrasts and speed matching with matched contrast.

I was able to reproduce Thompson's (1982) findings that at low contrast and speeds below 8 Hz (4 deg/sec) there is an under-estimation in perceived speed. This result has been consistent within the literature (Stone & Thompson, 1992; Thompson, 1982; Thompson et al., 2006; Thompson & Stone, 1997) despite differences in stimulus parameters such as stimulus size, number of cycles, and mean luminance. The effect of low contrast increasing perceived speed at high temporal frequencies has not been consistently found in previous studies (e.g. Hammett & Larsson, 2012) but the current results show that, for both constant physical and matched contrast, perceived speed was over-estimated above 4 deg/sec (8 Hz), consistent with previous reports using physically constant contrast comparisons (e.g. Thompson et al., 2006).

I conclude that the estimation of perceived speed at low contrasts is unlikely to reflect changes in the perceived contrast of the comparison stimuli as a function of temporal frequency or speed. Rather, it seems reasonable to assume that this shift is a genuine reflection of underlying speed-processing mechanisms. All

in all, the results indicate that the effect of contrast on perceived speed is reliable and is not an artefact of contrast encoding.

Chapter 5

5 Perceived speed in peripheral vision

5.1 Introduction

It is well-known that visual stimuli presented in peripheral vision generally have higher detection and discrimination thresholds than those presented to central vision and that contours in the periphery fade with steady fixation, the well-known Troxler effect (Troxler, 1804). This Troxler fading is particularly pronounced at low stimulus contrast (Livingstone & Hubel, 1987) and has been attributed to the adaptation of edge detectors (Krauskopf, 1963; Ramachandran & Gregory, 1991).

Similarly, MacKay (1982) reported that moving stimuli in near-peripheral vision (<10 degrees from the fixation point) appear to slow and stop but their spatial structure can still be resolved. Moving into the far periphery (30-70 degrees), Hunzelmann and Spillmann (1984) confirmed the slow-down in the perceived speed of moving stimuli in peripheral vision and also observed that the apparent contrast of these stimuli was reduced. If it is the case that peripherally viewed moving stimuli appear reduced in contrast then their slowed speed might be expected, as it has been well-established that moving patterns generally appear to move more slowly at low contrast (Stone & Thompson, 1992; Thompson, 1976, 1982).

In Experiment 4 I tested the hypothesis that the perceived slowing of stimuli in peripheral vision can be accounted for entirely in terms of a perceived reduction in contrast. In Experiment 5 I investigated how luminance affects perceived speed in order to further investigate the mechanisms underlying this perceptual bias.

5.2 Experiment 4a: The effect of speed upon perceived contrast in the periphery

5.3 Methods

5.3.1 Subjects

Four (two male and two female) subjects aged between 22 and 27 participated in this experiment. One of the subjects (OH) was an author; the other three were naïve to the purpose of the experiment. All subjects had normal or corrected-to-normal acuity.

5.3.2 Apparatus and stimuli

All stimuli were horizontally oriented sinusoidal gratings of 2 c/deg generated using the Psychophysics Toolbox extensions (Brainard, 1997; Kleiner et al., 2007; Pelli, 1997) for MATLAB 7.11 (MathWorks, Cambridge, UK) and displayed on an EIZO 6600-M (Hakusan, Ishikawa, Japan) monochrome monitor at a frame rate of 100 Hz. The monitor was gamma corrected using the CRS Optical photometric system (Cambridge Research Systems, Rochester, UK). The display subtended $68^{o} \times 47^{o}$ at a viewing distance of 28.5 cm. Mean luminance was 25 cd m^{-2}. On each trial stimuli were presented simultaneously for 500 msec in elliptical windows with sharp edges that subtended 2 degrees horizontally by 4 degrees vertically. A small bright fixation spot was situated at the centre of the display. The standard pattern was situated at the centre of the display and the test pattern was situated to the right of the standard pattern centred at one of five eccentricities (0^{o}, 6^{o}, 12^{o}, 24^{o} and 32^{o}). The stimuli drifted downward at one of four speeds (1, 2, 4 and 6 deg/sec). The Michelson contrast of the standard pattern was 0.1 and the contrast of the test pattern was altered by a QUEST routine (Watson & Pelli, 1983) depending on the subject's

responses.

5.3.3 Procedure

Subjects adapted to a blank screen of mean luminance for at least 5 minutes at the beginning of each session. The subject's task was to indicate which pattern (standard or test) appeared to have greater contrast by pressing a mouse button. For each block the QUEST procedure was terminated after 50 trials, the data were fit to a cumulative Gaussian function using the method of least squares and the 50% point of the function was estimated. The mean of five such estimates was taken as the PSE. A blank screen of mean luminance was presented between each trial, and subjects pressed a mouse button to initiate each trial. At 0^{o}, stimuli were presented sequentially at the centre of the display for 500 msec with an inter-stimulus interval of 500 msec and the mean of three estimates was taken as the PSE. The experiments were conducted binocularly in a semi-darkened room using a chin and headrest.

5.4 Results

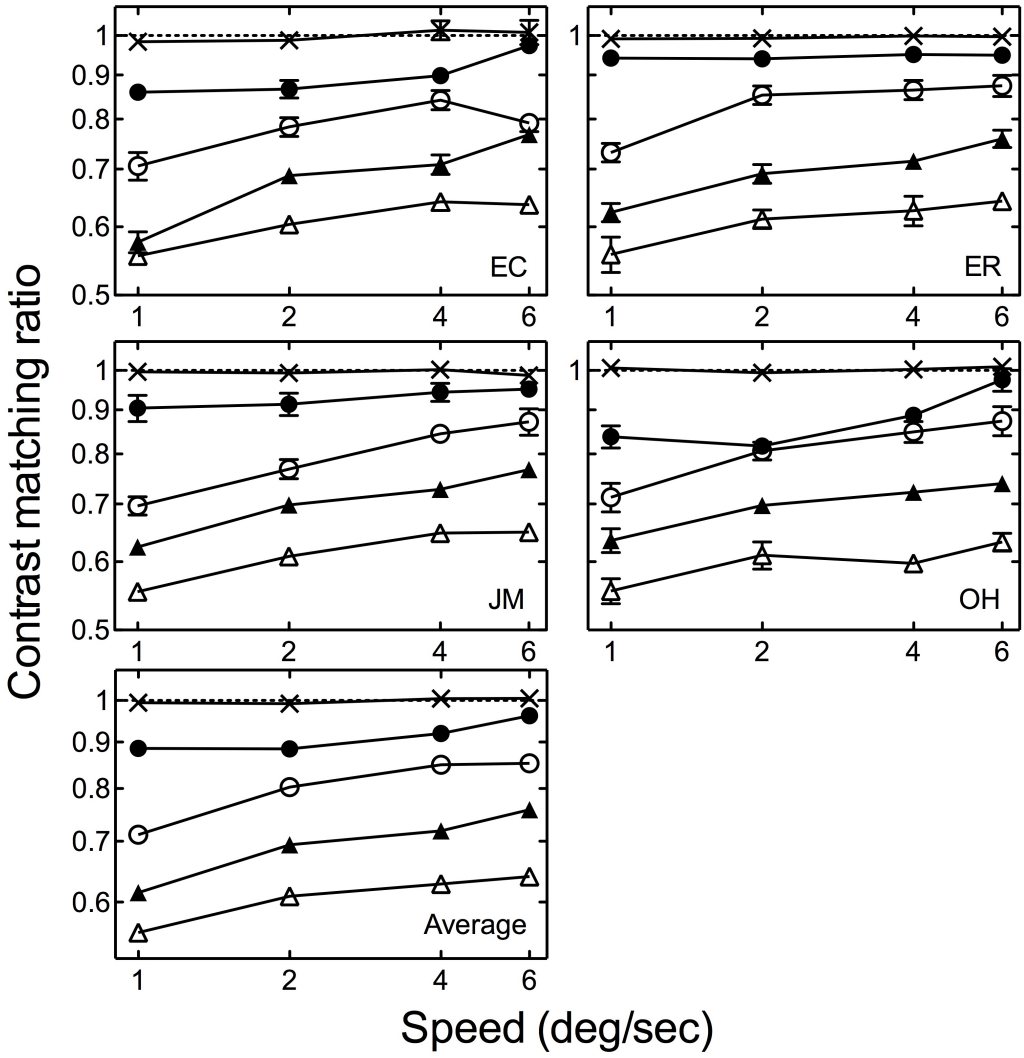

Figure 5.1: The ratio of physical to perceived contrasts as a function of speed at five eccentricities: 0^o the control condition (crosses), 6^o (closed circles), 12^o (open circles), 24^o (closed triangles), and 32^o (open triangles). Subjects' initials are indicated in the bottom right of each panel, the average across subjects is indicated in the lowermost left panel. A value of 1 (broken line) represents a veridical estimate. Values less than 1 indicate an under-estimation of contrast. Error bars represent ±1 SEM.

Figure 5.1 plots the average contrast match as a function of speed for each eccentricity. The results indicate that subjects accurately matched the contrast of patterns in foveal vision but under-estimated the contrast of patterns in the periphery. The further into the periphery the test stimuli were, the greater the under-estimation of contrast. Furthermore, at all eccentricities the slower the speed of the stimuli, the more their contrast is under-estimated.

5.5 Experiment 4b: The effect of perceived contrast upon biases in perceived speed in the periphery

5.6 Methods

The experimental details were identical to those described for Experiment 4a except that the subject's task was to indicate which pattern appeared faster, the speed of the test pattern was altered by a QUEST routine depending upon the subject's response. Perceived speed was measured for stimuli of both equal physical and equal perceived contrast. In the equal physical contrast condition, the contrast of both patterns was fixed at 0.1. In the equal perceived contrast condition, the contrast of the standard pattern was set at 0.1 and the contrast of the test pattern was set to that of the subject's contrast match value estimated in Experiment 4a. Five (three in the control condition) estimates were taken at each speed and eccentricity. The order of each condition was randomised.

5.7 Results

Figure 5.2 plots the perceived speed matches for equal physical and equal perceived contrast as a function of speed for each eccentricity. The results indicate that subjects progressively under-estimated the speed of patterns as eccentricity increased. Equalising the perceived contrast of the patterns reduced this effect at slower speeds so that all speeds suffered a similar reduction in perceived speed at any particular eccentricity.

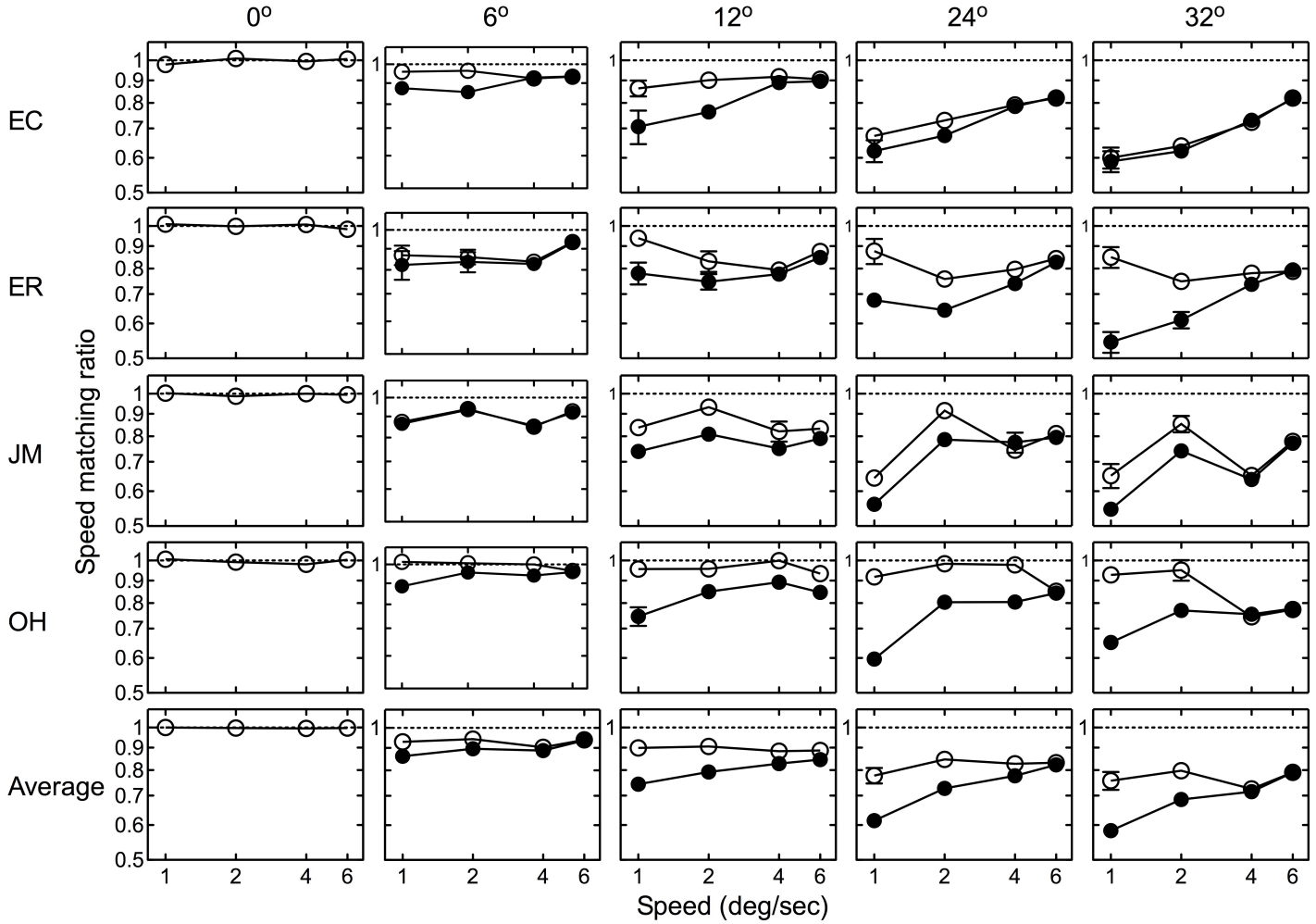

Figure 5.2: The ratio of physical speed and matched speed at equal physical contrast (closed symbols) and equal perceived contrast (open symbols) as a function of physical speed for a range of eccentricities (indicated above panels). Subjects' initials are indicated on the left of each row, the average across subjects is indicated in the lowermost row. A value of 1 (broken line) represents a veridical speed estimate. Values less than 1 indicate an under-estimation of perceived speed. Error bars represent ±1 SEM.

This pattern of results suggests that there are two components contributing to the reductions in perceived speed observed. Firstly there appears to be a component which is independent of speed and contrast but increases with eccentricity. Secondly there is a component that can be ascribed to the reduction in perceived contrast in the periphery. This effect is greatest at the slowest speeds and greatest eccentricity.

A three-way repeated measures ANOVA revealed no significant main effect of speed, $F(3, 9) = 2.43$, $p = 0.132$; a significant main effect of contrast, $F(1, 3) = 16.77$, $p < 0.05$; a significant main effect of eccentricity, $F(3, 9) = 57.92$, $p < 0.001$; a significant interaction between speed and contrast, $F(3, 9) = 12.76$, $p < 0.010$; no significant interaction between speed and eccentricity, $F(9, 27) = 1.70$, $p = 0.137$; no significant interaction between contrast and eccentricity, $F(3, 9) = 2.58$, $p = 0.118$; and no significant interaction between speed, contrast and eccentricity, $F(9, 27) = 1.25$, $p = 0.306$.

5.8 Experiment 5: The effect of luminance upon peripheral speed perception

5.9 Introduction

The results of Experiment 4 indicate that the reduction in perceived contrast that accompanies increasing eccentricity does contribute to the perceptual slowing down of moving patterns in the periphery. However, when one accounts for this contrast-induced reduction in perceived speed by equalising the perceived contrast of peripherally presented patterns the results indicate that eccentric patterns are still perceived as slower – around 10% slower at 6 degrees and 20% slower at 32 degrees. How might one account for this residual effect of eccentricity upon perceived speed? One possibility is that the known changes in the ratio of M and P cells with eccentricity (Dacey, 1994) contribute to this effect. It is known that the contrast gain of P cells is more greatly reduced than that of M cells as luminance is reduced (Purpura et al., 1988). I therefore reason that should the effect of eccentricity on perceived speed be in part mediated by the changing ratio of M and P cells with eccentricity, this should result in an increase rather than decrease in perceived speed under conditions where the response of M cells prevails – at low luminance, low contrast and large eccentricities. In order to investigate this notion further I estimated perceived speed as a function of eccentricity at both high and low luminance and contrast.

5.10 Methods

All the experimental details were the same as those of Experiment 4b except that stimuli had a spatial frequency of 1 c/deg. Perceived speed was estimated for two contrasts (0.1 and 0.7) at two luminance levels (2.5 cd m^{-2} and 25 cd m^{-2}) and three eccentricities (6, 12 and 24 degrees). During the low luminance

conditions 1 log unit neutral density filters (NDF) (Thorlabs Inc., Newton, New Jersey, USA) were inserted into drop-cell trial frames (Skeoch, Sussex, UK) that were worn by the subjects in all conditions.

5.11 Results

Figure 5.3 and Figure 5.4 plot the speed matches as a function of speed for high and low luminance and contrast at three eccentricities. At high luminance (open symbols), as the test stimuli moved further into the periphery there was an increase in the under-estimation of perceived speed for all speeds tested, confirming the results of Experiment 4b. At low luminance (closed symbols), in the near-periphery (6^o eccentricity) the data showed a similar under-estimation of perceived speed as at high luminance. Further into the periphery (12^o and 24^o) an under-estimation of perceived speed occurred only for slow moving stimuli (< 6 deg/sec), for faster moving stimuli (12 deg/sec) perceived speed was over-estimated.

At high luminance a reduction in contrast of both the standard and test gratings from 0.7 (open triangles) to 0.1 (open circles) showed an increase in the under-estimation of perceived speed, across all eccentricities and for all speeds tested. At low luminance the reduction in stimulus contrast did not appear to affect the perceived speed.

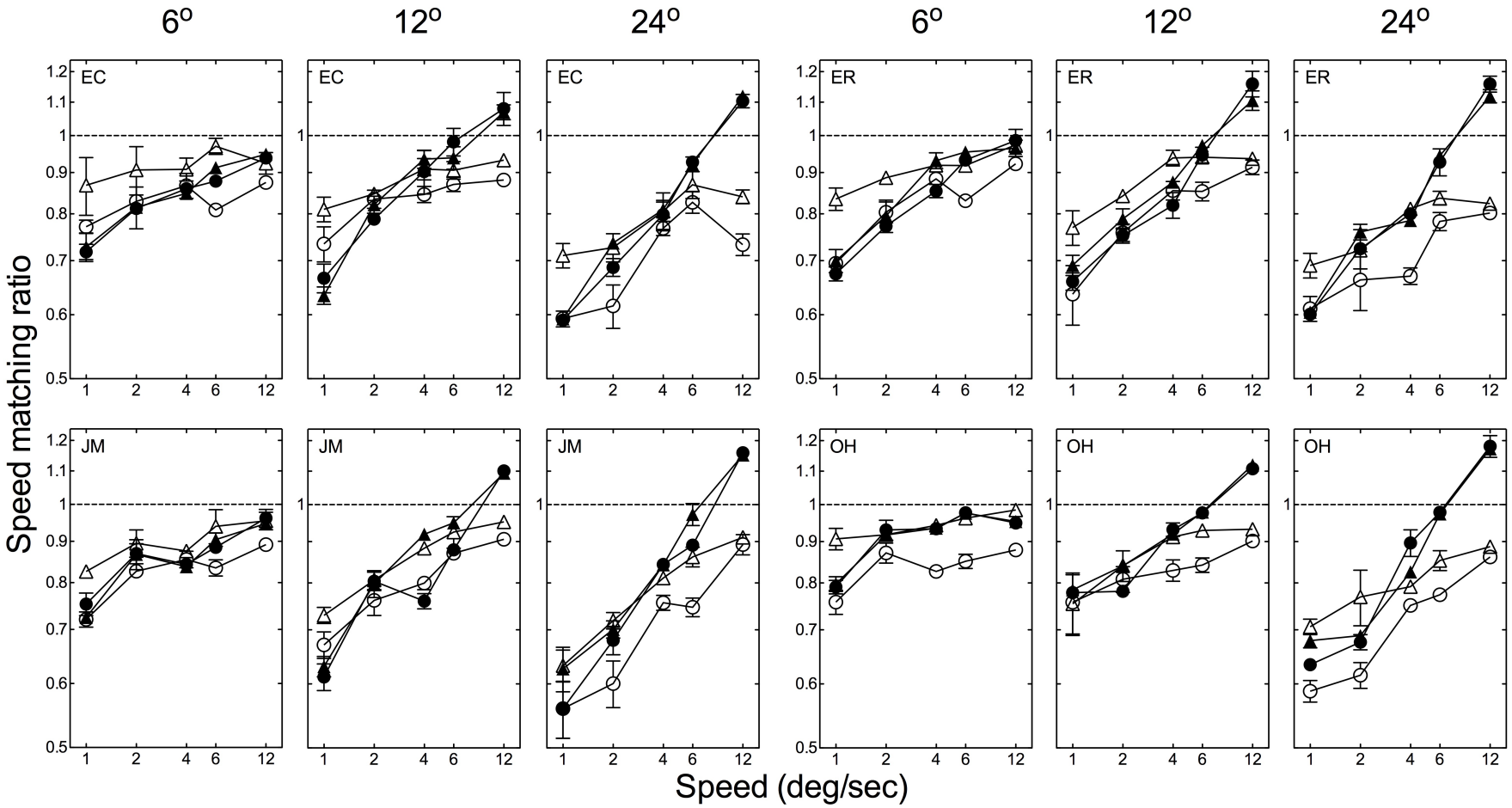

Figure 5.3: Speed matching at high (open symbols) and low (closed symbols) luminance for 0.1 (circles) and 0.7 (triangles) contrast stimuli as a function of speed for all subjects. Subjects' initials are indicated in the top left of each panel. Test grating eccentricity is indicated above panels. The broken horizontal line represents a veridical speed estimate. Speed match values greater than 1 indicate an over-estimation of matched speed, values less than 1 indicate an under-estimation of matched speed. Error bars represent ±1 SEM.

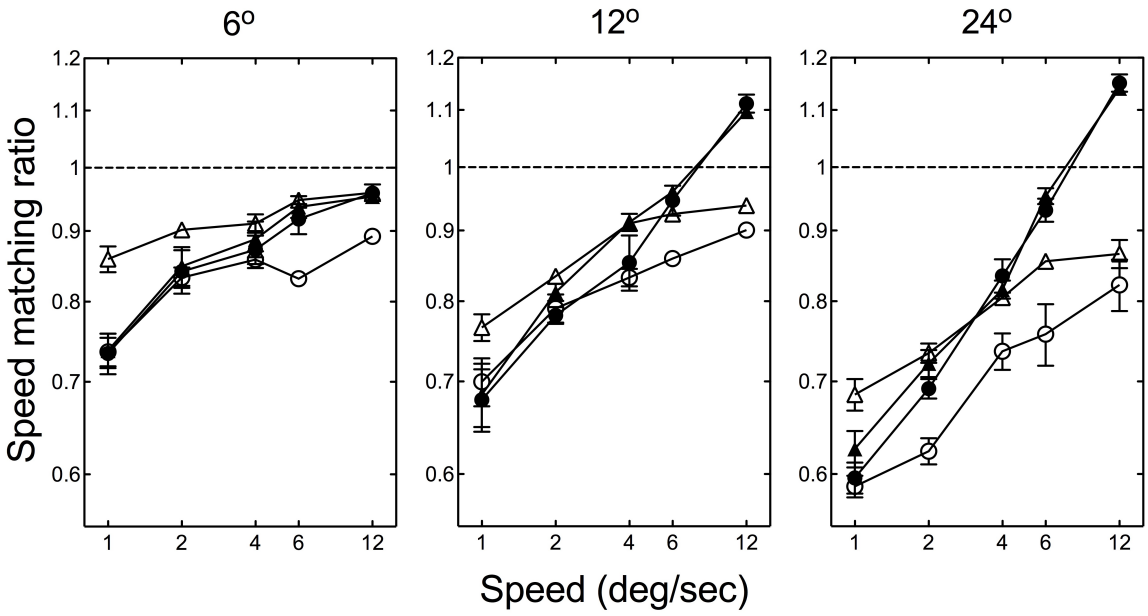

Figure 5.4: Average speed matching at high (open symbols) and low (closed symbols) luminance for 0.1 (circles) and 0.7 (triangles) contrast stimuli as a function of speed. Test grating eccentricity is indicated above panels. The broken horizontal line represents a veridical speed estimate. Speed match values greater than 1 indicate an over-estimation of matched speed, values less than 1 indicate an under-estimation of matched speed. Error bars represent ±1 SEM.

A four-way repeated measures ANOVA revealed a significant main effect of eccentricity, $F(2, 6) = 104.34$, $p < 0.001$; a significant main effect of contrast, $F(1, 3) = 336.49$, $p < 0.001$; a significant main effect of luminance, $F(1, 3) = 24.70$, $p < 0.05$; a significant main effect of speed, $F(4, 12) = 206.73$, $p < 0.001$; no significant interaction between eccentricity and contrast, $F(2, 6) = 0.44$, $p = 0.663$; a significant interaction between eccentricity and luminance, $F(2, 6) = 121.37$, $p < 0.001$; a significant interaction between eccentricity and speed, $F(8, 24) = 16.09$, $p < 0.001$; a significant interaction between contrast and luminance, $F(1, 3) = 169.15$, $p < 0.010$; no significant interaction between contrast and speed, $F(4, 12) = 2.83$, $p = 0.072$; a significant interaction between luminance and speed, $F(4, 12) = 62.14$, $p < 0.001$; no significant interaction between eccentricity, contrast and luminance, $F(2, 6) = 4.67$, $p = 0.059$; no significant interaction between eccentricity, contrast and speed, $F(8, 24) = 1.70$, $p = 0.150$; a significant interaction between eccentricity, luminance and speed,

$F(8, 24) = 9.21$, $p < 0.001$; no significant interaction between contrast, luminance and speed, $F(4, 12) = 1.41$, $p = 0.288$; and no significant interaction between eccentricity, contrast, luminance and speed, $F(8, 24) = 0.92$, $p = 0.516$.

5.12 Experiment 6: The effect of luminance upon time-to-collision estimates

Generally, studies of speed perception require the observer to make a judgement as to which of two stimuli is moving faster (e.g. Thompson et al., 2006; Thompson & Hammett, 2004; Thompson, 1982). This experimental paradigm provides us with an accurate measure of *relative* perceived speed. However, we usually observe moving stimuli as a unitary perceptual experience. I sought to investigate whether the biases in perceived speed measured in Experiment 5 occur in more typical perceptual conditions by measuring subjects' estimates of time-to-collision (TTC).

5.13 Methods

5.13.1 Subjects

Four (two male and two female) subjects aged between 23 and 27 participated in this experiment. One of the subjects (OH) was an author; the other three were naïve to the purpose of the experiment. All subjects had normal or corrected-to-normal acuity.

5.13.2 Apparatus and stimuli

All stimuli were elliptical (2^o wide × 4^o high) patches of 1 c/deg horizontally orientated sinusoidal gratings whose contrast was modulated by a 2D Gaussian ($\sigma = 16.45$ horizontally, $\sigma = 24.67$ vertically) generated using the Psychophysics

Toolbox extensions (Brainard, 1997; Kleiner et al., 2007; Pelli, 1997) for MATLAB 7.11 (MathWorks, Cambridge, UK) and displayed on an EIZO 6600-M (Hakusan, Ishikawa, Japan) monochrome monitor at a frame rate of 100 Hz. The monitor was gamma corrected using the CRS Optical photometric system (Cambridge Research Systems, Rochester, UK). The Michelson contrast of the stationary and moving patches was equal (either 0.1 or 0.7). The phases of the sinusoidal gratings in the patches were randomised from trial-to-trial. The display subtended $68^{o} \times 47^{o}$ at a viewing distance of 28.5 cm. Mean luminance was 25 cd m^{-2} for the high luminance conditions. During the low luminance conditions 1 log unit neutral density filters (NDF) (Thorlabs Inc., Newton, New Jersey, USA) were inserted into optometrist drop-cell trial frames (Skeoch, Sussex, UK) worn by the subjects, reducing the mean luminance to 2.5 cd m^{-2}. A stationary patch was located at the centre of the screen, while the moving patch was displaced horizontally to the centre of the screen. A small dark fixation spot was situated at the centre of the display.

5.13.3 Procedure

Before beginning the experiment subjects were dark adapted for at least 5 min. Two stimulus patches were presented simultaneously, a stationary patch at the centre of the screen and a drifting patch whose initial location was 32^{o} ± 10% to the right. The drifting patched moved toward the central patch at one of two speeds (6 and 12 deg/sec) and disappeared at 24^{o} ± 10% (Figure 5.5). The initial and disappearing positions of the drifting patch were randomised (within ± 10% of 32^{o} and 24^{o}, respectively) from trial-to-trial. Both speeds were presented 50 times randomly within a block of 100 trials. A small dark fixation spot surrounded by mean luminance was presented between each trial, and subjects

pressed a mouse button to initiate each trial. The subject's task was to estimate the TTC between the stationary patch and drifting patch while assuming that the drifting patch maintained the same trajectory and speed prior to disappearing by pressing a mouse button. The experiments were conducted binocularly in a semi-darkened room using a chin and headrest.

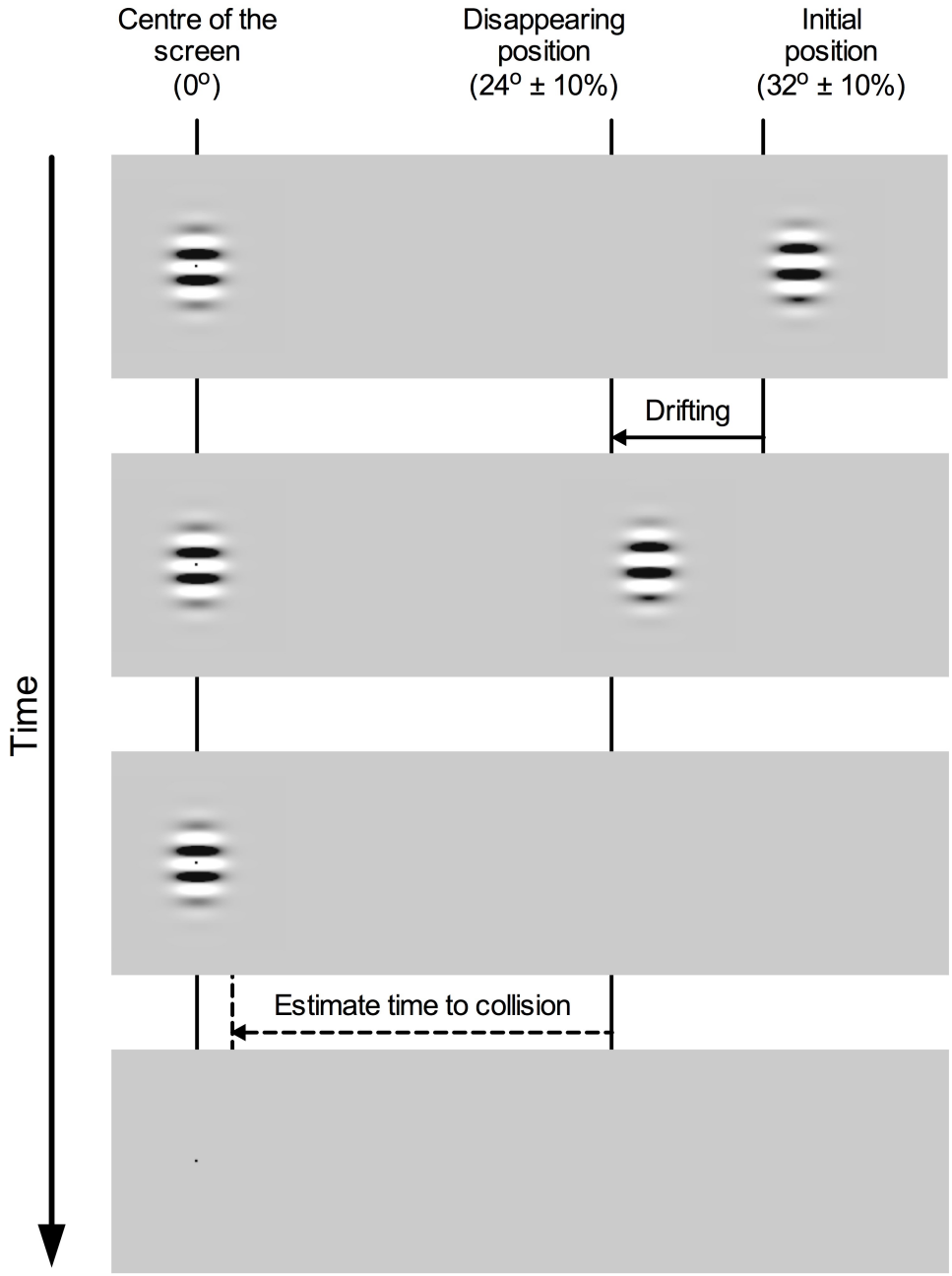

Figure 5.5: In each trial, while fixated on a central dot subjects viewed a stationary patch and drifting patch moving towards the centre of the screen. The drifting patch subsequently disappeared. Subjects estimated the TTC between the stationary patch and drifting patch.

5.14 Results

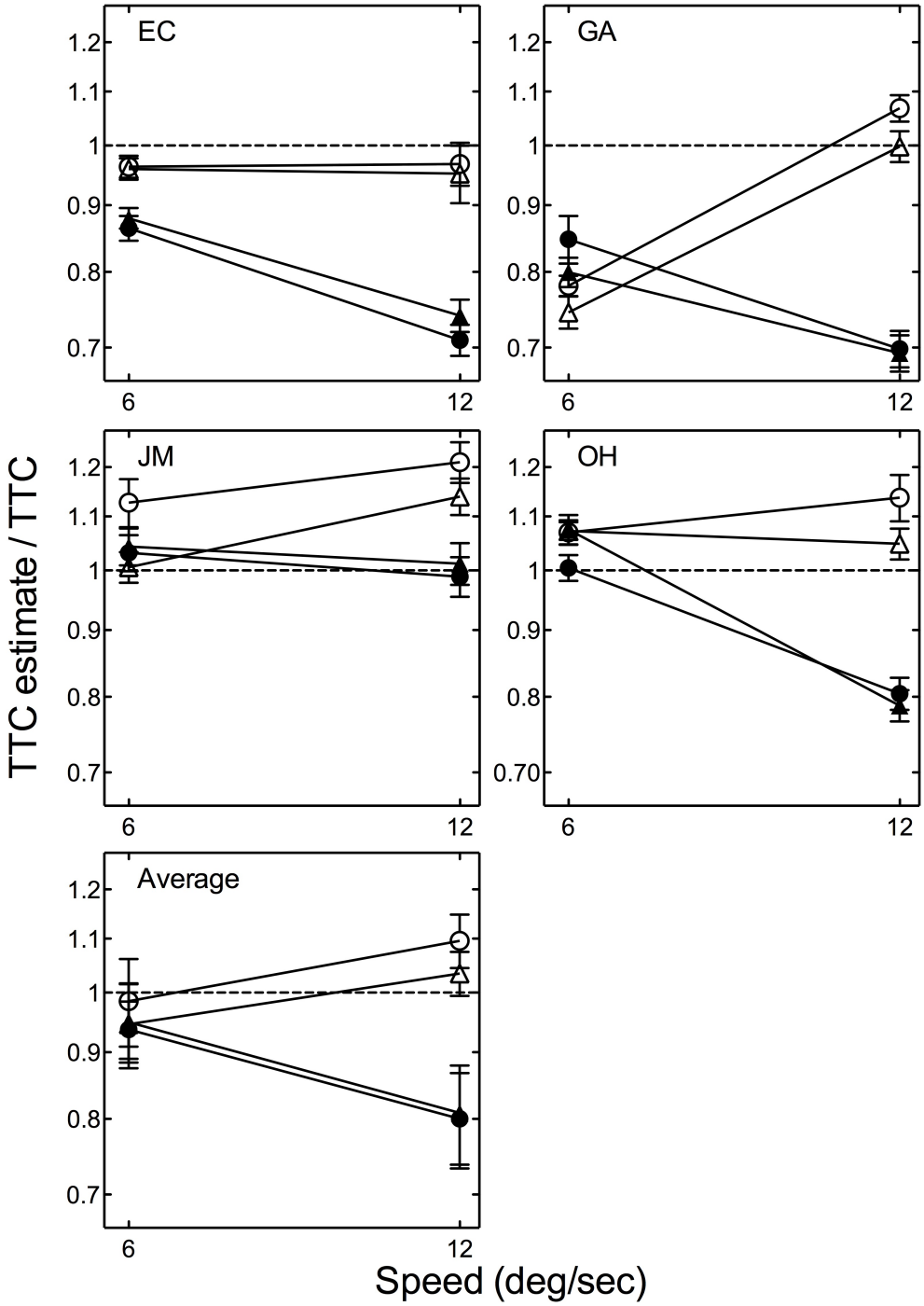

Figure 5.6: The error in TTC estimates between two patches at equal contrasts of 0.1 (open and closed circles) and 0.7 (open and closed triangles) as a function of drift speed (6 and 12 deg/sec) at high (open symbols) and low (closed symbols) luminance. Subjects' initials are indicated in the top left of each panel, the average across subjects is indicated in the lowermost left panel. The broken horizontal line at 1 represents a veridical time estimate. TTC values greater than 1 indicate an over-estimation of TTC, values less than 1 indicate an under-estimation of TTC. Error bars represent ±1 SEM.

Figure 5.6 plots the ratio of TTC estimate to veridical TTC for patches of equal contrast at high and low luminance. As speed increases from 6 to 12 deg/sec at high luminance for both 0.1 and 0.7 contrast stimuli the perceived TTC is over-estimated. However, at low luminance the perceived TTC is under-estimated. At high luminance high speed stimuli moving towards the fovea from the periphery are perceived as moving slower, at low luminance the same stimuli are perceived as moving faster.

A three-way repeated measures ANOVA revealed no significant main effect of contrast, $F(1, 3) = 1.87$, $p = 0.264$; a significant main effect of luminance, $F(1, 3) = 28.43$, $p < 0.05$; no significant main effect of speed, $F(1, 3) = 0.00$, $p = 0.950$; no significant interaction between contrast and luminance, $F(1, 3) = 7.70$, $p = 0.069$; no significant interaction between contrast and speed, $F(1, 3) = 0.89$, $p = 0.413$; a significant interaction between luminance and speed, $F(1, 3) = 27.19$, $p < 0.05$; and no significant interaction between contrast, luminance and speed, $F(1, 3) = 0.13$, $p = 0.739$.

5.15 Discussion

Moving stimuli in peripheral vision appear to move slower and have reduced contrast compared with foveally presented stimuli. The results of Experiment 4b indicate that when perceived contrast is equalised across eccentricities perceived speed is still slower in peripheral vision, showing that the perceived slowing is not just an artefact of reduced perceived contrast. This reduction in perceived speed is roughly equal at all speeds and increases with eccentricity.

A number of researchers (e.g., De Valois et al., 2000; Hammett et al., 2000; Smith & Edgar, 1994; Tolhurst et al., 1973) have previously speculated that the

code for speed may be related to the relative activity of Magno- and Parvo-cellular populations. Since these are driven by retinal parasol and midget cells respectively (Kaplan & Shapley, 1986) changes in the ratio of these populations should yield at least a qualitative prediction of how perceived speed changes with eccentricity. However, inspection of the relative densities of midget and parasol cells as a function of eccentricity poses a serious problem for such ratio models. The proportion of midget cells decreases from around 90% near the fovea to around 50% in the far periphery (ca 52 degrees), whereas the density of parasol cells increases from around 6% in the fovea to around 25% in the far periphery (Dacey, 1994, see also Watson (2014) for corroborative estimates of midget cell densities). Thus traditional ratio models would predict that perceived speed in the periphery should increase given the increased proportion of parasol cells. However, I find clear evidence that perceived speed is reduced in the periphery. Moreover, once the effect of perceived contrast is accounted for, I find that whilst perceived speed decreases with eccentricity, it is not speed-dependent. Thus the reduction in perceived speed may not be closely linked with the neural processing of speed *per se.*

How may this general reduction in perceived speed come about? One possibility is that absolute levels of neural activity may bias speed encoding such that speed is under-estimated if fewer units are active. Whilst the *proportion* of parasol cells increases with eccentricity, total ganglion cell density falls from around 27860 cells/mm^2 in the fovea to 1080 cells/mm^2 at 24 degrees eccentricity (estimated from Dacey, 1994, Figure 3A). If this, or some other phenomenon, simply serves to modulate the speed code with eccentricity, then

speed-dependent biases in perceived speed in the periphery should be observable under conditions where Parvocellular activity is reduced.

In order to test whether such a scheme could account for the changes in perceived speed found in Experiment 4 I therefore measured perceived speed in the periphery at both high and low contrast and luminance in Experiment 5. Since reducing luminance reduces the contrast gain of the Parvocellular system far more than that of the Magnocellular system (Purpura et al., 1988), I predicted that reducing luminance should lead to an increase in perceived speed in the periphery in much the same way as has been documented for central vision (Hammett et al., 2007).

The results of Experiment 5 indicate that at high luminance perceived speed was reduced as eccentricity increased, consistent with previous research (Campbell & Maffei, 1979, 1981; Cohen, 1965; Hunzelmann & Spillmann, 1984; Lichtenstein, 1963; MacKay, 1982; Tynan & Sekuler, 1982). At lower luminance, the speed of slower moving stimuli (< 6 deg/sec) was similarly under-estimated with increasing eccentricity. However, the speed of faster moving stimuli was over-estimated (> 6 deg/sec) as eccentricity increased. This pattern of results is consistent with the increases in perceived speed found in central vision at low luminance which are adequately accounted for by a simple ratio model of speed encoding (Hammett et al., 2007).

5.15.1 Estimates of TTC

The results of Experiment 6 show that at high luminance high speed stimuli moving towards the fovea from the periphery are perceived to collide later while at low luminance the same stimuli are perceived to collide sooner. There are a number of factors that could influence TTC judgements, including the method used to estimate TTC, spatial-acuity, speed, time and distance distortions in the periphery.

Three main explanations for how visual information is used to obtain an estimate of TTC have been proposed. First, TTC could be based on object speed and distance from the observer, according to the following equation:

$$TTC = \frac{distance}{speed} \quad \text{.....} \quad (5.1)$$

For this method to work both distance and speed must be estimated in order to provide the observer with enough information.

A second method for obtaining TTC in line with the approach of ecological optics (e.g. Gibson, 1966, 1979; Lee, 1976), relies upon TTC information being directly available at the eye of the observer through the changes in optic-flow information. Lee (1976, 2009) hypothesised that object distance and velocity information do not need to be estimated in order to calculate TTC. As long as the object is moving towards the observer (or the observer is moving towards the object) at a constant velocity then TTC may be estimated by the optic variable tau, which is the size of the object's retinal image divided by its rate of

expansion. Based upon this model McLeod and Ross (1983) proposed the following equation:

$$TTC = \frac{\theta_1}{(\theta_2 - \theta_1)/(t_2 - t_1)} \quad \text{..... (5.2)}$$

where θ_1 and θ_2 are the angular separations between any two target image points at times t_1 and t_2 respectively.

A third method for obtaining TTC is based upon distance change information and can be expressed as:

$$TTC = \frac{d_1}{(d_1 - d_2)/(t_1 - t_2)} \quad \text{..... (5.3)}$$

where d_1 and d_2 are the distance between the observer and the object at times t_1 and t_2 respectively (Cavallo & Laurent, 1988).

Since Experiment 6 employed a stimulus moving in the picture plane rather than motion-in-depth there was no change in the size of the stimulus's retinal image. Thus a tau strategy of estimating TTC (Lee, 1976) could not have been used by subjects. However, subjects may have been judging TTC using alternative methods such as a ratio of distance and speed or relying on distance-change information. Early psychophysical studies show that subjects are able to estimate both distance (Ross, 1967; Teghtsoonian & Teghtsoonian, 1969) and speed (Evans, 1970) in visual environments where TTC judgements may be critical, providing some support for the idea that TTC may be estimated using

these computational methods. However, it is well known that visual acuity decreases in the peripheral visual field (Millodot, 1966). A number of studies have investigated sensitivity to spatial position in the periphery and found that relative position-acuity (i.e. observers were asked to localise the position of one peripheral stimulus relative to another peripheral stimulus) decreases as eccentricity increases (e.g. Levi, Klein, & Aitsebaomo, 1985; Westheimer, 1982; Whitaker, Rovamo, Macveigh, & Makela, 1992; Yap, Levi, & Klein, 1989). Other studies that investigated absolute position-acuity (i.e. observers were asked to localise the position of one peripheral stimulus relative to the fovea) also found that position-acuity is dependent upon eccentricity and independent of contrast (Waugh & Levi, 1993). Thus there is greater uncertainty as to the initial spatial location of the stimulus in Experiment 6 than its final point of disappearance. It is not clear as to how such uncertainty might affect TTC judgements and how this might interact with luminance but there is a clear prima facie case that, had subjects been using a method to estimate TTC that required distance information, the non-veridical matching reported may have been due, at least in part, to inaccurate distance judgements made in the periphery.

Johnston and Wright (1986) reported that the reduction in perceived speed found in the periphery, at least within the range of speeds tested, can be accounted for by the reduction in spatial grain in peripheral vision. Indeed, they report that the spatial scaling factor required to account for the reduction in perceived speed is proportional to the change in mean cortical receptive field area of the macaque (Dow, Snyder, Vautin, & Bauer, 1981) as a function of eccentricity. Thus they conclude that the reduction in perceived speed in the periphery is determined by changes in spatial scale. Indeed, a range of findings

are consistent with the notion that biases in motion can be accounted for by M-scaling, for instance nulling of the motion aftereffect (Johnston & Wright, 1983) and velocity discrimination thresholds (McKee & Nakayama, 1984) are found to be consistent across eccentricity once M-scaling is accounted for. The stimuli in Experiment 6 were not M-scaled thus if subjects were using a method to estimate TTC that required an accurate measure of speed then the over-estimation in TTC at high luminance for fast moving stimuli may be due to the reduction in perceived speed with eccentricity.

Since subjects are making responses to predicted motion in the absence of visual information, cognitive operations may be been implicated (Tresilian, 1995). Two possible classes of cognitive operations for how prediction motion tasks are accomplished have been proposed, cognitive clocking and cognitive tracking (DeLucia & Liddell, 1998). Observers using cognitive clocking would obtain a TTC estimate at the onset of occlusion and mentally count down this duration before responding (e.g. Lyon & Waag, 1995; Tresilian, 1995). Alternatively, observers using cognitive tracking would continue to track the occluded object with eye movements or a spotlight of spatial attention (if required to fixate) and respond once their gaze or attention reaches the point of collision (e.g. Cooper, 1989; Finke & Shyi, 1988; Jagacinski, Johnson, & Miller, 1983; Rosenbaum, 1975). It may be the case that the non-veridical TTC judgements reported are associated with errors in these cognitive mechanisms or biases that may affect such strategies.

Studies have shown that time estimation is influenced by a number of factors such as length of duration to be estimated (Eisler, 1976), attentional demands

of a task (Zakay & Block, 1995, 1996, 1997) sex (Block, Hancock, & Zakay, 2000) and age (Block, Zakay, & Hancock, 1998). As Zakay and Block (1997) noted in their review there appear to be many contradictory findings in time estimation literature. Thus it is difficult to identify whether a particular factor would elicit an under-estimation or over-estimation of TTC. However, a range of psychophysical studies have shown that perceived duration increases when subjects view stimuli moving at fast speeds (e.g. Beckmann & Young, 2009; Brown, 1995; Johnston, Arnold, & Nishida, 2006; Kaneko & Murakami, 2009; Leiser, Stern, & Meyer, 1991). For example, Kaneko and Murakami (2009) measured the perceived duration of moving stimuli by asking subjects to compare the duration of two consecutively presented stimuli (moving at different speeds) and indicate which seemed to last longer. They found that the over-estimation in perceived duration reported by subjects increased proportionally with log speed. Any such speed-induced temporal dilation would serve to delay TTC judgements for fast stimuli in our experiment but, unfortunately, to date, the effect of luminance on this effect is unknown.

Humans are also known to make position extrapolation errors. Freyd and Finke (1984) investigated the changes in mental representation of a visually presented pattern induced by a prior sequence of displays. They presented subjects with three presentations of a rectangle which implied rotation, the duration of each presentation was 250 msec with an inter-stimulus interval of 250 msec. A test stimulus was then presented in an identical position to the third position, or in a position that is backward or forward relative to the third position of the rectangle. Subjects were asked whether the test stimulus had the same orientation as the third position and often reported the forward position as

the same as the third position. Freyd and Finke (1984) termed this memory distortion representational momentum, in which observers remembered the final position of a moving object as being more forward in its motion trajectory. Furthermore, Finke, Freyd, and Shyi (1986) found that location memory distortions are not only sensitive to the direction of implied motion but the forward memory shift associated with representational momentum increases as velocity and acceleration increase. Thus if an observer were using cognitive tracking, any under-estimation of TTC for fast stimuli may be explained by representational momentum.

In conclusion, the results of Experiment 6 appear consistent with those of Experiment 5 but there are a number of factors that may affect TTC judgements which were not controlled for in Experiment 6 and may have contributed to the subjects' judgements. Amongst these are temporal dilation, heterogeneity in positional certainty and spatial grain across the retina and cognitive strategies that may well have been influenced by all or some of these low-level biases. Thus, the results of Experiment 6 are consistent with those of Experiment 5 but no direct link can be assumed.

I conclude that, once the reduction in perceived contrast in the periphery is accounted for, speed encoding in the periphery is essentially similar to central vision. The source of the speed-independent reduction in perceived speed is uncertain but may possibly be related to the reduction in absolute cell density in the peripheral retina. The results of my initial TTC study are tentatively consistent with such a scheme.

Chapter 6

6 The effect of luminance upon biases in perceived speed

6.1 Introduction

There is still no consensus on the nature of the processes that underlie the encoding of speed in the human visual system. Much of the work that addresses this problem has looked to biases in our perception of speed to inform models of speed encoding. Human speed perception has been shown to be readily influenced by the contrast of the scene viewed (e.g. Hammett et al., 2007; Thompson, 1982; Thompson et al., 2006) and it is now well established, at slow speeds, low contrast stimuli appear to move more slowly than their higher contrast analogues but, conversely, they can appear to move more quickly at higher speeds (> 8 Hz)[1] (e.g. Thompson, 1982; Thompson et al., 2006). This observation and others has led Thompson (1982) and many others (e.g. Adelson & Bergen, 1986; Hammett et al., 2000; Harris, 1980; Smith & Edgar, 1994; Tolhurst et al., 1973) to the suggestion that speed may be encoded as the ratio of two mechanisms tuned to low and high temporal frequencies (or 'slow' and 'fast' mechanisms) (Figure 6.1, left hand panel). The ratio model can adequately account for the Thompson Effect and other perceptual biases in speed such as those induced by changes in luminance and adaptive state (Hammett et al., 2005, 2007; Thompson, 1981).

However, subsequent to the popularisation of modelling brain processes as Bayesian operations (e.g. Jaynes, 1988) a number of workers (e.g. Ascher & Grzywacz, 2000; Hürlimann et al., 2002; Stocker & Simoncelli, 2006; Weiss &

---

[1] Not all studies (e.g. Hawken et al., 1994; Stone & Thompson, 1992) find evidence of a reversal (i.e. an over-estimation) at high speed, most likely due to disparate stimulus parameters (see Hammett & Larsson, 2012).

Adelson, 1998; Weiss et al., 2002) have proposed an alternative account of how the brain encodes speed. Whilst the details of the models vary, this class of model shares the assumption that speed is encoded as the product of a likelihood (the sensory signal including noise) and a Bayesian prior that favours slow speeds. Given these two assumptions it follows that reducing the sensory signal (for instance by reducing contrast) must result in a phenomenal slow-down. The well-established Thompson Effect is thus broadly consistent with both the ratio and Bayesian class of models of speed encoding and both approaches have had some degree of success in modelling it (e.g. Ascher & Grzywacz, 2000; Hammett et al., 2000; Stocker & Simoncelli, 2006; Thompson et al., 2006).

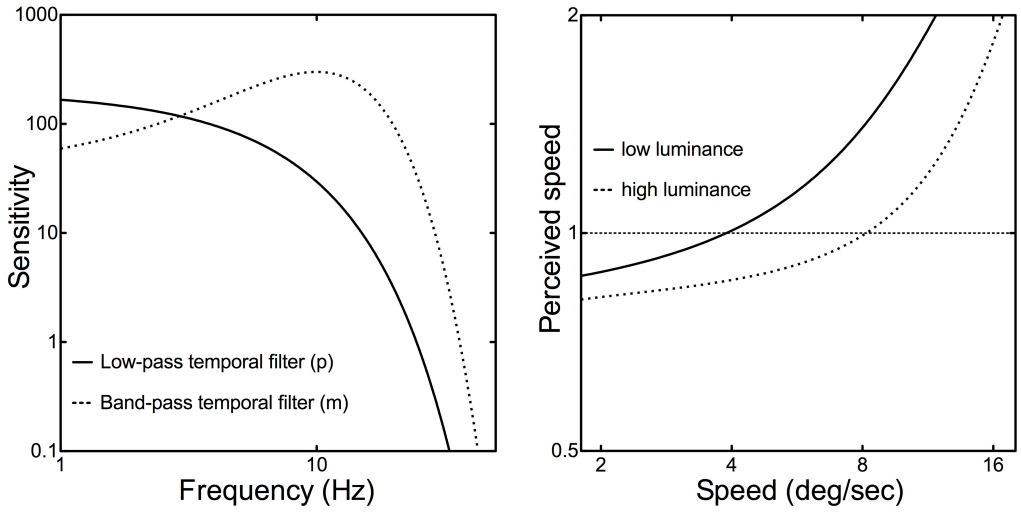

Figure 6.1: The ratio of the responses of low-pass and band-pass temporal filters (left panel, after Smith and Edgar (1994)) provides a monotonic code for speed that is consistent with under- and over-estimation of speed at low contrast. Perceived speed of a low contrast pattern encoded by a ratio model at high and low luminance is plotted in the right hand panel: values below 1 indicate an under-estimation of perceived speed at low contrast and values above 1 indicate an over-estimation of perceived speed. The ratio model shows a reduction in the under-estimation of slow speeds and an over-estimation of higher speeds at reduced luminance. Details of the simulation may be found in Appendix 2.

Vintch and Gardner (2014) have reported that the fMRI BOLD population response in V1 effectively mirrors the contrast-induced perceptual biases in speed experienced by their subjects and suggest that these biases constitute

evidence for the encoding of perceptual priors for slow speed. However, they also note that their results could be interpreted as evidence for a scheme where speed was encoded by two mechanisms whose gains varied differentially as a function of speed.

Thus there are currently two competing accounts of how speed is encoded in the human visual system that are broadly consistent with much behavioural data. One of the problems in resolving which (if either) approach provides a more consonant framework for understanding speed encoding is that both class of models tend to make similar predictions and, where they diverge, can be readily modified to accommodate empirical evidence. For instance, whilst Stocker and Simoncelli's (2006) model does not predict the reversal in perceptual bias frequently found in the Thompson Effect at higher speed, they note that their model "*would be able to fit these behaviours with a prior that increases at high speeds*" (p. 583).

There is therefore a need to identify cases where the Bayesian and ratio approaches yield unequivocally different predictions. In order to do so, I used the logic and model invoked by Hammett et al. (2007) to derive divergent predictions for Bayesian and ratio class models of speed encoding. Hammett et al. (2007) (see also Vaziri-Pashkam & Cavanagh, 2008) found that low luminance (mesopic) patterns appeared faster than higher luminance (photopic) patterns at fast (> 4 Hz) speeds. They demonstrated that a simple ratio model comprising two temporally tuned mechanisms could account for this perceptual bias if the gain of the lower frequency channel is reduced proportionately more than that of the higher frequency channel at low luminance – an assumption

that is consistent with the known properties of retinal ganglion cells that project to the M and P layers of the primate LGN (Purpura et al., 1988). In such a scheme the response of the lower frequency tuned mechanism is reduced at low luminance (relative to its response to the same contrast at high luminance) and thus the ratio model yields an increase in perceived speed relative to photopic levels. Thus this class of model predicts that at low luminance the reduction in perceived speed at low contrast will be attenuated since a proportionately larger input to the ratio will be derived from the higher frequency-tuned mechanism. Figure 6.1 shows the qualitative effect of reducing luminance (and concomitantly the gain of the 'slow' mechanism) predicted by ratio models: the Thompson Effect is reduced at slow speeds, increases at faster speeds and the speed at which the perceptual bias reverses is reduced. The Bayesian approach posits that the precision of the speed signal is reduced at low luminance. Since reducing luminance effectively reduces the contribution of the signal input equally for high and low contrast patterns, Bayesian models predict that reducing luminance will have no effect upon the contrast-induced perceptual bias but will increase discrimination thresholds as the precision of the signal is reduced. In other words, since the precision of the speed signal is reduced at low luminance, Bayesian models would predict that speed discrimination performance will deteriorate (since the certainty associated with speed is diminished). However, since the relative contrast ratio is constant, Bayesian models would predict that there should be no change in the effect of contrast on speed biases across luminance condition since the relative change in certainty with contrast is the same in both conditions. In order to test these predictions I therefore measured perceived speed and estimated discrimination

thresholds of low contrast patterns over a range of speeds and at high and low luminance.

6.2 Methods

6.2.1 Subjects

Five (two male and three female) subjects aged between 20 and 29 participated in this experiment. One of the subjects (OH) was an author; the other four were naïve to the purpose of the experiment. All subjects had normal or corrected-to-normal acuity.

6.2.2 Apparatus and stimuli

All stimuli were horizontally orientated sinusoidal gratings of 2 c/deg generated using the Psychophysics Toolbox extensions (Brainard, 1997; Kleiner et al., 2007; Pelli, 1997) for MATLAB 7.11 (MathWorks, Cambridge, UK) and displayed on an EIZO 6600-M (Hakusan, Ishikawa, Japan) monochrome monitor at a frame rate of 100 Hz. The monitor was gamma corrected using the CRS Optical photometric system (Cambridge Research Systems, Rochester, UK). The Michelson contrast of the standard (fixed speed) grating was 0.7, and the contrast of the test (variable speed) grating was 0.1. During the control conditions both the standard and test gratings were of equal contrast (either 0.1 or 0.7). The spatial and temporal phase of the standard and test gratings was randomised. The display subtended $68^{o} \times 47^{o}$ at a viewing distance of 28.5 cm. Mean luminance was 25 cd m^{-2} for the high luminance conditions and 2.5 cd m^{-2} in the low luminance conditions. In the low luminance conditions 1 log unit neutral density filters (NDF) (Thorlabs Inc., Newton, New Jersey, USA) were inserted into drop-cell trial frames (Skeoch, Sussex, UK) worn by subjects.

Stimuli were presented through two 6^{o} diameter circular windows with hard edges. Each window was located equidistant from the horizontal centre of the screen and separated by 2°. A small bright fixation spot was situated at the centre of the display.

6.2.3 Procedure

Before beginning the experiment subjects were dark adapted for at least 5 min. Two patterns were presented simultaneously for 500 msec to the right and left of a central fixation point. The standard patterns (always presented on the left) were drifting in a downward direction at one of four speeds (1, 2, 4, and 8 deg/sec). The speed of the test pattern was altered by a QUEST routine (Watson & Pelli, 1983) depending on the subject's responses. For each block the QUEST procedure was terminated after 50 trials, the data were fit to a cumulative Gaussian function using the method of least squares fit, and the 50% point of the function was derived. The mean of five (three in the control condition) such estimates was taken as the point of subjective equality (PSE). Both patterns were presented at equal luminance, in both the high or low luminance conditions. A blank screen of mean luminance was presented between each test pair and subjects had to press a mouse button in order for each test pair to be presented. The subject's task was to indicate which pattern appeared faster, by pressing a mouse button. The experiments were conducted binocularly in a semi-darkened room using a chin and headrest.

6.3 Results

At all speeds tested in the control condition speed matching was near veridical at both high and low luminance. For 0.1 contrast patterns, a two-way repeated

measures ANOVA revealed no significant main effect of speed, $F(3, 12) = 0.77$, $p = 0.532$; no significant main effect of luminance, $F(1, 4) = 2.21$, $p = 0.211$; and no significant interaction between speed and luminance, $F(3, 12) = 1.92$, $p = 0.180$. Similarly, for patterns at 0.7 contrast, a two-way repeated measures ANOVA revealed no significant main effect of speed, $F(3, 12) = 2.19$, $p = 0.142$; no significant main effect of luminance, $F(1, 4) = 0.26$, $p = 0.639$; and no significant interaction between speed and luminance, $F(3, 12) = 0.28$, $p = 0.840$, on the speed match ratio.

Figure 6.2 plots the ratio of the match speed for the low contrast stimuli to the standard speed. A value greater than one represents an over-estimate of the perceived speed of low contrast with respect to high contrast patterns and a value less than one represents an under-estimate of the perceived speed of low contrast with respect to high contrast patterns. The results clearly indicate that low contrast patterns appear slower for most speeds tested. In line with many other studies, the results also indicate that the perceptual bias in speed reverses at faster speeds such that low contrast patterns appear faster at fast speeds. A two-way repeated measures ANOVA revealed a significant main effect of speed, $F(3, 12) = 247.96$, $p < 0.001$; a significant main effect of luminance, $F(1, 4) = 727.83$, $p < 0.001$; and a significant interaction between speed and luminance, $F(3, 12) = 14.55$, $p < 0.001$, on the speed match ratio. The results clearly indicate that the speed at which this reversal in perceptual bias occurs varies with luminance. At high luminance, the perceived speed of low contrast patterns is under-estimated for speeds up to 4 deg/sec (temporal frequencies up to 8 Hz) but over-estimated at 8 deg/sec (16 Hz). At low luminance a similar reversal in the bias occurs but at a lower speed - only

speeds less than 4 deg/sec (8 Hz) were under-estimated. One-sample t tests at 4 deg/sec (8 Hz) revealed that there was no significant difference between perceived and veridical speed at low luminance (t = 0.89, df = 4, p = 0.422), but at high luminance, perceived speed was significantly lower than veridical (t = -16.15, df = 4, p < 0.001).

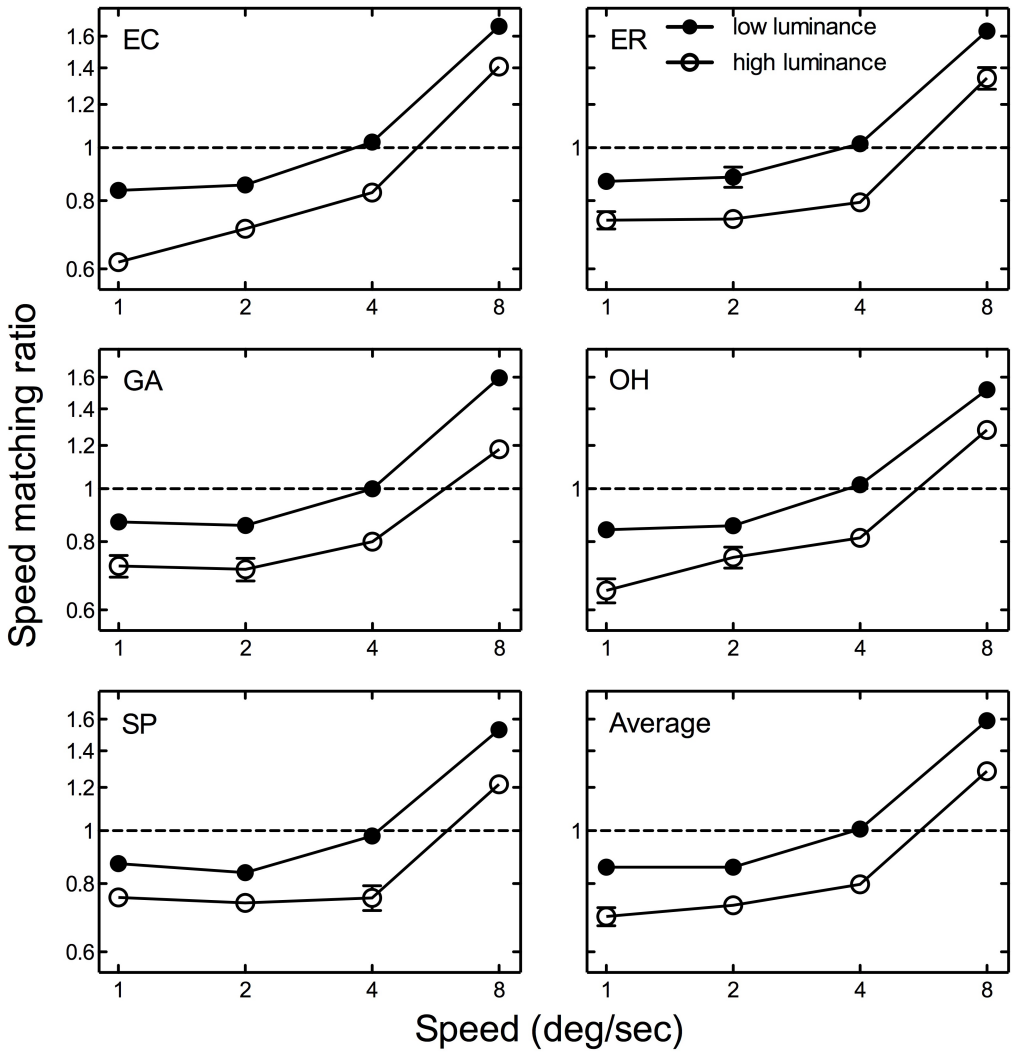

Figure 6.2: The ratio between perceived speed and physical speed of the low contrast (0.1) pattern is plotted as a function of speed at high (open symbols) and low luminance (closed symbols). Subjects' initials are indicated in the top left of each panel, the average across subjects is indicated in the lowermost right panel. The broken horizontal line represents a veridical match. Speed match values greater than 1 indicate an over-estimation of matched speed, values less than 1 indicate an under-estimation of matched speed. Error bars represent ±1 SEM.

Following Freeman, Champion, and Warren (2010) I calculated the average standard deviations of the underlying cumulative Gaussian psychometric

functions for the control conditions in order to estimate speed discrimination thresholds at high and low luminance. Figure 6.3 plots these thresholds as fractions of the standard speed for test and standard patterns of 0.1 contrast. A two-way repeated measures ANOVA revealed no significant main effect of speed, $F(3, 12) = 1.48$, $p = 0.269$; no significant main effect of luminance, $F(1, 4) = 1.43$, $p = 0.297$; and no significant interaction between speed and luminance, $F(3, 12) = 0.53$, $p = 0.668$.

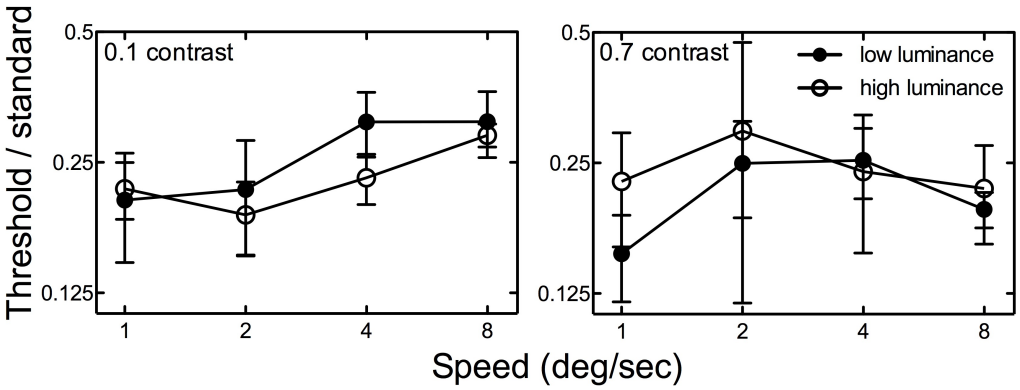

Figure 6.3: Estimated discrimination thresholds are reported as fractions of the standard speed for test and standard patterns of equal contrast (left panel, 0.1, right panel, 0.7), at high (open symbols) and low (closed symbols) luminance. Data points represent the mean of five subjects. Error bars represent ±1 SEM.

Similarly, for test and standard patterns with a contrast of 0.7, a two-way repeated measures ANOVA revealed no significant main effect of speed, $F(3, 12) = 0.56$, $p = 0.649$; no significant main effect of luminance, $F(1, 4) = 0.20$, $p = 0.677$; and no significant interaction between speed and luminance, $F(3, 12) = 0.22$, $p = 0.883$, on estimated discrimination thresholds.

At both high and low luminance the estimated discrimination thresholds as fractions of the standard speed were not affected by changes in contrast. At low luminance, a two-way repeated measures ANOVA revealed no significant main effect of speed, $F(3, 12) = 2.13$, $p = 0.150$; no significant main effect of contrast,

$F(1, 4) = 1.81$, $p = 0.249$; and no significant interaction between speed and contrast, $F(3, 12) = 0.59$, $p = 0.635$. At high luminance, a two-way repeated measures ANOVA revealed no significant main effect of speed, $F(3, 12) = 0.07$, $p = 0.976$; no significant main effect of contrast, $F(1, 4) = 0.03$, $p = 0.862$; and no significant interaction between speed and contrast, $F(3, 12) = 1.19$, $p = 0.354$.

6.4 Discussion

There is currently no consensus on how speed is encoded in the human visual system. Both Bayesian and ratio class models have been proposed and previous investigations have found perceptual biases consistent with both class of model. Recently, Sotiropoulos, Seitz, and Seriès (2014) reported that a model that combined Stocker and Simoncelli's (2006) Bayesian model with Thompson et al.'s (2006) ratio model accounted for their measurements of the Thompson Effect better than a Bayesian model alone. However, the model required 10 free parameters and the resultant best fitting parameters render the temporal filters underlying the ratio stage to be both effectively low-pass with the peak and cut-off of the ‘m’ filter at around 2 Hz and 20 Hz respectively. Thus whilst the large number of parameters does allow for a good fit to the data, the underlying filters lose the physiological plausibility of the original fixed parameter model proposed by Perrone (2005).

Vintch and Gardner's (2014) finding that the population response in V1 mirrors the contrast-induced perceptual biases in speed and flicker gave further weight to a Bayesian approach. However, Vintch and Gardner’s measurements were restricted to speeds no faster than 4 deg/sec (well below the speeds at which a

reversal in perceptual bias may be expected) and, whilst pointing to the consistency of their results with a Bayesian prior, they also note that their results are consistent with a two-channel model of speed where the prior can be considered as a frequency-dependent difference in the gain of the mechanisms. I therefore set out to provide a direct test of the predictions of ratio and Bayesian class models of speed encoding by assessing the effect of luminance upon the Thompson Effect: An early slow prior should be readily differentiated from a ratio mechanism upon the basis of the effect of luminance on speed biases. A ratio model of speed encoding that incorporates known luminance-induced changes in gain (Purpura et al., 1988) predicts that the perceptual bias will be greater at slow speeds at high luminance and greater at fast speeds at lower luminance.

In order to evaluate the effect of the luminance reduction upon Bayesian models I followed the logic of Freeman et al. (2010). They observed that a reduction of the slope of the underlying psychometric function (and thus discrimination threshold) should yield less certainty and therefore a slower perceived speed. I estimated the slopes of the underlying psychometric functions of the control conditions at 0.1 and 0.7 contrast (Figure 6.3). There is no significant difference between low and high luminance discrimination thresholds, nor is there any significant difference in discrimination thresholds at high and low contrasts. Thus, the Bayesian class of model predicts that luminance should have no effect on the contrast-induced bias in these measurements since the discriminability of the patterns is equally affected by the luminance reduction. Moreover, given the lack of any significant difference in discrimination

thresholds between high and low contrast, Bayesian models would also not predict perceptual biases as a function of contrast.

The results clearly indicate that the perceived speed of low contrast patterns is under-estimated at slow speeds and over-estimated at faster speeds as has previously been reported. I also find that this shift in perceptual bias *is* influenced by the average luminance of the image such that at lower luminance there is significantly less reduction in perceived speed and greater increase in perceived speed and a concomitant reduction in the speed at which the bias is reversed. This increase in perceived speed and the associated reduction in the speed at which the perceptual bias reversed at low luminance is predicted by the ratio class of model (e.g. Hammett et al., 2007) that incorporates the biologically plausible (Purpura et al., 1988) assumption that the gain of the lower temporal frequency tuned mechanism reduces proportionately more at low luminance.

Others (e.g. Thompson et al., 2006) have pointed out that Bayesian approaches do not predict the reversal in perceptual bias found here and elsewhere and Hammett et al. (2007) noted that the finding that stimuli appear faster at mesopic than photopic levels was also inconsistent with Bayesian models. The present finding that the perceived slowing of low contrast patterns is greater at high luminance provides a strong challenge to the plausibility of Bayesian accounts of speed encoding since they predict that lower contrast patterns should have the same relative perceived speed at either luminance and cannot explain the shift in frequency at which the bias reverses. Conversely, the perceptual biases induced by luminance and contrast (Hammett et al., 2007;

Thompson, 1982; Thompson et al., 2006; Vaziri-Pashkam & Cavanagh, 2008) and the effect of luminance I find here are all consistent with a simple, biologically plausible two-mechanism ratio model.

6.5 Conclusions

Bayesian approaches to characterising brain function have become very popular in recent years and have been used to model a range of processes such as perceived speed under smooth pursuit, sensorimotor learning and tactile perception (Freeman et al., 2010; Goldreich & Tong, 2013; Körding & Wolpert, 2004). Indeed, the impressive range of studies proposing a Bayesian characterisation of sensory processes (Geisler & Kersten, 2002; Langer & Bülthoff, 2001) led Körding and Wolpert (2006) to suggest that *"the Bayesian process may be a fundamental element of sensory processing"* (p. 321). Amongst the evidence cited by Körding and Wolpert to support this suggestion was Stocker and Simoncelli's (2006) Bayesian model of speed encoding. However, their model (like all pure Bayesian models) fails to predict the reversal in perceptual bias found at higher speeds in the Thompson Effect and is inconsistent with both previous work that has manipulated luminance (e.g. Hammett et al., 2007; Vaziri-Pashkam & Cavanagh, 2008) and the results presented here.

It is important to stress that these data may be consistent with a range of models of speed encoding (e.g. Heeger, 1987; Simoncelli & Heeger, 1998) other than ratio models and it is not my intention to make any strong claim in support of ratio models upon the basis of my results. Indeed, it is appropriate to acknowledge that the basis of proposed ratio models is itself *ad hoc* in nature

and rests upon assumptions regarding gain changes with luminance that rely upon relatively sparse evidence. However, the evidence I report here, and previous reports of perceptual biases in speed perception, are not readily reconciled with Bayesian accounts of speed encoding in the human brain.

Chapter 7

7 General Discussion

Despite remarkable advances in our understanding of visual processing there is surprisingly little consensus on the question of how object speed is encoded. The various computational approaches may be characterised as Bayesian, gradient and ratio based. The experiments reported in the previous chapters were designed to cast light upon how our biases in speed perception may inform the viability of these various classes of model.

Chapter 3 described two experiments that investigated which adaptation parameters determined the ramp after-effect. The ramp after-effect has previously been invoked to support gradient-based models of motion perception (e.g. Anstis, 1997; Ashida & Scott-Samuel, 2014; Scarfe & Johnston, 2010). If gradient motion detectors mediate the ramp after-effect it would be reasonable to assume that gradient would determine the strength of the ramp after-effect. The results of Experiments 1 and 2 indicate that this is not the case. Several ramp profiles were tested and the results showed that ramp profile (gradient shape) had no effect on the duration of the after-effect. Rather, the duration of the after-effect is well characterised by the amplitude of the luminance ramps, consistent with the findings of Arnold and Anstis (1993). These experiments also sought to test the proposition that the ramp after-effect is mediated by ON- and OFF- channels (Anstis, 1967; Arnold & Anstis, 1993). Subjects were adapted to ascending and descending luminance ramps at high and low luminance. The results indicated that the duration of after-effect was attenuated only for descending ramps at low luminance. Since OFF cell responses are known to be reduced at low luminance (Dolan & Schiller, 1989, 1994; Ramoa et

al., 1985) this finding is entirely consistent with the proposition that the ramp after-effect is mediated by ON- and OFF-channels.

Chapter 4 described an experiment that measured the biases in speed perception attributable to contrast. Thompson (1982) showed that at low contrast slow moving stimuli appeared to move slower while fast moving stimuli appeared to move faster. However, temporal frequency also changes the perception of contrast (Georgeson, 1987). Thus Experiment 3 attempted to answer the question of whether the shift in perceived speed is a true reflection of speed processing mechanisms or simply an artefact of changes in perceived contrast with temporal frequency. The results showed that speed matching with matched contrasts produced the same biases in speed perception as speed matching with constant physical contrasts. The biases in perceived speed at low contrasts do not appear to be due to changes in perceived contrast due to temporal frequency but a genuine effect of underlying speed-processing mechanisms.

Chapter 5 documents an investigation of whether perceived slowing of stimuli in the periphery may be accounted for in terms of a perceived reduction in contrast. The results of Experiment 4 indicate that the reduction in perceived contrast as eccentricity is increased does contribute to the perceptual slowing down of moving patterns in the periphery. However, when contrast is matched for peripherally presented patterns they are still perceived as slower. Traditional ratio models would predict that perceived speed in the periphery should increase given the increased proportion of parasol cells. Currently, it is not clear why perceived speed is reduced in the periphery but one possibility is that the

reduction in absolute density of cells as a function of eccentricity leads to the effect upon the basis of a relative reduction in gross neural activity.

In Experiment 5 I investigated how luminance and eccentricity affect perceived speed in order to further investigate the mechanisms underlying this perceptual bias. The results of Experiment 5 indicate that at high luminance perceived speed was reduced as eccentricity increased, consistent with previous research (Campbell & Maffei, 1979, 1981; Cohen, 1965; Hunzelmann & Spillmann, 1984; Lichtenstein, 1963; MacKay, 1982; Tynan & Sekuler, 1982). At lower luminance, the speed of slower moving stimuli was similarly under-estimated with increasing eccentricity. However, the speed of faster moving stimuli was over-estimated as eccentricity increased. This pattern of results is consistent with the increases in perceived speed found in central vision at low luminance which are adequately accounted for by a simple ratio model of speed encoding (e.g. Hammett et al., 2007; Thompson et al., 2006; Vaziri-Pashkam & Cavanagh, 2008). Once the reduction in perceived contrast in the periphery is accounted for, speed encoding in the periphery is essentially similar to central vision. The source of the speed-independent reduction in perceived speed is uncertain but may possibly be related to the reduction in absolute cell density in the peripheral retina.

The experiments reported thus far have used relative judgements of speed. This protocol leaves open the possibility that the perceptual biases they reveal are due to the relativity of the task and do not pertain to more realistic scene processing. In order to evaluate the extent to which these findings based upon relative speed judgements can be applied to unitary perceptual experience,

Experiment 6 inferred biases in speed perception as a function of eccentricity by measuring subjects' estimates of TTC. The results indicate that luminance and speed had a significant effect upon TTC estimation and that these effects are consistent with the results of Experiment 5 which deployed a relative judgement of speed. At high luminance, high speed stimuli moving towards the fovea from the periphery are perceived as moving slower, at low luminance, the same stimuli are perceived as moving faster. It is possible that changes in perceived duration may have influenced TTC estimates (e.g. Ayhan et al., 2009; Bruno et al., 2011) but this seems an unlikely explanation given the consistency of the results with those of Experiment 5 where such an explanation could not be invoked to explain the perceptual biases observed.

Chapter 6 described an experiment that investigated the effects of contrast and luminance upon speed perception. While there are several models of speed perception and no consensus on how speed is encoded in the human visual system both Bayesian and ratio class of models are consistent with much behavioural data and tend to make similar predictions. In order to differentiate between the two class of models I investigated speed perception at low luminance for which the two class of models produce different predictions. Bayesian models predict that lower contrast patterns would have the same relative perceived speed at both high and low luminance. The ratio model I deployed predicts that at low luminance the under-estimation in perceived speed at low contrast and slow speeds will be attenuated while the over-estimation at higher speeds would increase. The results of Experiment 7 showed that at low luminance the Thompson Effect is still present, but across all speeds tested low luminance patterns appeared faster than high luminance

patterns. The shift in changes in speed perception at low luminance can be accounted for by a ratio model. The results of Experiment 7 are inconsistent with Bayesian models since a slow prior simply cannot account for the changes in the Thompson Effect found at low luminance.

Overall, the results of these studies are entirely consistent with ratio-type approaches to modelling speed encoding in the human visual system. Experiments 1 and 2 are not consistent with gradient models and Experiments 4 - 7 are inconsistent with Bayesian approaches. However, whilst the present findings are consistent with the ratio class of model they do not offer any clear evidence for such an implementation within the visual system and in a number of the studies reported here conclusions have been based upon speed judgements using only one spatial frequency of sinusoidal grating. Thus the possibility remains in these experiments that the subjects made their judgements upon the basis of the temporal frequency of the gratings rather than their speed. Clearly a parametric study that repeated these measurements for a range of spatial and temporal frequencies would be of benefit in disambiguating the interpretation of my results in this respect. Moreover this problem of disambiguating speed and temporal frequency also resides within imaging studies. For instance, Hammett, Smith, Wall and Larsson (2013) showed that whilst there was no unambiguous response in the fMRI Bold signal to varying speed in visual cortex, a multivariate classifier could predict speed in all cortical areas measured. Thus it may be that the encoding of speed is distributed in the multivariate neuronal population response of visual cortex. However, Hammett et al.'s use of a single spatial frequency sinusoidal grating leaves open the possibility that the multivariate BOLD response encodes temporal frequency

rather than speed per se, thus a parametric study that employed stimuli with a range of spatial and temporal frequencies would be of great value in this respect. Similarly, direct electrophysiological measurements of the inputs to early speed-sensitive neurones in V1 could prove invaluable in furthering our understanding of the origins of a code for speed. It has been known for some time that two sub-populations of non-directional macaque V1 cells are in temporal quadrature phase and have differing spatial phases of their receptive fields (De Valois et al., 2000). De Valois et al. demonstrated that the receptive fields of directionally tuned V1 cells can be constructed by linear combination of the spatio-temporal characteristics of the two sub-populations of non-directional cells in approximate quadrature phase (see also Peterson, Li and Freeman (2004) for similar evidence in the cat). However, there is still no direct anatomical or physiological evidence to support De Valois et al.'s suggestion that the two V1 sub-populations receive discrete inputs from magno- and parvo-cellular pathways. Clearly, further studies in both these areas will cast a strong light upon the origins of the earliest speed signals in the visual cortex which, in turn, will serve to inform our understanding of the more robust velocity estimates which are likely extracted from these early V1 cells in higher cortical areas.

References

Adelson, E. H., & Bergen, J. R. (1985). Spatiotemporal energy models for the perception of motion. *Journal of the Optical Society of America A*, *2*(2), 284–299.

Adelson, E. H., & Bergen, J. R. (1986). The extraction of Spatio-temporal Energy in Human and Machine Vision. In *Proceedings from the Workshop on Motion: Representation and Analysis* (pp. 151–155). Charleston, SC: IEEE Computer Society Press.

Adelson, E. H., & Movshon, J. A. (1982). Phenomenal coherence of moving visual patterns. *Nature*, *300*(5892), 523–525.

Allen, H., & Derrington, A. M. (2001). Distracting attention from Contrast-defined motion. *Investigative Ophthalmology and Visual Science*, *42*(4), 5061.

Allen, H., & Ledgeway, T. (2003). Attentional modulation of threshold sensitivity to first-order motion and second-order motion patterns. *Vision Research*, *43*(27), 2927–2936.

Anderson, S. J., & Burr, D. (1985). Spatial and temporal selectivity of the human motion detection system. *Vision Research*, *25*(8), 1147–1154.

Anderson, T. W., McCarthy, P. J., & Tukey, J. W. (1946). “Staircase” method of sensitivity testing. In *NAVORD Report 65-46*. Washington, D. C.

Anstis, S. (1967). Visual Adaptation to Gradual Change of Intensity. *Science*, *155*(3763), 710–712.

Anstis, S. (1980). The perception of apparent movement. *Philosophical Transactions of the Royal Society of London B: Biological Sciences*, *290*, 153–168.

Anstis, S. (1997). Experiments on motion aftereffects. In M. Jenkin & L. Harris (Eds.), *Computational and Psychophysical Mechanisms of Visual Coding*.

Cambridge: Cambridge University Press.

Anstis, S., & Cavanagh, P. (1981). What Goes Uo Need Not Come Down: Moving Flicker Edges Give Position Motion Aftereffects. In J. Long & A. Baddeley (Eds.), *Attention and Performance IX*. Hillsdale, N.J.: Lawrence Erlbaum Associates.

Anstis, S., & Harris, J. (1987). Magnification factor for adaptation of a visual transient mechanism. *Journal of the Optical Society of America A*, *4*(8), 1688–1698.

Anstis, S., & Moulden, B. (1970). After effect of seen movement: Evidence for peripheral and central components. *Quarterly Journal of Experimental Psychology*, *22*(2), 222–229.

Arnold, K., & Anstis, S. (1993). Properties of the Visual Channels that Underlie Adaptation to Gradual Change of Luminance. *Vision Research*, *33*(1), 47–54.

Ascher, D., & Grzywacz, N. M. (2000). A Bayesian model for the measurement of visual velocity. *Vision Research*, *40*(24), 3427–3434.

Ashida, H., & Scott-Samuel, N. E. (2014). Motion influences the perception of background lightness. *I-Perception*, *5*(1), 41–49. doi:10.1068/i0628

Ayhan, I., Bruno, A., Nishida, S., & Johnston, A. (2009). The spatial tuning of adaption-based time compression. *Journal of Vision*, *9*(11), 1–12.

Baker, C. (1999). Central neural mechanisms for detecting second-order motion. *Current Opinion in Neurobiology*, *9*(4), 461–466.

Baker, C., & Braddick, O. (1985). Eccentricity-dependent scaling of the limits for short-range apparent motion perception. *Vision Research*, *25*(6), 803–812.

Baker, C., & Cynader, M. (1988). Space-time separability of direction selectivity in cat striate cortex neurons. *Vision Research*, *28*(2), 239–246.

Banks, W., & Kane, D. (1972). Discontinuity of seen motion reduces the visual motion aftereffect. *Perception & Psychophysics*, *12*, 69–72.

Barfield, L. P., & Tolhurst, D. J. (1975). The detection of complex gratings by the human visual system. *The Journal of Physiology*, *248*(1), 37–38.

Beaton, A., & Blakemore, C. (1981). Orientation selectivity of the human visual system as a function of retinal ecentricity and visual hemfield. *Perception*, *10*(3), 273–282.

Beckmann, J. S., & Young, M. E. (2009). Stimulus dynamics and temporal discrimination: implications for pacemakers. *Journal of Experimental Psychology: Animal Behavior Processes*, *35*(4), 525.

Benton, C., & Johnston, A. (2001). A new approach to analysing texture-defined motion. *Proceedings of the Royal Society of London B: Biological Sciences*, *268*, 2435–2443.

Benton, C., Johnston, A., McOwan, P. W., & Victor, J. (2001). Computational modeling of non-Fourier motion: further evidence for a single luminance-based mechanism. *Journal of the Optical Society of America A*, *18*(9), 2204–2208.

Blakemore, C., & Campbell, F. W. (1969). On the existence of neurones in the human visual system selectively sensitive to the orientation and size of retinal images. *The Journal of Physiology*, *203*(1), 237–260.

Blakemore, C., Muncey, J. P., & Ridley, R. M. (1973). Stimulus specificity in the human visual system. *Vision Research*, *13*(10), 1915–1931.

Blakemore, C., & Vital-Durand, F. (1986). Organization and post-natal development of the monkey's lateral geniculate nucleus. *The Journal of Physiology*, *380*, 453–491.

Blakemore, M. R., & Snowden, R. J. (1999). The effect of contrast upon

perceived speed: A general phenomenon? *Perception*, *28*(1), 33–48.

Block, R. A., Hancock, P., & Zakay, D. (2000). Sex differences in duration judgments: a meta-analytic review. *Memory & Cognition*, *28*(8), 1333–1346.

Block, R. A., Zakay, D., & Hancock, P. A. (1998). Human aging and duration judgments: A meta-analytic review. *Psychology and Aging*, *13*(4), 584.

Bracewell, R. (1999). *The Fourier Transform and Its Application* (3rd ed.). New York: McGraw-Hill.

Braddick, O. J. (1974). A short-range process in apparent motion. *Vision Research*, *14*, 519–527.

Braddick, O. J. (1980). Low-level and high-level processes in apparent motion. *Philosophical Transactions of the Royal Society of London B: Biological Sciences*, *290*, 137–151.

Braddick, O. J., Campbell, F. W., & Atkinson, J. (1978). Channels in vision: basic aspects. In *Handbook of sensory physiology: Vol VIII. Perception*. Heidelberg: Springer.

Brainard, D. (1997). The psychophysics toolbox. *Spatial Vision*, 433–436.

Brooks, K. (2001). Stereomotion speed perception is contrast dependent. *Perception*, *30*(6), 725–731.

Brown, J. F. (1931). The visual perception of velocity. *Psychologische Forschung*, *14*(1), 199–232.

Brown, S. W. (1995). Time, change, and motion: The effects of stimulus movement on temporal perception. *Perception & Psychophysics*, *57*, 105–116.

Bruno, A., Ayhan, I., & Johnston, A. (2011). Duration expansion at low luminance levels. *Journal of Vision*, *11*(14), 1–13.

Callaway, E. M. (2005). Structure and function of parallel pathways in the primate early visual system. *The Journal of Physiology*, *566*(1), 13–19.

Campbell, F. W., Cooper, G. F., & Enroth-Cugell, C. (1969). The spatial selectivity of the visual cells of the cat. *The Journal of Physiology*, *203*(1), 223–235.

Campbell, F. W., & Maffei, L. (1979). Stopped visual motion. *Nature*, *278*, 192–193.

Campbell, F. W., & Maffei, L. (1981). The influence of spatial frequency and contrast on the perception of moving patterns. *Vision Research*, *21*(5), 713–721.

Campbell, F. W., & Robson, J. G. (1968). Application of Fourier analysis to the visibility of gratings. *The Journal of Physiology*, *197*(3), 551–566.

Carlson, V. R. (1962). Adaptation in the perception of visual velocity. *Journal of Experimental Psychology*, *64*(2), 192–197.

Carter, B. E., & Henning, G. B. (1971). The detection of gratings in narrow-band visual noise. *The Journal of Physiology*, *219*(2), 355–365.

Cavallo, V., & Laurent, M. (1988). Visual information and skill level in time-to-collision estimation. *Perception*, *17*(5), 623–632.

Cavanagh, P. (1992). Attention-Based Motion Perception.

Cavanagh, P., & Anstis, S. (1986). Brightness shift in drifting ramp gratings isolates a transient mechanism. *Vision Research*, *26*(6), 899–908.

Cavanagh, P., Boeglin, J., & Favreau, O. (1985). Perception of motion in equiluminous kinematograms. *Perception*, *14*(2), 151–162.

Cavanagh, P., & Mather, G. (1989). Motion: The long and short of it. *Spatial Vision*, *3*(2), 103–129.

Champion, R. A., Hammett, S. T., & Thompson, P. G. (2007). Perceived

direction of plaid motion is not predicted by component speeds. *Vision Research*, *47*(3), 375–383.

Chang, J., & Julesz, B. (1983). Displacement limits for spatial frequency filtered random-dot cinematograms in apparent motion. *Vision Research*, *23*(12), 1379–1385.

Chubb, C., & Sperling, G. (1988). Drift-balanced random stimuli: a general basis for studying non-Fourier motion perception. *Journal of the Optical Society of America A*, *5*(11), 1986–2007.

Cohen, R. L. (1965). Adaptation effects and after effects of moving patterns viewed in the periphery of the visual field. *Scandinavian Journal of Psychology*, *6*(2), 257–264.

Comptes Rendus des Séances de la 16e Conférence Générale des Poids et Mesures (CGPM). (1979). Sèvres, France: BIPM.

Cooper, L. A. (1989). Mental models of the structure of visual objects. In B. E. Shepp & S. Ballesteros (Eds.), *Object perception: Structure and process* (pp. 91–119). Hillsdale, N.J.: Lawrence Erlbaum Associates.

Cornsweet, T. N. (1962). The Staircase-Method in Psychophysics. *The American Journal of Psychology*, *75*(3), 485–491.

Dacey, D. M. (1994). Physiology, morphology and spatial densities of identified ganglion cell types in primate retina. In *Higher-Order Processing in the Visual System, Ciba Foundation Symposium 184* (pp. 12–34). Chichester, UK: Wiley.

De Valois, K. K. (1977). Spatial frequency adaptation can enhance contrast sensitivity. *Vision Research*, *23*, 249–256.

De Valois, K. K., De Valois, R. L., & Yund, E. W. (1979). Responses of striate cortex cells to grating and checkerboard patterns. *The Journal of*

Physiology, *291*(1), 483–505.

De Valois, R. L., Albrecht, D. G., & Thorell, L. G. (1977). Spatial tuning of LGN and cortical cells in the monkey visual system. In H. Spekreijse & H. van der Tweel (Eds.), *Spatial contrast* (pp. 60–63). Amsterdam: Elsevier.

De Valois, R. L., Albrecht, D. G., & Thorell, L. G. (1982). Spatial frequency selectivity of cells in macaque visual cortex. *Vision Research*, *22*(5), 545–559.

De Valois, R. L., Cottaris, N. P., Mahon, L. E., Elfar, S. D., & Wilson, J. A. (2000). Spatial and temporal receptive fields of geniculate and cortical cells and directional selectivity. *Vision Research*, *40*(27), 3685–3702.

De Valois, R. L., & De Valois, K. K. (1980). SPATIAL VISION. *Annual Review of Psychology*, *31*, 309–341.

De Valois, R. L., & De Valois, K. K. (1988). *Spatial Vision*. Oxford, UK: Oxford University Press.

DeLucia, P. R., & Liddell, G. W. (1998). Cognitive motion extrapolation and cognitive clocking in prediction motion task. *Journal of Experimental Psychology. Human Perception and Performance*, *24*(3), 901–914.

Derrington, A. M., Krauskopf, J., & Lennie, P. (1984). Chromatic mechanisms in lateral geniculate nucleus of macaque. *The Journal of Physiology*, *357*, 241–265.

Derrington, A. M., & Lennie, P. (1984). Spatial and temporal contrast sensitivities of neurones in lateral geniculate nucleus of macaque. *The Journal of Physiology*, *357*, 219–240.

Derrington, A. M., & Suero, M. (1991). Motion of complex patterns is computed from the perceived motions of their components. *Vision Research*, *31*(1), 139–149.

Derrington, A. M., & Ukkonen, O. (1999). Second-order motion discrimination by feature-tracking. *Vision Research*, *39*(8), 1465–1475.

Dixon, W. J., & Mood, A. M. (1948). A Method for Obtaining and Analyzing Sensitivity Data. *Journal of the American Statistical Association*, *43*(241), 109–126.

Dolan, R. P., & Schiller, P. H. (1989). Evidence for only depolarizing rod bipolar cells in the primate retina. *Visual Neuroscience*, *2*(5), 421–424.

Dolan, R. P., & Schiller, P. H. (1994). Effects of ON channel blockade with 2-amino-4-phosphonobutyrate (APB) on brightness and contrast perception in monkeys. *Visual Neuroscience*, *11*(1), 23–32.

Dow, B. M., Snyder, A. Z., Vautin, R. G., & Bauer, R. (1981). Magnification factor and receptive field size in foveal striate cortex of the monkey. *Experimental Brain Research*, *44*(2), 213–228.

Edgar, G. K., & Smith, A. T. (1990). Hemifield differences in perceived spatial frequency. *Perception*, *19*(6), 759–766.

Eisler, H. (1976). Experiments on subjective duration 1868-1975: A collection of power function exponents. *Psychological Bulletin*, *83*(6), 1154–1171.

Emerson, R. C., Bergen, J. R., & Adelson, E. H. (1992). Directionally Selective Complex Cells and the Computation of Motion Energy in cat Visual Cortex. *Vision Research*, *32*(2), 203–218.

Enroth-Cugell, C., & Robson, J. G. (1966). The contrast sensitivity of retinal ganglion cells of the cat. *The Journal of Physiology*, *187*, 517–552.

Evans, L. (1970). Automobile-speed estimation using movie-film simulation. *Ergonomics*, *13*(2), 231–237.

Exner, S. (1894). *Entwurf zu einer physiologischen Erklärung der psychischen Erscheinungen*. Vienna: F. Deuticke.

Fennema, C. L., & Thompson, W. B. (1979). Velocity Determination in Scenes Containing Several Moving Objects. *Computer Graphics and Image Processing*, *9*, 301–315.

Ferrera, V. P., & Wilson, H. R. (1990). Perceived direction of moving two-dimensional patterns. *Vision Research*, *30*(2), 273–287.

Finke, R. A., Freyd, J. J., & Shyi, G. C. (1986). Implied velocity and acceleration induce transformations of visual memory. *Journal of Experimental Psychology: General*, *115*(2), 175–188.

Finke, R. A., & Shyi, G. C. (1988). Mental extrapolation and representational momentum for complex implied motions. *Ournal of Experimental Psychology: Learning, Memory, and Cognition*, *14*(1), 112.

Foster, K. H., Gaska, J. P., Nagler, M., & Pollen, D. A. (1985). Spatial and temporal frequency selectivity of neurones in visual cortical areas V1 and V2 of the macaque monkey. *The Journal of Physiology*, *365*, 331–363.

Fourier, J. B. J. (1822). *Théorie analytique de la chaleur*. Paris: Firmin Didot.

Fredericksen, R. E., & Hess, R. F. (1998). Estimating multiple temporal mechanisms in human vision. *Vision Research*, *38*(7), 1023–1040.

Freeman, T. C. A., Champion, R. A., & Warren, P. A. (2010). A Bayesian Model of Perceived Head-Centered Velocity during Smooth Pursuit Eye Movement. *Current Biology*, *20*(8), 757–762.

Freyd, J. J., & Finke, R. A. (1984). Representational momentum. *Journal of Experimental Psychology: Learning, Memory, and Cognition*, *10*(1), 126–132.

Geisler, W. S., & Kersten, D. (2002). Illusions, perception and Bayes. *Nature Neuroscience*, *5*(6), 508–510.

Georgeson, M. A. (1975). *Mechanisms of Visual Image Processing: Studies on*

Pattern Interaction and Selective Channels in Human Vision. University of Sussex.

Georgeson, M. A. (1987). Temporal properties of spatial contrast vision. *Vision Research*, *27*(5), 765–780.

Gibson, J. J. (1966). *The Senses Considered as Perceptual Systems*. Boston, MA: Houghton Mifflin.

Gibson, J. J. (1979). *The Ecological Approach to Visual Perception*. Boston, MA: Houghton Mifflin.

Goldreich, D., & Tong, J. (2013). Prediction, postdiction, and perceptual length contraction: a bayesian low-speed prior captures the cutaneous rabbit and related illusions. *Frontiers in Psychology*, *4*(221), 1–26.

Gouras, P. (1968). Identification of cone mechanisms in monkey ganglion cells. *The Journal of Physiology*, *199*(3), 533–547.

Graham, N. (1972). Spatial frequency channels in the human visual system: Effects of luminance and pattern drift rate. *Vision Research*, *12*(1), 53–68.

Hall, J. L. (1981). Hybrid adaptive procedure for estimation of psychometric functions. *The Journal of the Acoustical Society of America*, *69*(6), 1763–1769.

Hall, J. L. (1983). A procedure for detecting variability of psychophysical thresholds. *The Journal of the Acoustical Society of America*, *73*(2), 663–667.

Hammett, S. T., Champion, R. A., Morland, A. B., & Thompson, P. G. (2005). A ratio model of perceived speed in the human visual system. *Proceedings of the Royal Society B: Biological Sciences*, *272*(1579), 2351–2356.

Hammett, S. T., Champion, R. A., Thompson, P. G., & Morland, A. B. (2007). Perceptual distortions of speed at low luminance: Evidence inconsistent

with a Bayesian account of speed encoding. *Vision Research*, *47*(4), 564–568.

Hammett, S. T., & Larsson, J. (2012). The effect of contrast on perceived speed and flicker. *Journal of Vision*, *12*(12), 1–8.

Hammett, S. T., & Smith, A. T. (1992). Two Temporal Channels or Three? A Re-evaluation. *Vision Research*, *32*(2), 285–291.

Hammett, S. T., Smith, A. T., Wall, M. B., & Larsson, J. (2013). Implicit representations of luminance and the temporal structure of moving stimuli in multiple regions of human visual cortex revealed by multivariate pattern classification analysis. *Journal of Neurophysiology*, *110*(3), 688–99.

Hammett, S. T., Thompson, P. G., & Bedingham, S. (2000). The dynamics of velocity adaptation in human vision. *Current Biology*, *10*(18), 1123–1126.

Harris, M. G. (1980). Velocity specificity of the flicker to pattern sensitivity ratio in human vision. *Vision Research*, *20*(8), 687–691.

Hassenstein, B., & Reichardt, W. (1956). Systemtheoretische Analyse der Zeit-, Reihenfolgen- und Vorzeichenauswertung bei der Bewegungsperzeption des Rüsselkäfers Chlorophanus. *Zeitschrift Für Naturforschung B*, *11*(9), 513–524.

Hawken, M. J., Gegenfurtner, K. R., & Tang, C. (1994). Contrast dependence of colour and luminance motion mechanisms in human vision. *Nature*, *367*(6460), 268–270.

Hawken, M. J., Shapley, R. M., & Grosof, D. H. (1996). Temporal-frequency selectivity in monkey visual cortex. *Visual Neuroscience*, *13*(3), 477–492.

Heeger, D. J. (1987). Model for the extraction of image flow. *Journal of the Optical Society of America A*, *4*(8).

Heeger, D. J., & Simoncelli, E. P. (1993). Model of visual motion sensing. In L.

Harris & M. Jenkin (Eds.), *Spatial vision in humans and robots* (pp. 367–392). New York: Cambridge University Press.

Hess, R. F., & Plant, G. T. (1985). Temporal frequency discrimination in human vision: Evidence for an additional mechanism in the low spatial and high temporal frequency region. *Vision Research*, *25*(10), 1493–1500.

Hess, R. F., & Snowden, R. J. (1992). Temporal properties of human visual filters: Number, shapes and spatial covariation. *Vision Research*, *32*(1), 47–59.

Hicks, T. P., Lee, B. B., & Vidyasagar, T. R. (1983). The responses of cells in macaque lateral geniculate nucleus to sinusoidal gratings. *The Journal of Physiology*, *337*, 183–200.

Horn, B. K. P., & Schunck, B. G. (1981). Determining optical flow. *Artificial Intelligence*, *17*, 185–203.

Hubel, D. H., & Wiesel, T. N. (1961). Integrative action in the cat's lateral geniculate body. *The Journal of Physiology*, *155*(2), 385–398.

Hubel, D. H., & Wiesel, T. N. (1972). Laminar and columnar distribution of geniculo-cortical fibers in the macaque monkey. *The Journal of Comparative Neurology*, *146*(4), 421–450.

Hubel, D. H., Wiesel, T. N., & Stryker, M. P. (1977). Orientation columns in macaque monkey visual cortex demonstrated by the 2-deoxyglucose autoradiographic technique. *Nature*, *269*(5626), 328–330.

Hunzelmann, N., & Spillmann, L. (1984). Movement adaptation in the peripheral retina. *Vision Research*, *24*(12), 1765–1769.

Hürlimann, F., Kiper, D. C., & Carandini, M. (2002). Testing the Bayesian model of perceived speed. *Vision Research*, *42*(19), 2253–2257.

Jagacinski, R. J., Johnson, W. W., & Miller, R. A. (1983). Quantifying the

cognitive trajectories of extrapolated movements. *Journal of Experimental Psychology: Human Perception and Performance*, *9*(1), 43–57.

Jaynes, E. T. (1988). How does the brain do plausible reasoning? In G. J. Erickson & C. R. Smith (Eds.), *Maximum entropy and Bayesian methods in science and engineering* (pp. 1–24). Netherlands: Kluwer Academic.

Johnston, A., Arnold, D., & Nishida, S. (2006). Spatially localized distortions of event time. *Current Biology*, *16*(5), 472–479.

Johnston, A., McOwan, P. W., & Buxton, H. (1992). A computational model of the analysis of some first-order and second-order motion patterns by simple and complex cells. *Proceedings of the Royal Society of London B*, *250*(1329), 297–306.

Johnston, A., & Wright, M. J. (1983). Visual motion and cortical velocity. *Nature*, *304*(5925), 436–438.

Johnston, A., & Wright, M. J. (1986). Matching velocity in central and peripheral vision. *Vision Research*, *26*(7), 1099–1109.

Jones, R. M., & Tulunay-Keesey, U. (1975). Local retinal adaptation and spatial frequency channels. *Vision Research*, *15*(11), 1239–1244.

Julesz, B. (1971). *Foundations of cyclopean perception*. Chicago: Chicago Press.

Kaneko, S., & Murakami, I. (2009). Perceived duration of visual motion increases with speed. *Journal of Vision*, *9*(7), 14.

Kaplan, E., Lee, B. B., & Shapley, R. M. (1990). New Views of Primate Retinal Function. In N. Osborn & G. Chader (Eds.), *Progress in Retinal Research* (pp. 273–336). Oxford, UK: Pergamon.

Kaplan, E., & Shapley, R. M. (1986). The primate retina contains two types of ganglion cells, with high and low contrast sensitivity. *Proceedings of the*

National Academy of Sciences, *83*(8), 2755–2757.

Kleiner, M., Brainard, D., & Pelli, D. G. (2007). “Whats new in Psychtoolbox-3?” *Perception ECVP Abstract Supplement*, *36*.

Körding, K. P., & Wolpert, D. M. (2004). Bayesian integration in sensorimotor learning. *Nature*, *427*(6971), 244–247.

Körding, K. P., & Wolpert, D. M. (2006). Bayesian decision theory in sensorimotor control. *Trends in Cognitive Sciences*, *10*(7), 319–326.

Krauskopf, J. (1963). Effect of retinal image stabilization on the appearance of heterochromatic targets. *Journal of the Optical Society of America A*, *53*(6), 741–744.

Krekelberg, B., van Wezel, R. J., & Albright, T. D. (2006). Interactions between speed and contrast tuning in the middle temporal area: implications for the neural code for speed. *The Journal of Neuroscience*, *26*(35), 8988–8998.

Langer, M. S., & Bülthoff, H. H. (2001). A prior for global convexity in local shape-from-shading. *Perception*, *30*(4), 403–410.

Ledgeway, T., & Smith, A. T. (1994). Evidence for separate motion-detecting mechanisms for first-and second-order motion in human vision. *Vision Research*, *34*(20), 2727–2740.

Ledgeway, T., & Smith, A. T. (1997). Changes in perceived speed following adaptation to first-order and second-order motion. *Vision Research*, *37*(2), 215–224.

Lee, D. N. (1976). A theory of visual control of braking based on information about time-to-collision. *Perception*, *5*(4), 437–459.

Lee, D. N. (2009). General Tau Theory: evolution to date. *Perception*, *38*(6), 837–858.

Leek, M. R. (2001). Adaptive procedures in psychophysical research.

Perception & Psychophysics, *63*(8), 1279–1292.

Leiser, D., Stern, E., & Meyer, J. (1991). Mean velocity and total time estimation effects of order and proportions. *Journal of Environmental Psychology*, *11*(4), 347–358.

Lennie, P., Trevarthen, C., Van Essen, D., & Wässle, H. (1990). Parallel processing of visual information. In L. S. Spillmann & J. S. Werner (Eds.), *Visual perception: The neurophysiological foundations* (pp. 103–128). San Diego, California: Academic Press.

Levi, D. M., Klein, S. A., & Aitsebaomo, A. P. (1985). Vernier acuity, crowding and cortical magnification. *Vision Research*, *25*(7), 963–977.

Levitt, H. (1971). Transformed Up-Down methods in psychoacoustics. *The Journal of the Acoustical Society of America*, *49*(2), 467–477.

Lichtenstein, M. (1963). Spatio-Temporal Factors in Cessation of Smooth Apparent Motion. *Journal of the Optical Society of America*, *53*(2), 304–306.

Livingstone, M. S., & Hubel, D. H. (1987). Psychophysical evidence for separate channels for the perception of form, color, movement, and depth. *The Journal of Neuroscience*, *7*(11), 3416–3468.

Livingstone, M. S., & Hubel, D. H. (1988). Segregation of form, color, movement, and depth: anatomy, physiology, and perception. *Science*, *240*(4853), 740–749.

Lu, Z., Liu, C., & Dosher, B. (2000). Attention mechanisms for multi-location first-and second-order motion perception. *Vision Research*, *40*(2), 173–186.

Lu, Z., & Sperling, G. (1995). The Functional Architecture of Human Visual Motion Perception. *Vision Research*, *35*(19), 2697–2722.

Lund, J. S., & Boothe, R. G. (1975). Interlaminar connections and pyramidal neuron organisation in the visual cortex, area 17, of the Macaque monkey. *The Journal of Comparative Neurology*, *159*(3), 305–334.

Lyon, D. R., & Waag, W. L. (1995). Time course of visual extrapolation accuracy. *Acta Psychologica*, *89*(3), 239–260.

MacKay, D. M. (1982). Anomalous perception of extrafoveal motion. *Perception*, *11*(3), 359–360.

Maffei, L., & Fiorentini, A. (1973). The visual cortex as a spatial frequency analyser. *Vision Research*, *13*(7), 1255–1267.

Maffei, L., Morrone, C., Pirchio, M., & Sandini, G. (1979). Responses of visual cortical cells to periodic and non-periodic stimuli. *The Journal of Physiology*, *296*(1), 27–47.

Mandler, M. B. (1984). Temporal frequency discrimination above threshold. *Vision Research*, *24*(12), 1873–1880.

Mandler, M. B., & Makous, W. (1984). A three channel model of temporal frequency perception. *Vision Research*, *24*(12), 1881–1887.

Markram, H. (2003). Elementary principles of nonlinear synaptic transmission. In R. Hecht-Nielsen & T. McKenna (Eds.), *Computational Models for Neuroscience: Human Cortical Information Processing* (pp. 125–169). London: Springer.

Marr, D., & Ullman, S. (1981). Directional selectivity and its use in early visual processing. *Proceedings of the Royal Society of London B*, *211*(1183), 151–180.

Maunsell, J. H. (1987). Physiological evidence for two visual subsystems. In L. Vaina (Ed.), *Matters of Intelligence* (Vol. 188, pp. 59–87). Dordrecht, Holland: Reidel Press.

Maunsell, J. H., & Schiller, P. H. (1984). Evidence for the segregation of parvo- and magnocellular channels in the visual cortex of macaque monkey. *Neuroscience Abstracts*, *10*(520), 4155–4157.

Maunsell, J. H., & Van Essen, D. (1983). Functional Properties of Neurons in Middle Temporal Visual Area of the Macaque Monkey. I. Selectivity for Stimulus Direction, Speed, and Orientation. *Journal of Neurophysiology*, *49*(5), 1127–1147.

McKee, S. P., & Nakayama, K. (1984). The direction of motion in the peripheral visual field. *Vision Research*, *24*(1), 25–32.

McLean, J., & Palmer, L. A. (1989). Contribution of linear spatiotemporal receptive field structure to velocity selectivity of simple cells in area 17 of cat. *Vision Research*, *29*(6), 675–679.

McLean, J., Raab, S., & Palmer, L. A. (1994). Contribution of linear mechanisms to the specification of local motion by simple cells in areas 17 and 18 of the cat. *Visual Neuroscience*, *11*(2), 271–294.

McLeod, R., & Ross, H. (1983). Optic-flow and cognitive factors in time-to-collision estimates. *Perception*, *12*(4), 417–423.

Merigan, W. H., Byrne, C. E., & Maunsell, J. H. (1991). Does primate motion perception depend on the Magnocellular pathway? *The Journal of Neuroscience*, *11*(11), 3422–3429.

Merigan, W. H., & Eskin, T. A. (1986). Spatio-temporal vision of macaques with severe loss of P beta retinal ganglion cells. *Vision Research*, *26*(11), 1751–1761.

Merigan, W. H., Katz, L. M., & Maunsell, J. H. (1991). The effects of parvocellular lateral geniculate lesions on the acuity and contrast sensitivity of macaque monkeys. *The Journal of Neuroscience*, *11*(4), 994–1001.

Merigan, W. H., & Maunsell, J. H. (1993). How parallel are the primate visual pathways? *Annual Review of Neuroscience*, *16*(1), 369–402.

Michael, C. R. (1988). Retinal afferent arborization patterns, dendritic field orientations, and the segregation of function in the lateral geniculate nucleus of the monkey. *Proceedings of the National Academy of Sciences*, *85*(13), 4914–4918.

Millodot, M. (1966). Foveal and extra-foveal acuity with and without stabilized retinal images. *The British Journal of Physiological Optics*, *23*(2), 75.

Moulden, B., Renshaw, J., & Mather, G. (1984). Two channels for flicker in the human visual system. *Perception*, *13*(4), 387–400.

Movshon, J. A., & Blakemore, C. (1973). Orientation specificity and spatial selectivity in human vision. *Perception*, *2*(1), 53–60.

Movshon, J. A., Thompson, I. D., & Tolhurst, D. J. (1978). Spatial and temporal contrast sensitivity of neurones in areas 17 and 18 of the cat's visual cortex. *The Journal of Physiology*, *283*(1), 101–120.

Nakayama, K., & Silverman, G. (1984). Temporal and spatial characteristics of the upper displacement limit for motion in random dots. *Vision Research*, *24*(4), 293–299.

Nilsson, T. H., Richmond, C. F., & Nelson, T. M. (1975). Flicker adaptation shows evidence of many visual channels selectively sensitive to temporal frequency. *Vision Research*, *15*(5), 621–624.

Nishida, S., Ledgeway, T., & Edwards, M. (1997). Dual Multiple-scale Processing for Motion in the Human Visual System. *Vision Research*, *37*(19), 2685–2698.

Nyquist, H. (1928). Certain topics in telegraph transmission theory. *Transactions of the American Institute of Electrical Engineers*, *47*(2), 617–

644.

O'Keefe, L., & Movshon, J. (1998). Processing of first-and second-order motion signals by neurons in area MT of the macaque monkey. *Visual Neuroscience*, *15*, 305–317.

Pantle, A. (1971). Flicker adaptation—I. Effect on visual sensitivity to temporal fluctuations of light intensity. *Vision Research*, *11*(9), 943–952.

Pantle, A., & Sekuler, R. (1968). Size-detecting mechanisms in human vision. *Science*, *162*(3858), 1146–1148.

Papert, S. (1964). Stereoscopic synthesis as a technique for localizing visual mechanisms. *MIT Quarterly Progress Report No. 73*, *239*, 239.

Pavan, A., Campana, G., Guerreschi, M., Manassi, M., & Casco, C. (2009). Separate motion-detecting mechanisms for first-and second-order patterns revealed by rapid forms of visual motion priming and motion aftereffect. *Journal of Vision*, *9*(11), 1–16.

Pelli, D. G. (1997). The VideoToolbox software for visual psychophysics: Transforming numbers into movies. *Spatial Vision*, *10*(4), 437–442.

Pentland, A. (1980). Maximum likelihood estimation: The best PEST. *Perception & Psychophysics*, *28*(4), 377–379.

Perrone, J. A. (2005). Economy of scale: A motion sensor with variable speed tuning. *Journal of Vision*, *5*(1), 28–33.

Perrone, J. A., & Thiele, A. (2002). A model of speed tuning in MT neurons. *Vision Research*, *42*(8), 1035–1051.

Peterson, M. R., Li, B., & Freeman, R. D. (2004). The derivation of direction selectivity in the striate cortex. *Journal of Neuroscience*, *24*(14), 3583–91.

Plant, G., Laxer, K., Barbaro, N., Schiffman, J., & Nakayama, K. (1993). Impaired visual motion perception in the contralateral hemifield following

unilateral posterior cerebral lesions in humans. *Brain*, *116*(6), 1303–1335.

Plant, G., & Nakayama, K. (1993). The characteristics of residual motion perception in the hemifield contralateral to lateral occipital lesions in humans. *Brain*, *116*(6), 1337–1353.

Pollen, D. A., & Ronner, S. F. (1981). Phase relationships between adjacent simple cells in the visual cortex. *Science*, *212*(4501), 1409–1411.

Purpura, K., Kaplan, E., & Shapley, R. M. (1988). Background light and the contrast gain of primate P and M retinal ganglion cells. *Proceedings of the National Academy of Sciences*, *85*(12), 4534–4537.

Purpura, K., Tranchina, D., Kaplan, E., & Shapley, R. M. (1990). Light adaptation in the primate retina: Analysis of changes in gain and dynamics of monkey retinal ganglion cells. *Visual Neuroscience*, *4*(1), 75–93.

Ramachandran, V. S., & Gregory, R. (1978). Does colour provide an input to human motion perception? *Nature*.

Ramachandran, V. S., & Gregory, R. L. (1991). Perceptual filling in of artificially induced scotomas in human vision. *Nature*, *350*(6320), 699–702.

Ramoa, A. S., Freeman, R. D., & Macy, A. (1985). Comparison of response properties of cells in the cat's visual cortex at high and low luminance levels. *Journal of Neurophysiology*, *54*(1), 61–72.

Rao, S. M., Rourke, D., & Whitman, R. D. (1981). Spatio-temporal discrimination of frequency in the right and left visual fields: a preliminary report. *Perceptual and Motor Skills*, *53*(1), 311–316.

Reichardt, W. (1961). Autocorrelation, a principle for the evaluation of sensory information by the central nervous system. In W. A. Rosenblith (Ed.), *Sensory Communication* (pp. 303–317). New York: MIT Press and John Wiley and Sons.

Rodman, H. R., & Albright, T. D. (1987). Coding of visual stimulus velocity in area MT of the macaque. *Vision Research*, *27*(12), 2035–2048.

Rosenbaum, D. A. (1975). Perception and extrapolation of velocity and acceleration. *Journal of Experimental Psychology: Human Perception and Performance*, *1*(4), 395–403.

Ross, H. (1967). Water, fog and the size—distance invariance hypothesis. *British Journal of Psychology*, *58*, 301–313.

Rovamo, J., & Virsu, V. (1979). An estimation and application of the human cortical magnification factor. *Experimental Brain Research*, *37*(3), 495–510.

Sachs, M. B., Nachmias, J., & Robson, J. G. (1971). Spatial-frequency channels in human vision. *The Journal of Optical Society of America*, *61*(9), 1176–1186.

Sato, T. (1988). Direction discrimination and pattern segregation with isoluminant chromatic random-dot cinematograms. *Invest. Ophthalmol. Visual Sci.(Suppl.)*, *29*, 449.

Scarfe, P., & Johnston, A. (2010). Perception of motion from the combination of temporal luminance ramping and spatial luminance gradients. *Journal of Vision*, *10*(7), 847–847. doi:10.1167/10.7.847

Schieting, S., & Spillmann, L. (1987). Flicker adaption in the peripheral retina. *Vision Research*, *27*(2), 277–284.

Schiller, P. H. (1982). Central connections of the retinal ON and OFF pathways. *Nature*, *297*(5867), 580–583.

Schiller, P. H. (1984). The connections of the retinal ON and OFF pathways to the lateral geniculate nucleus of the monkey. *Vision Research*, *24*(9), 923–932.

Schiller, P. H. (1992). The ON and OFF channels of the visual system. *Trends*

in Neurosciences, *15*(3), 86–92.

Schiller, P. H., & Colby, C. L. (1983). The responses of single cells in the lateral geniculate nucleus of the rhesus monkey to color and luminance contrast. *Vision Research*, *23*(12), 1631–1641.

Schiller, P. H., Logothetis, N. K., & Charles, E. R. (1990). Functions of the colour-opponent and broad-band channels of the visual system. *Nature*, *343*(6253), 68–70.

Schiller, P. H., & Malpeli, J. G. (1978). Functional specificity of lateral geniculate nucleus laminae of the rhesus monkey. *Journal of Neurophysiology*, *41*(3), 788–797.

Schiller, P. H., Sandell, J. H., & Maunsell, J. H. (1986). Functions of the ON and OFF channels of the visual system. *Nature*, *322*(6082), 824–825.

Seiffert, A., & Cavanagh, P. (1998). Position displacement, not velocity, is the cue to motion detection of second-order stimuli. *Vision Research*, *38*(22), 3569–3582.

Seiffert, A., & Cavanagh, P. (1999). Position-based motion perception for color and texture stimuli: effects of contrast and speed. *Vision Research*, *39*(25), 4172–4185.

Shadlen, M., & Carney, T. (1986). Mechanisms of human motion perception revealed by a new cyclopean illusion. *Science*, *232*(4746), 95–97.

Shannon, C. E. (1949). Communication in the presence of noise. *Proceedings of the IRE*, *37*(1), 10–21.

Shapley, R. M. (2009). Linear and nonlinear systems analysis of the visual system: Why does it seem so linear? A review dedicated to the memory of Henk Spekreijse. *Vision Research*, *49*(9), 907–921.

Shapley, R. M., & Lennie, P. (1985). Spatial frequency analysis in the visual

system. *Annual Review of Neuroscience*, *8*(1), 547–583.

Shipley, W., Kenney, F., & King, M. (1945). Beta apparent movement under binocular, monocular and interocular stimulation. *The American Journal of Psychology*, *58*(4), 545–549.

Simoncelli, E. P., & Heeger, D. J. (1998). A Model of Neuronal Responses in Visual Area MT. *Vision Research*, *38*(5), 743–761.

Simoncelli, E. P., & Heeger, D. J. (2001). Representing retinal image speed in visual cortex. *Nature Neuroscience*, *4*(5), 461–462.

Smith, A. T. (1994). Correspondence-based and energy-based detection of second-order motion in human vision. *Journal of the Optical Society of America A*, *11*(7), 1940–1948.

Smith, A. T., & Edgar, G. K. (1991). Perceived speed and direction of complex gratings and plaids. *Journal of the Optical Society of America A*, *8*(7), 1161–1171.

Smith, A. T., & Edgar, G. K. (1994). Antagonistic comparison of temporal frequency filter outputs as a basis for speed perception. *Vision Research*, *34*(2), 253–265.

Smith, A. T., Greenlee, M., Singh, K., Kraemer, F., & Hennig, J. (1998). The processing of first-and second-order motion in human visual cortex assessed by functional magnetic resonance imaging (fMRI). *The Journal of Neuroscience*, *18*(10), 3816–3830.

Snowden, R. J., Stimpson, N., & Ruddle, R. A. (1998). Speed perception fogs up as visibility drops. *Nature*, *392*(6675), 450.

Sotiropoulos, G., Seitz, A. R., & Seriès, P. (2014). Contrast dependency and prior expectations in human speed perception. *Vision Research*, *97*, 16–23.

Stecher, S., Sigel, C., & Lange, R. V. (1973). Spatial frequency channels in

human vision and the threshold for adaptation. *Vision Research*, *13*(9), 1691–1700.

Stocker, A. A., & Simoncelli, E. P. (2006). Noise characteristics and prior expectations in human visual speed perception. *Nature Neuroscience*, *9*(4), 578–585.

Stone, L. S., & Thompson, P. G. (1992). Human speed perception is contrast dependent. *Vision Research*, *32*(8), 1535–1549.

Stone, L. S., Watson, A. B., & Mulligan, J. B. (1990). Effect of contrast on the perceived direction of a moving plaid. *Vision Research*, *30*(7), 1049–1067.

Stromeyer, C. F., & Julesz, B. (1972). Spatial-frequency masking in vision: Critical bands and spread of masking. *Journal of the Optical Society of America*, *62*(10), 1221–1232.

Taylor, M. M., & Creelman, C. D. (1967). PEST: Efficient Estimates on Probability Functions. *The Journal of the Acoustical Society of America*, *41*, 782–787.

Teghtsoonian, M., & Teghtsoonian, R. (1969). Scaling apparent distance in natural indoor settings. *Psychonomic Science*, *16*(6), 281–283.

Thompson, P. G. (1976). *Velocity aftereffects and the perception of movement*. University of Cambridge.

Thompson, P. G. (1981). Velocity aftereffects: the effects of adaptation to moving stimuli on the perception of subsequently seen moving stimuli. *Vision Research*, *21*, 337–345.

Thompson, P. G. (1982). Perceived rate of movement depends on contrast. *Vision Research*, *22*, 377–380.

Thompson, P. G. (1983). Discrimination of moving gratings at and above detection threshold. *Vision Research*, *23*(12), 1533–1538.

Thompson, P. G., Brooks, K., & Hammett, S. T. (2006). Speed can go up as well as down at low contrast: Implications for models of motion perception. *Vision Research*, *46*(6), 782–786.

Thompson, P. G., & Hammett, S. T. (2004). Perceived speed in peripheral vision: it can go up as well as down. *Journal of Vision*, *4*(8), 83.

Thompson, P. G., & Stone, L. S. (1997). Contrast affects flicker and speed perception differently. *Vision Research*, *37*(10), 1255–1260.

Thompson, P. G., Stone, L. S., & Swash, S. (1996). Speed estimates from grating patches are not contrast--normalized. *Vision Research*, *36*(5), 667–674.

Tolhurst, D. J. (1972). Adaptation to square-wave gratings: Inhibition between spatial frequency channels in the human visual system. *The Journal of Physiology*, *226*(1), 231–248.

Tolhurst, D. J., & Barfield, L. P. (1978). Interactions between spatial frequency channels. *Vision Research*, *18*(8), 951–958.

Tolhurst, D. J., Sharpe, C. R., & Hart, G. (1973). The analysis of the drift rate of moving sinusoidal gratings. *Vision Research*, *13*(12), 2545–2555.

Tresilian, J. R. (1995). Perceptual and cognitive processes in time-to-contact estimation: analysis of prediction-motion and relative judgment tasks. *Perception & Psychophysics*, *57*(2), 231–245.

Troxler, I. P. V. (1804). Uber das Verschwinden gegebener Gegenstande innerhalb unseres Gesichtskreises. In J. Himly & J. A. Schmidt (Eds.), *Ophthalmologische Bibliothek* (Vol. 2, pp. 1–119). Jenna: Fromann.

Tynan, P. D., & Sekuler, R. (1982). Motion processing in peripheral vision: Reaction time and perceived velocity. *Vision Research*, *22*, 61–68.

Ullman, S. (1979). *The interpretation of visual motion*. Massachusetts: MIT

Press.

Vaina, L., Cowey, A., & Kennedy, D. (1999). Perception of first-and second-order motion: separable neurological mechanisms? *Human Brain Mapping*, *7*(1), 67–77.

Vaina, L., Makris, N., Kennedy, D., & Cowey, A. (1996). The neuroanatomical damage producing selective deficits to first or second order motion in stroke patients provides further evidence for separate mechanisms. *NeuroImage*, *3*(3), S360.

Vaina, L., Makris, N., Kennedy, D., & Cowey, A. (1998). The selective impairment of the perception of first-order motion by unilateral cortical brain damage. *Visual Neuroscience*, *15*, 333–348.

Vaina, L., & Soloviev, S. (2004). First-order and second-order motion: neurological evidence for neuroanatomically distinct systems. *Progress in Brain Research*, *144*, 197–212.

van Santen, J. P., & Sperling, G. (1985). Elaborated Reichardt detectors. *Journal of the Optical Society of America A*, *2*(2), 300–321.

Vaziri-Pashkam, M., & Cavanagh, P. (2008). Apparent speed increases at low luminance. *Journal of Vision*, *8*(16), 1–12.

Victor, J. D., & Conte, M. M. (1994). Investigation of a patient with severely impaired direction discrimination: evidence against the intersection-of-constraints model. *Vision Research*, *34*(2), 267–277.

Vintch, B., & Gardner, J. L. (2014). Cortical correlates of human motion perception biases. *The Journal of Neuroscience*, *34*(7), 2592–2604.

von Békésy, G. (1947). A new audiometer. *Acta Oto-Laryngologica*, *35*, 411–422.

Von Grünau, M. (1986). A motion aftereffect for long-range stroboscopic

apparent motion. *Perception & Psychophysics*, *40*(1), 31–38.

Watson, A. B. (2014). A formula for human retinal ganglion cell receptive field density as a function of visual field location. *Journal of Vision*, *14*(7), 1–17.

Watson, A. B., & Pelli, D. G. (1983). QUEST: A Bayesian adaptive psychometric method. *Perception & Psychophysics*.

Watson, A. B., & Robson, J. G. (1981). Discrimination at threshold: Labelled detectors in human vision. *Vision Research*, *21*(7), 1115–1122.

Waugh, S. J., & Levi, D. M. (1993). Visibility and vernier acuity for separated targets. *Vision Research*, *33*(4), 539–552.

Weiss, Y., & Adelson, E. H. (1998). *Slow and Smooth: A Bayesian theory for the combination of local motion signals in human vision*. Cambridge, MA.

Weiss, Y., Simoncelli, E. P., & Adelson, E. H. (2002). Motion illusions as optimal percepts. *Nature Neuroscience*, *5*(6), 598–604.

Westheimer, G. (1982). The spatial grain of the perifoveal visual field. *Vision Research*, *22*(1), 157–162.

Whitaker, D., Rovamo, J., Macveigh, D., & Makela, P. (1992). Spatial scaling of vernier acuity tasks. *Vision Research*, *32*(8), 1481–1491.

Wiesel, T. N., & Hubel, D. H. (1966). Spatial and chromatic interactions in the lateral geniculate body of the rhesus monkey. *Journal of Neurophysiology*, *29*, 1115–1156.

Wilson, H. R., Ferrera, V. P., & Yo, C. (1992). A psychophysically motivated model for two-dimensional motion perception. *Visual Neuroscience*, *9*(1), 79–97.

Yap, Y. L., Levi, D. M., & Klein, S. A. (1989). Peripheral position acuity: Retinal and cortical constraints on 2-dot separation discrimination under photopic and scotopic conditions. *Vision Research*, *29*, 789–802.

Zakay, D., & Block, R. A. (1995). An attentional-gate model of prospective time estimation. *Time and the Dynamic Control of Behavior*, (11), 167–178.

Zakay, D., & Block, R. A. (1996). The role of attention in time estimation processes. *Advances in Psychology*, *115*, 143–164.

Zakay, D., & Block, R. A. (1997). Temporal cognition. *Current Directions in Psychological Science*, *6*(1), 12–16.

Żychaluk, K., & Foster, D. H. (2009). Model-free estimation of the psychometric function. *Attention, Perception, & Psychophysics*, *71*(6), 1414–1425.

Appendix 1

MATLAB code

The script used in Experiment 3a to run a contrast matching task:

```
% Contrast Matching

% Omar Hassan 12/09/12

function ContrastMatch


%% Subject ID and trial parameters

subject = input('Subject ID:', 's');

C_P = str2double(input('Standard Contrast (e.g. 0.1 or 0.7): ',...
    's'));

% S_S = str2double(input('Standard Speed (e.g. 1 (deg/sec)): ',...
% 's'));

T_S =str2double(input('Test Speed (e.g. 1, 2, 4, 8 (deg/sec)):'...
    , 's'));


%% Screen

%Remove 'Welcome to psychtoolbox' screen
Screen('Preference', 'VisualDebuglevel', 1);

%ResolutionTest;
%screenres=Screen('Resolution', 1)
%1152x864 100Hz


%% Gamma correction and open window

%Gamma correction
PsychImaging('PrepareConfiguration');
PsychImaging('AddTask', 'FinalFormatting',...
    'DisplayColorCorrection','SimpleGamma');

%Open window
[wPtr,rect]=PsychImaging('OpenWindow',1);

%Gamma correction
PsychColorCorrection('SetEncodingGamma', wPtr, 0.4562002);

Screen('BlendFunction', wPtr, GL_SRC_ALPHA,...
    GL_ONE_MINUS_SRC_ALPHA);


%% Mean luminance

lummean=128;


%% Initial screen of mean luminance

Screen('FillRect',wPtr,lummean);
Screen('Flip', wPtr);
```

```
%% Experimenter defined parameters

params.stimulusDuration=0.5; % (sec)

params.stimulusSize=100; % Window size (pixels) = 3 deg

params.stimulusLeftANGLE=270; % Angle of standard grating
params.stimulusRightANGLE=270; % Angle of test grating

params.stimulusLeftSF=0.12; % Standard SF (cycles/pixel)= 2 c/deg
params.stimulusRightSF=0.12; % Test SF (cycles/pixel)= 2 c/deg

params.stimulusLeftSPEED=1*2; % Standard TF (cycles/sec)
params.stimulusRightSPEED=T_S*2; % Test TF (cycles/sec)

params.screenNum = 1;
params.wPtr=wPtr;
params.rect=rect;

params.ITI = 1; % (sec)
params.ISI=0.5; % (sec)

params.totalTrials=50; % Number of trials

wrongRight = {'wrong','right'}; % Response displayed

% Standard contast used to create stimulus
params.stimulusLeftCONTRAST=C_P;


%% QuestCreate

% Create prior threshold estimate.
contrastGuess = C_P+(0+0.1*rand(1,1));

% Contast used in QUEST is log10 contrast
tGuess = log10(contrastGuess);

% Range of possible values of threshold
tGuessSd = 2.5;

% Threshold criterion expressed as probability of response==1.
pThreshold=0.82;

beta=3.5; delta=0.01; gamma=0.5; grain=0.01; range=4;

q=QuestCreate(tGuess,tGuessSd,pThreshold,beta,delta,gamma,...
    grain,range,[]);

q.normalizePdf=1;


%% Mean luminance screen

Screen('FillRect',wPtr,lummean);
Screen('Flip', wPtr);
WaitSecs(5);


%% Create array for save file
```

```
trialcomplete=ones(4,params.totalTrials);


%% Trials

for k=1:params.totalTrials

      % Get recommended level.
      tTest=QuestQuantile(q);

    % Restrict to range of log contrasts.
    tTest=min(0,max(-2,tTest));


    %% Present Stimuli

    % Test contrast
    RightCONTRAST=10^tTest

    texsize =params.stimulusSize / 2;

    % Find the color values which correspond to white and black:
    white=WhiteIndex(params.screenNum);
    black=BlackIndex(params.screenNum);

    % Round gray to integral number:
    gray=round((white+black)/2); %128

    % Contrast 'inc'rement range for given white and gray values:
    inc=white-gray;


    % Calculate parameters of the gratings:

    % Compute pixels/cycle:
    p=ceil(1/params.stimulusLeftSF); % Standard
    pRight=ceil(1/params.stimulusRightSF); % Test

    % Frequency in radians:
    fr=params.stimulusLeftSF*2*pi; % Standard
    frRight=params.stimulusRightSF*2*pi; % Test

    % Visible size of the grating:
    visiblesize=2* texsize +1;

    % Create single static grating images:

    x = meshgrid(-texsize:texsize + p*10, 1); % Standard

    xRight = meshgrid(-texsize:texsize + pRight*10, 1); % Test

    % Compute cosine gratings:
    grating=gray + inc*cos(fr*x); % Standard
    %Random spatial phase
    gratingchangeL=grating(1:25);
    phlL=randi([1 20]);
    gratingchL=gratingchangeL(phlL:end);
    gratingcutL = grating(1:end-numel(gratingchL));
    grating = horzcat(gratingchL, gratingcutL);

    gratingRight=gray + inc*cos(frRight*xRight); % Test
```

```
%Random spatial phase
gratingchangeR=gratingRight(1:25);
phlR=randi([1 20]);
gratingchR=gratingchangeR(phlR:end);
gratingcutR = gratingRight(1:end-numel(gratingchR));
gratingRight = horzcat(gratingchR, gratingcutR);

% Store 1-D single row grating in texture:
gratingtexLeft=Screen('MakeTexture', params.wPtr,...
    grating); % Standard
gratingtexRight=Screen('MakeTexture', params.wPtr,...
    gratingRight); % Test

% Create a mask:

% Create a single hard edged mask
% and store it to a texture:

mask=ones(2*texsize+1, 2*texsize+1, 2) * gray;
[x,y]=meshgrid(-texsize:texsize,-texsize:texsize);
mask(:, :, 2)=white * (1-(x.^2 + y.^2 <= texsize^2));
masktex=Screen('MakeTexture', params.wPtr, mask);

% OR

% Create a single gaussian transparency mask
% and store it to a texture:

%     [x,y]=meshgrid(-texsize:texsize, -texsize:texsize);
%     maskblob=uint8(ones(2*texsize+1, 2*texsize+1, 2) * gray);
%     size(maskblob);
%
%     % Layer 2 (Transparency aka Alpha) is filled with
%     % gaussian transparency mask.
%
%     xsd=texsize/2.0;
%     ysd=texsize/2.0;
%     maskblob(:,:,2)=uint8(round...
%         (255 - exp(-((x/xsd).^2)-((y/ysd).^2))*255));
%
%     masktex=Screen('MakeTexture', params.wPtr, maskblob);

% Definition of the drawn rectangle on the screen:
dstRect=[0 0 visiblesize visiblesize];
dstRectd=[0 0 2 2];
dstRectdot=CenterRectOnPoint(dstRectd, params.rect(3)*0.5,...
    params.rect(4)*0.5); % Fixation
dstRectLeft=CenterRectOnPoint(dstRect, params.rect(3)*0.44,...
    params.rect(4)*0.5); % Standard
dstRectRight=CenterRectOnPoint(dstRect,...
    params.rect(3)*0.56,params.rect(4)*0.5); % Test

% Query duration of one monitor refresh interval:
ifi=Screen('GetFlipInterval', params.wPtr);

waitframes = 1;

% Translate frames into seconds for screen update interval:
waitduration = waitframes * ifi;

% Recompute p, without the ceil() operation.
p=1/params.stimulusLeftSF;  % Standard (pixels/cycle)
```

```
pRight=1/params.stimulusRightSF; % Test (pixels/cycle)

% Translate requested speed of the grating (in cycles/sec)
% into a shift value in "pixels per frame", for
% given waitduration:
% Standard:
shiftperframe= params.stimulusLeftSPEED * p * waitduration;
% Test:
shiftperframeRight= params.stimulusRightSPEED *...
    pRight * waitduration;

% Perform initial Flip to sync us to the VBL and for
% getting an initial VBL-Timestamp as timing baseline
% for our redraw loop:
vbl=Screen('Flip', params.wPtr);

% Run 'params.stimulusDuration' seconds
vblendtime = vbl + params.stimulusDuration;
i=0;

% Animationloop:
while(vbl < vblendtime)

    xoffset = mod(i*shiftperframe,p); % Standard
    xoffsetRight = mod(i*shiftperframeRight,pRight); % Test
    i=i+1;

    % Define shifted srcRect that cuts out the properly
    % shifted rectangular area from the texture:
    % Standard:
    srcRect=[xoffset 0 xoffset + visiblesize visiblesize];
    % Test:
    srcRectRight=[xoffsetRight 0 xoffsetRight + visiblesize...
        visiblesize];

    % Draw grating textures:
    % Standard:
    Screen('DrawTexture', params.wPtr, gratingtexLeft,...
        srcRect,dstRectLeft, params.stimulusLeftANGLE,...
        [],params.stimulusLeftCONTRAST, [], [], [], []);
    % Test:
    Screen('DrawTexture', params.wPtr, gratingtexRight,...
        srcRectRight,dstRectRight,...
        params.stimulusRightANGLE,[],RightCONTRAST,...
        [], [], [], []);

    % Draw gaussian mask over grating:
    % Standard
    Screen('DrawTexture', params.wPtr, masktex,...
        [0 0 visiblesize visiblesize], dstRectLeft,...
        params.stimulusLeftANGLE,[], [], [], [], [], []);
    % Test
    Screen('DrawTexture', params.wPtr, masktex,...
        [0 0 visiblesize visiblesize], dstRectRight,...
        params.stimulusRightANGLE,[], [], [], [], [], []);

    % Draw fixation dot
    Screen('FillOval', params.wPtr, uint8(white), dstRectdot);

    % Flip 'waitframes' monitor refresh intervals
    % after last redraw.
    vbl = Screen('Flip', params.wPtr, vbl +...
```

```
        (waitframes - 0.5) * ifi);

end;

%dstRectd=[0 0 2 2];
%dstRectdot=CenterRectOnPoint(dstRectd, params.rect(3)*0.5,...
%params.rect(4)*0.5);
Screen('FillOval', params.wPtr, uint8(white), dstRectdot);
Screen('Flip', params.wPtr);
Screen('FillOval', params.wPtr, uint8(white), dstRectdot);


%% Response

[x,y,buttons] = GetMouse(1);

while ~any(buttons)

    [x,y,buttons] = GetMouse(1);

end

% a=buttons
if buttons(1)==0;

    response=1;% Right mouse button pressed so subjects think
               % right grating has higher contrast.
else

    response=0;% Sbjts think left grating has higher contrast.

end


%% Display trial data to experimenter

% Trial data for save file:
trialcomplete(1,k)=k;
trialcomplete(2,k)=response;
trialcomplete(3,k)=RightCONTRAST;

if response==1 && (params.stimulusLeftCONTRAST...
        <= RightCONTRAST)

    wrongR=2; % Correct

elseif response==0 && (params.stimulusLeftCONTRAST...
        < RightCONTRAST)

    wrongR=1; % Incorrect

elseif response==1 && (params.stimulusLeftCONTRAST...
        > RightCONTRAST)

    wrongR=1; % Incorrect

elseif response==0 && (params.stimulusLeftCONTRAST...
        >= RightCONTRAST)

    wrongR=2; % Correct

end
```

```
    trialcomplete(4,k)=wrongR;

    fprintf('Trial %3d at %5.2f cont %5.5f is %s\n',k,tTest,...
        RightCONTRAST,char(wrongRight(wrongR)));


    %% Screen of mean luminance
    Screen('Flip', params.wPtr);

    % Intertrial interval
    WaitSecs (params.ITI);


    %% Update the pdf
    q=QuestUpdate(q,tTest,response);


end


%% Ask Quest for the final estimate of threshold.

% Log10 contrast:
t=QuestMean(q);

sd=QuestSd(q);

% Actual contrast:
realt=10^t;

% Display final threshold to experimenter
fprintf('Final threshold estimate (mean sd) is %.4f  %.2f\n',...
    realt,sd);


%% Save data

C_Pname=C_P*10; % Remove decimal point

file_name=sprintf('%s_%sC_%sS_%s', subject, num2str(C_Pname),...
    num2str(T_S), datestr(now,30));
save(file_name,'q', 'params','t','sd','realt','trialcomplete');


Screen('CloseAll');
```

Appendix 2

The simulation in Figure 6.1 used the temporal filters originally proposed by Smith and Edgar (1994) for their close fit to behavioural data. They take the form $m = 300e^{-0.5(\omega-10)^2/(24+\omega)}$ and $p = 15000e^{-0.5(\omega-50)^2/(17)}$ where *m* and *p* define the sensitivity of the 'fast' and 'slow' mechanisms. The simulation assumes that their responses (*M* and *P*) are determined by a modified Naka-Rushton relation such that sensitivity at any given temporal frequency, w, and contrast, *c*, is given by $P(\omega, c) = \frac{c.p(\omega)}{|c|.p(\omega)+\alpha_p}$ and $M(\omega, c) = \frac{c.m(\omega)}{|c|.m(\omega)+\alpha_m/\omega}$ where α_m and α_p are the semi-saturation constants. In the high luminance simulation these values were set to 0.13 and 1.79 which is consistent with the known properties of M and P cells (Blakemore & Vital-Durand, 1986; Derrington & Lennie, 1984; Hicks, Lee, & Vidyasagar, 1983; Kaplan, Lee, & Shapley, 1990; Schiller & Colby, 1983). The value of α_m varied inversely as a function of frequency such that the contrast response became more compressive at higher frequencies consistent with physiological reports (Kaplan & Shapley, 1986). In the low luminance condition the values were set to 0.15 and 8.95 in order to simulate a large reduction in gain of the P mechanism (Purpura et al., 1988). Speed, *S,* at each contrast, *c*, was calculated as the ratio of the two mechanisms' responses such that $S(\omega, c) = \frac{M(\omega,c)}{P(\omega,c)}$.